Investigating the role of epigenetic regulators in MYC-driven prostate cancer

M.Sc. thesis presented by

LÉA-KRISTINE DEMERS

Faculty of Medicine and Health Sciences

Division of Experimental Medicine

McGill University

July 2022

A thesis submitted to McGill University in partial fulfillment of the requirements of the degree of Master of Science

ABSTRACT

Prostate cancer is the second most common cancer among men worldwide and a leading cause of cancer-related mortality. Chromatin integrity and accessibility for transcriptional regulation are central features altered in prostate cancer progression. The proto-oncogene c-*MYC* (*MYC*) is a key driver of human prostate cancer tumorigenesis and progression involved in transcriptional reprogramming. MYC-overexpression is found in 8% of primary prostate tumors and 37% of metastatic tumors and is associated with poor overall survival. Critically, MYC overexpression in normal luminal cells of murine prostate is sufficient to initiate prostate cancer, indicating the key role of MYC in driving prostate cancer initiation. A hallmark of MYC-overexpression is the induction of global metabolic reprograming events which support cancer cell survival and growth. While MYC is known as a master regulator of cellular metabolism, the role of epigenetic modifications which rely on metabolites as substrates or cofactors to alter chromatin structure and DNA accessibility in MYC-driven prostate cancer growth remains elusive. We hypothesize that in the context of MYC-overexpression, prostate cancer cells are dependent on the expression of key epigenetic regulators for survival and growth.

To decipher the role of epigenetic regulators in the context of MYC-overexpression in prostate cancer, we performed pooled *in vitro* CRISPR/Cas9 knockout (KO) screens using a MYC-driven murine prostate cancer cell line (MyC-CaP). Briefly, we designed and amplified two custom CRISPR/Cas9 sgRNA libraries that are created to target 1,343 genes, mostly focused on epigenetic processes, with distinct sets of 5 sgRNAs per targeted gene. Our *in vitro* CRISPR/Cas9 KO screens revealed around 100 genes that were significantly depleted or enriched (P-value ≤ 0.05) in both screens, 30 of which are non-commonly essential across human cancer cell lines. Namely, our *in vitro* CRIPSR/Cas9 KO screens identified the pioneer transcription factor *Foxa1,* the ligand-

inducible transcription factor *Ar*, and the methyltransferases *Mettl1* and *Setd8*, to function as critical players in MYC-driven prostate cancer. Further, our *in vitro* CRISPR/Cas9 KO screens revealed that the disruption of the transcriptional corepressor *Rb1*, the histone demethylase *Kdm3b* and the histone chaperone *Hira* confers a selective growth advantage in MYC-overexpressing prostate cancer. Overall, our results revealed the specific patterns of epigenetic expression that must be maintained for prostate cancer cells to survive or proliferate in a MYC-driven context. We expect that our findings will contribute to unraveling the role of epigenetic remodeling in MYC-driven prostate cancer growth and enable the identification of novel therapeutically targetable chromatin-related mechanisms, which could ultimately be used to treat patients with MYC-overexpressing prostate cancer tumors.

RÉSUMÉ

Le cancer de la prostate est le deuxième cancer le plus fréquent chez les hommes dans le monde et l'une des principales causes de mortalité liée au cancer. L'intégrité et l'accessibilité de la chromatine pour la régulation transcriptionnelle sont des caractéristiques centrales altérées dans la progression du cancer de la prostate. Le proto-oncogène c-*MYC* (MYC) est un facteur clé de la tumorigenèse et de la progression du cancer de la prostate étant impliqué dans la reprogrammation transcriptionnelle. La surexpression de MYC est présente dans 8 % des tumeurs localisées et 37 % des tumeurs métastatiques du cancer de la prostate et est associée à un faible taux de survie globale. La surexpression de MYC dans les cellules luminales normales de la prostate murine est suffisante pour initier le cancer de la prostate, indiquant un rôle clé de MYC dans l'initiation du cancer de la prostate. L'une des caractéristiques de la surexpression de MYC est l'induction d'évènements de reprogrammation métabolique globaux qui favorisent la survie et la croissance des cellules cancéreuses. Alors que MYC est connu comme un régulateur principal du métabolisme cellulaire, le rôle des modifications épigénétiques, qui reposent sur des métabolites en tant que substrats ou cofacteurs pour modifier la structure de la chromatine et l'accessibilité de l'ADN, dans la croissance du cancer de la prostate induite par MYC reste inconnu. Notre hypothèse est donc que dans le contexte de la surexpression de MYC, les cellules cancéreuses de la prostate dépendent de l'expression de régulateurs épigénétiques clés pour leurs survies et leurs croissances.

Pour déchiffrer le rôle des régulateurs épigénétiques dans le contexte de la surexpression de MYC dans le cancer de la prostate, nous avons effectué des cribles CRISPR/Cas9 knockout (KO) *in vitro* à l'aide d'une lignée cellulaire de cancer de la prostate murine qui surexprime MYC (MyC-CaP). En bref, nous avons conçu et amplifié deux bibliothèques d'ARN guides synthétiques (ARNgs) CRISPR/Cas9 personnalisées qui sont créées pour cibler 1 343 gènes, principalement

axés sur les processus épigénétiques, avec des ensembles distincts de 5 ARNgs par gène ciblé. Nos cribles CRISPR/Cas9 KO *in vitro* ont révélé environ 100 gènes significativement réduits ou enrichis (valeur $P \leq 0,05$) dans les deux cribles, dont 30 ne sont généralement pas essentiels dans les lignées cellulaires cancéreuses humaines. À savoir, nos cribles CRIPSR/Cas9 *in vitro* ont identifié le facteur de transcription pionnier *Foxa1*, le facteur de transcription *Ar* et les méthyltransférases *Mettl1* et *Setd8,* comme étant des gènes essentiels dans le cancer de la prostate induit par MYC. De plus, nos cribles CRISPR/Cas9 *in vitro* ont révélé que la perturbation du corépresseur transcriptionnel *Rb1*, de l'histone déméthylase *Kdm3b* et du chaperon d'histones *Hira* confère un avantage de croissance sélectif dans le cancer de la prostate surexprimant MYC. Dans l'ensemble, nos résultats ont révélé l'archétype spécifique d'expression épigénétique qui doit être maintenu pour que les cellules cancéreuses de la prostate survivent ou prolifèrent dans un contexte axé sur la surexpression de MYC. Nous nous attendons à ce que nos découvertes contribuent à éclaircirent-le rôle du remodelage épigénétique dans la croissance du cancer de la prostate induite par MYC et permettent l'identification de nouveaux mécanismes liés à la chromatine pouvant être thérapeutiquement ciblées, et qui pourraient être utilisé pour traiter les patients atteints avec le cancer de la prostate surexprimant MYC.

TABLE OF CONTENT

LIST OF FIGURES

LIST OF TABLES

LIST OF ABBREVIATIONS

ADT	androgen-deprivation therapy
AJCC	American Joint Committee on Cancer
BFP	blue fluorescent protein
BPH	benign hyperplastic hyperplasia
BRD4	bromodomain protein 4
BSA	bovine serum albumin
Cas	CRISPR-associated protein
CgA	chromogranin A
CRIPSRi	CRISPR interference
CRISPR KO	CRISPR knockout
CRISPRa	CRIPSR activation
CRISPRs	clusters of regulatory interspaced short palindromic repeats
CRPC	castration-resistant prostate cancer
crRNAs	CRISPR RNAs
CTL-4	T-lymphocyte-associated protein 4
D-PBS	Dulbecco's phosphate-buffered saline
dCas9	dead Cas9
DDR	DNA damage repair genes
DMEM	Dulbecco's modified eagle medium
DNMTS	DNA methyltransferases
DRE	digital rectal examen

EBRT	external-bean radiation therapy
EED	embryonic ectoderm development protein
EMT	epithelial-mesenchymal transition
EZH2	enhancer of zeste homolog 2
gDNA	genomic DNA
GFP	green-fluorescent protein
GnRH	gonadotropin-releasing hormone
GO	gene Ontology
GSEA	gene set enrichment analysis
GWAS	genome-wide association studies
HATS	histone acetyltransferases
HDACs	histone deacetylase
HDR	homology-directed repair
Hi-MYC	transgenic mice with high MYC overexpression in the prostate
HMT	histone methyltransferase
IMRT	intensity-modulated radiation therapy
KEGG	kyoto encyclopedia of genes and genomes
LFC	log fold change
LHRH	luteinizing hormone-releasing hormone
mCRPC	metastatic castration-resistant prostate cancer
mCSPC	metastatic castration-sensitive prostate cancer
MMR	DNA mismatch repair genes
MOI	multiplicity of infection

MSigDB	molecular signatures database
NEPC	neuroendocrine prostate cancer
NGS	next-generation sequencing
NHEJ	non-homologous end-joining repair
NSE	neuron-specific enolase
ORA	over-representation analyses
PAM	protospacer adjacent motif
PARP	poly-ADP ribose polymerase
PCA	principal component analysis
PD-1	programmed cell death protein 1
PDL-1	programmed cell death protein ligand 1
PIN	prostatic intraepithelial neoplasia
PSA	prostate-specific antigen
PSMA	prostate-specific membrane antigen
PTMs	post-translational modifications
RIPA	radioimmunoprecipitation assay
RNAi	RNA interference
RNAi	RNA interference
RPMI	Rosewell park memorial institute medium
RRA	robust rank analysis
SAM	S-adenosylmethionine
sgRNA	single guide RNA
SNPs	single nucleotides polymorphisms

SYN	synaptophysin
TALENs	transcription activator-like effector nucleases
TCGA	The Cancer Genome Atlas
TNM	tumor-node-metastasis
tracrRNA	trans-activating CRISPR RNA
tRNAs	transfer RNAs
ZFNs	zinc-finger nucleases

ACKNOWLEDGEMENT

I would like to begin by thanking Dr. David P. Labbé, my supervisor, for giving me the chance to be a part of his lab as a graduate student. I am very grateful to have had the opportunity to work under the supervision of such a knowledgeable, passionate, and devoted scientist. The research and professional skills I have gained while working in the Labbé lab are invaluable tools that will serve me for the rest of my career in the scientific field.

I would also like to thank my lab members who have been by my side throughout my two years as a graduate student. I would like to give a special thank you to Dr. Nadia Boufaied, my mentor without whom the success of this research project would not have been possible. I admire Nadia for her fervent devotion and determination towards her work and for her ability to successfully juggle with so many responsibilities simultaneously. The combination of her knowledge, her expertise in bioinformatics, and her support as a mentor has allowed me to be successful as a graduate student. I would like to thank Tarek Hallal, former student, and current research assistant, for the extensive support he has provided throughout my time as a graduate student. From all the times he has stepped in to help with experiments to the many, many times he was there to listen and provide encouragement, he has made a big impact on my time in the lab. I would like to thank Walaa, Michelle, and Janie, for their companionship and support.

I would like to express my thanks to my research advisory committee members, Dr. Ilan Azuelos and Dr. Marc Fabian, who both acted as my committee chair, and Dr. Jacques Côté, Dr. Livia Garzia, and Dr. Richard Marcotte. Thank you for taking the time to provide your expertise, your advice, and your ideas to my project and training.

I would like to give a special thank you to Dr. Richard Marcotte, Dr. Simon Drouin, Marc Sasseville, and Yves Fortin, who provided help and ideas to different aspects of this project. Your

expertise and generosity have allowed us to successfully conduct and analyze *in vitro* CRISPR/Cas9 KO screens, which was a first for our lab.

My gratitude extends to the McGill University Division of Experimental Medicine for the Graduate Excellence Fellowship, the Fonds de Recherche du Québec – Santé (FRQS) for the Master's training Scholarship, the McGill Urology Research subdivision for the McGill Urology Claude Gagnon Research Studentship, and the Canadian Institutes of Health Research Project Grant (CIHR) for the project grant awarded to Dr. David P. Labbé (project grant PJT-162246); all of which have allowed me to pursue this project.

I would like to give a huge thank you to my mother, Annie, my brother, Karl-Éric, and my friends, who have been by my side and have provided tremendous support throughout this experience.

Finally, I would like to give a very special thank you to my father, Éric, who passed away a few months before the completion of my master's degree. I would not have been able to accomplish this milestone without his love and support.

CONTRIBUTION OF AUTHORS

This thesis follows the format of a traditional thesis. I wrote this thesis under the supervision of Dr. David P. Labbé. The project was conceptualized by Dr. David P. Labbé. Experiments were designed by Dr. David P. Labbé, Dr. Nadia Boufaied, and myself. The custom CRISPR/Cas9 sgRNA libraries were designed by Dr. David P. Labbé and Dr. X. Shirley Liu.

I performed the cloning of the custom sgRNA libraries. The MyC-CaP Cas9 stable cell line and the Cas9-expressing monoclonal cell lines were generated by Dr. Nadia Boufaied. The experiments for characterization of the MyC-CaP Cas9 monoclonal cell line including Western Blotting, the Cas9 activity assay and the proliferation assay were performed by me. Production of the lentiviral sgRNA libraries in HEK293-FT cells and MOI determination of the lentivirus in MyC-CaP cells was performed by me. The 48 h puromycin kill curve in MyC-CaP cells was performed by me. I conducted the *in vitro* CRISPR/Cas9 KO screen in the MyC-CaP Cas9 cell line and harvested the genomic DNA from the cells harvested throughout the screen. Sample preparation for Next-Generation Sequencing was done by Yves Fortin at the National Research Council Canada. Bioinformatic analyses of the next-generation sequencing data were done by Dr. Nadia Boufaied, Dr. Simon Drouin and Marc Sasseville. All collected results were interpreted by me, with the help of Dr. David P. Labbé and Dr. Nadia Boufaied. Marc Sasseville and Dr. Nadia Boufaied wrote the bioinformatics section of the Methods chapter.

Figure 1-1 to **Figure 1-4** are adapted from the literature. **Figure 3-1**, **Figure 3-3A-C**, **Supplementary Figure 4-1**, and **Supplementary Figure 4-3A-B** were prepared by me. **Figure 3-2** was prepared by Yves Fortin. **Figure 3-2D** and Supplementary **Figure 4-2C** were prepared by me with the help of Walaa Alahmadi. **Figure 3-4**, **Figure 3-5**, **Figure 3-6**, **Figure 3-7,** and

Supplementary Figure 4-4 were prepared by Dr. Nadia Boufaied. **Supplementary Figure 4-2** was prepared by Tarek Hallal. **Table 1** to **Table 7** were prepared by me.

Chapter 1. Literature Review

1.1. Prostate Cancer

1.1.1. Prostate anatomy and function

The prostate is an organ of the male reproductive and urinary systems located beneath the urinary bladder and in front of the rectum. The prostate surrounds the urethra, which carries urine and semen out of the body through the penis [1]. The normal prostate is about the size of a walnut and weighs 15 to 20 grams. Over time, the prostate can grow larger in a process called benign hyperplastic hyperplasia (BPH), or prostate gland enlargement [1]. During this process, benign overgrowth of the glands surrounding the prostatic urethra leads to compression of the urethra, producing uncomfortable urinary symptoms such as bladder obstruction [1, 2]. As part of the reproductive system, the prostate functions as an accessory sex gland that contributes to 70% of the seminal volume [2]. In aid of reproduction, the prostatic smooth muscles contract to expel the sperm from the body via the prostatic urethra, while secreting seminal fluids that protect and energize the sperm cells as they travel to the female egg.

The prostate is a gland with different histological zones, namely the peripheral zone, the transition zone and the central zone (**Figure 1-1**) [3, 4]. The peripheral zone, which is wrapped around the outer portion of the prostate, constitute about 70% of tissue in the normal prostate, and is the most common site of origin of prostate cancers (60-70%) [3, 4]. The transition zone is located near the prostatic urethra and constitute about 5% of normal prostate tissue in young men [3, 4]. In older men, the transition zone often becomes considerably enlarged through the process of BPH. About 10-20% of cancers arise from the transition zone, which are clinically and biologically different than peripheral zone cancers. Notably, although transition zone cancers are often diagnosed at larger tumor volume, they show better clinical outcome than peripheral zone cancers

with regards to biochemical recurrence, local, and distant metastasis [5]. Transition zone cancers also demonstrated reduced rates of lymphovascular invasion, lymph node involvement and extracapsular invasion [5]. The central zone represents the wider portion of the base of the prostate, surrounding the ejaculatory ducts, and accounts for 25% of prostatic tissue [3, 4]. The small portion of prostate cancers (5-10%) that arises from the central zone are more aggressive than cancers from the peripheral and transition zones.

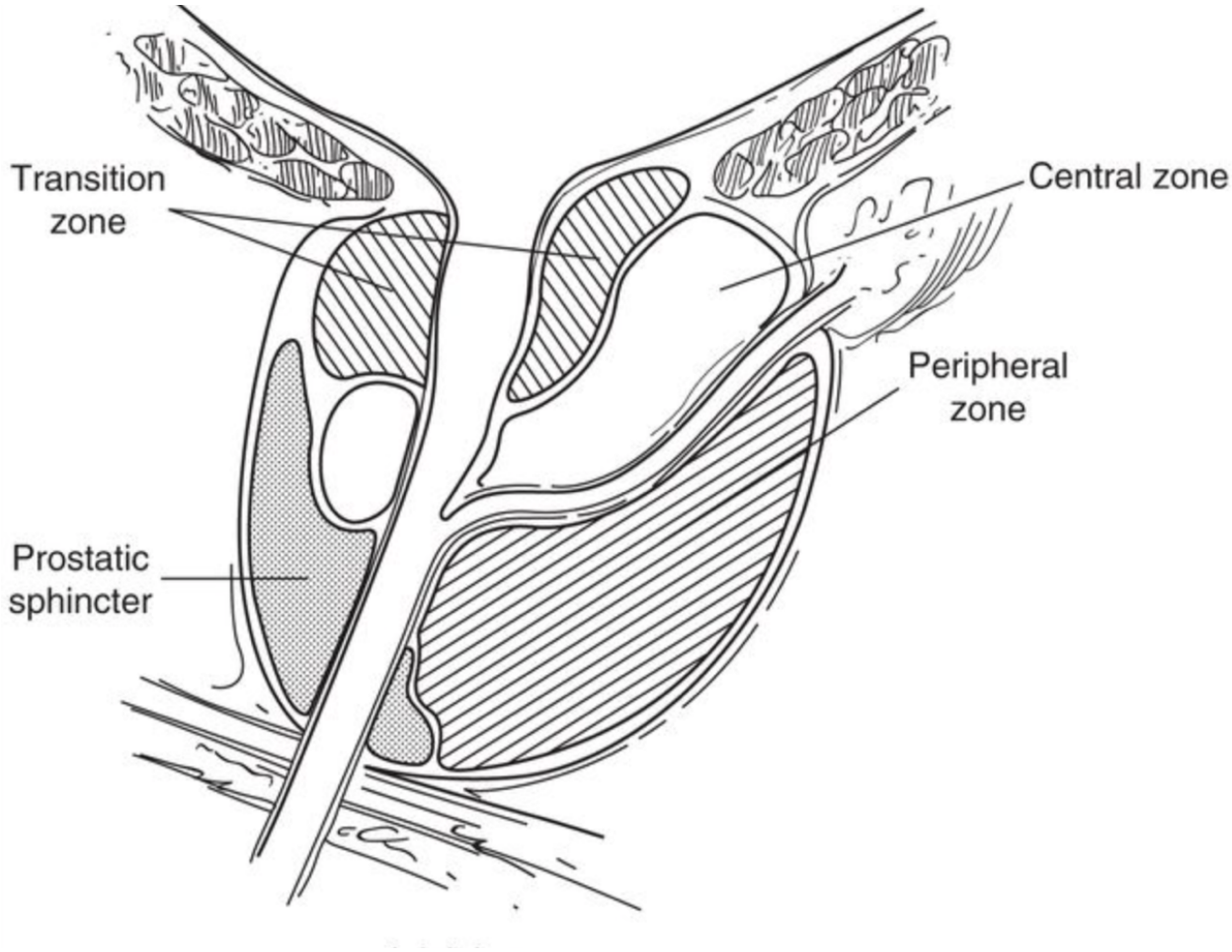

Figure 1-1. Zones of the human prostate.

The human prostate consists of the 3 histological zones: the peripheral zone, the transition zone and the central zone. Most cancer arises from the peripheral zone. Adapted from Ittmann M. (2018). Anatomy and Histology of the Human and Murine Prostate. *Cold Spring Harbor perspectives in medicine*, *8*(5), a030346. https://doi.org/10.1101/cshperspect.a030346. Permission received from Copyright © 2022 by Cold Spring Harbor Laboratory Press

The prostate glandular epithelium is composed of acini and ducts which are lined by three types of cells: luminal epithelial cells, basal epithelial cells, and neuroendocrine cells. Luminal cells are located on the luminal side of the glands and are specialized cells that synthesize and secrete prostate-specific antigen (PSA), which contribute to the formation of the luminal fluid [1, 6]. Luminal cells are terminally differentiated cells that express differentiation markers such as the androgen receptor (AR) and PSA. In contrast, basal cells are proliferating cells adjacent to the basement membrane that do not express AR and PSA, and are believed to play a critical role in maintaining ductal integrity and proper differentiation of luminal cells [7, 8]. Although evidence pinpointing to both basal cells [9] and luminal cells [10] as the cells of origin for prostate cancer has been discovered, the question of the origin of prostate cancer remains under debate. While basal and luminal cells constitute the vast majority of the epithelium in human prostate, neuroendocrine cells represent about 1% of the total epithelial population [7]. The neuroendocrine cells are scattered amongst the more abundant other two cell types, and can be identified using antibodies against markers of neuroendocrine differentiation such as neuron-specific enolase (NSE), chromogranin A (CgA) and synaptophysin (SYN). While the contribution of neuroendocrine cells in prostate cancer initiation is believed to be very minimal and their function in benign prostate remains largely unknown [7, 11], neuroendocrine cells are involved in the development of advanced prostate cancer [12, 13]. Indeed, tumors receiving androgen-deprivation therapy (ADT) eventually progress to an androgen resistant state known as castration resistant prostate cancer (CRPC). Neuroendocrine differentiation may arise in patients with CRPC, leading to a more lethal neuroendocrine prostate cancer (NEPC) [12, 13]. NEPC is an aggressive variant of prostate cancer and patients with this form of the disease are more likely to develop distant

metastases [12, 13]. NEPC still lacks effective diagnostic and therapeutic interventions, and patients diagnosed with NEPC generally survive less than year following diagnosis [13, 14].

1.1.2. Prostate cancer epidemiology

Prostate cancer is the second most common solid tumor in men worldwide and the fifth cause of cancer-related mortality [15]. In the year 2020, there was an estimated 1,41 million new cases of prostate cancer, which just a small 20,000 cases short from the most commonly diagnosed cancer (lung cancer), and an estimated 375 304 deaths worldwide due to prostate cancer [15]. More specifically, recent analyses from the Canadian Cancer Society suggest that 1 in 7 Canadian men will be diagnosed with prostate cancer in their lifetime, and 1 in 29 will die from the disease [16]. In the past few decades, there has been some fluctuations in prostate cancer incidence in Canada, starting with a dramatic increase in the early 1990s followed by several waves of increasing and decreasing incidence until 2015 [17]. More precisely, between the year of 1992 to 2011, the incidence rate of prostate cancer in Canada gradually increased, peaking at 19,325 cases in 2011, and then falling back down to 15,510 cases in 2015 [16]. The incidence rate of the disease has been relatively stable since 2015 and are expected to remain constant in 2022. Furthermore, mortality rates related to prostate cancer have been consistently declining in Canada since the year 1992, and are also expected to remain within the same trend in 2022 [17].

The unusual pattern in prostate cancer incidence can be mainly accredited to the changes in population-based testing practices. For instance, PSA testing became available in Canada in 1986 and was widely used by the early 1990s, which is believed to have played a major role in the peak of prostate cancer incidence through the 1990s and early 2000s [16, 18]. Of note, PSA-based screening has been associated with a high risk of overdiagnosis. There is currently an ongoing debated surrounding the cost versus the benefits of PSA screening. On one side, it is believed that

PSA screening should be reduced due to the fact that a large number of men with nonaggressive forms of the disease have been over-diagnosed [17]. Over-diagnosis may lead patients to seek treatment, which they do not actually require, and may hinder their quality of life (*i.e.*, castration). On the flip side, it is argued that reducing PSA-screening will lead to an increase in diagnosis of aggressive prostate cancers because of a reduction in early detection of the disease [17, 19].

On the other hand, the decrease in mortality rates related to prostate cancer over the past few decades can be attributed to the improvement in treatment modalities and earlier diagnosis. Altogether, the increasingly effective diagnostic tools for prostate cancer combined with the improvement of patient monitoring and disease surveillance and treatment has contributed to an elevated number of diagnoses while also decreasing the number of prostate cancer-related deaths. It is important to note that in most cases, prostate cancer follows a slow, indolent progress and can be effectively managed following an early diagnosis. However, in some cases the disease can become very aggressive and lethal, highlighting the need for a better understanding of disease progression at the molecular level [16-18].

1.1.3. Prostate cancer risk factors

As is the case with most other cancers, establishing the exact cause for prostate cancer initiation in men has been highly challenging. Certain predispositions, behaviours, conditions, or substances can affect a man's risk of developing prostate cancer. Epidemiological studies have pinpointed several different factors that increase a man's chance of getting prostate cancer, the most established ones being family history, genetic factors, age, ethnicity and diet and lifestyle factors.

1.1.3.1. Family history

Family history has been a focus in epidemiological studies relating to prostate cancer incidence since as early as the 1960s [20], and is now considered one of the most established risk factors for the disease. Prostate cancer is one of the most heritable cancers. Indeed, men with a close relative such as a father or a brother that has been diagnosed with prostate cancer have a two- to four-fold greater risk of developing the disease themselves [21]. Importantly, the relative risk increases according to the number of affected family members, their degree of relatedness, and the age at which they were affected [22, 23]. For example, men with a father diagnosed with prostate cancer before the age of 60 have a 20% chance of developing prostate cancer while men with a brother diagnosed before the age of 60 have a 25% chance of developing the disease, compared to an 8% chance for men with no family history of the disease [24, 25]. Furthermore, men with 3 or more affected male relatives have a 35-45% chance of developing prostate cancer [25]. Interestingly, studies have reported an increased prostate cancer risk in men with first-degree female relatives who had breast cancer. For instance, Ren *et al.* reported that men with a first-degree family history of breast cancer have a 28% chance of developing prostate cancer [26], reinforcing the importance of family of breast cancer in prostate cancer risk.

1.1.3.2. Genetic factors

There are three different phenotypes in which prostate cancer can be classified: sporadic, which refers to prostate cancer occurring in a man with no family history of the disease, familial, which is defined as a cancer in men with a first-degree relative or more affected by the disease, or hereditary, which represents a subset of familial prostate cancer that show a pattern of Mendelian inheritance of a susceptibility gene [20]. Genome-wide association studies (GWAS) have identified around 170 susceptibility loci for prostate cancer [27] and more than 180 independent

single nucleotide polymorphisms (SNPs) associated with prostate cancer risk [21]. Moreover, GWAS have uncovered several prostate cancer-related genes, with the vast majority showing a dominant autosomal inheritance pattern [28]. Indeed, inherited gene mutations are often found in DNA damage repair genes (DDR) such as *BRCA1*, *BRCA2*, *CHEK2*, *ATM*, and *PALB2* as well as in DNA mismatch repair genes (MMR) such as *MLH1*, *MSH2*, *MSH6*, and *PMS2*, and are involved in prostate cancer initiation and development [29, 30]. Interestingly, there is strong evidence that men with CRPC with germline mutations in DDR genes respond more positively to DNA-damaging therapies such as PARP inhibitors [31, 32] and platinum-based chemotherapy [32, 33]. Nonetheless, the clinical significance of mutations in many prostate cancer genes remains unclear.

1.1.3.3. Age

Prostate cancer is generally considered a disease of the elderly, with a median age of presentation of 66 years [34]. Indeed, the incidence rate of prostate cancer increases with age, and about 60% of cases are diagnoses in men over the age of 65. Interestingly, only 1 in 350 men worldwide under the age of 50 will be diagnosed with prostate cancer, while 1 in 52 men will be diagnosed with the disease between the ages of 50 to 59 years [34], highlighting the significant role of age in the incidence of the prostate cancer. On some rare occasion, prostate cancer is diagnosed in men well below the age of 50 years. For instance, Gupta *et al*. reported one of the youngest cases of prostate cancer at the age only 28 years [35]. Early onset prostate cancer is considered to be clinically different from prostate cancer diagnosed at an old age, with significantly less differentiation of the disease, but higher risk of lethality [35]. All things considered; age represents one of the most significant risk factors for prostate cancer.

1.1.3.4. Ethnicity

The incidence of prostate cancer has a significantly disproportionate distribution across different racial groups. Namely, in the United States, the incidence of prostate cancer in African-American men in is twice as high as Caucasian men and four times higher than Asian-American men [36]. Moreover, men of African ancestry are more likely to have an aggressive form of the disease than Caucasian men, and they tend to present with a more advanced or metastatic stage of the disease at the time of diagnosis [37]. The reason behind the disparities in the diagnosis and survival between these ethnic groups remain unclear, but are likely multifactorial, including a combination of different genetic susceptibility [38], socioeconomic factors and access to healthcare [39], and environmental factors (*e.g.*, dietary intake) [40].

1.1.3.5. Diet and lifestyle factors

Globally, a wide variation of prostate cancer incidence exists between different populations and regions. Indeed, higher incidence rate of prostate cancer is found in Northern America, Europe, and Oceania, while lower incidence rates are found in Africa and Asia [34]. Interestingly, an epidemiological study of Japanese immigrants in the United States found that incidence rate of prostate cancer is 4-fold higher in US-born Japanese than in Japanese living in their homeland, suggesting an important role of environmental factors in the etiology of the disease [41]. A variety of diet and lifestyle factors such as obesity, smoking, exercising, and diet have been studied with respect to prostate cancer risk. For example, several epidemiological studies suggest that obesity is an independent predictor of prostate cancer and is associated with the progression of the disease to an advanced stage [42]. Furthermore, smoking tobacco has been identified as a significant risk factor for cancer-related mortality and recurrence [43], while exercising has been found to reduce prostate cancer risks [44].

Numerous studies repeatedly show that dietary fat intake is associated with prostate cancer risk and induces more rapid prostate cancer growth. For example, Labbé *et al.* demonstrated that a high saturated fat consumption increases disease progression in a prostate cancer mouse model overexpressing the c-*MYC* transgene [45].

Conversely, certain types of food have been found to have beneficial effects with regards to prostate cancer risk. Vegetables such as broccoli, cauliflower, cabbage, kale, brussels sprouts, mustard greens and chard greens are believed to reduce cancer cell proliferation and promote apoptosis due to detoxification of carcinogenic compounds with metabolites such as isothiocyanates and indoles [46]. Several studies have also shown that consumption of tomato products reduces the risk of developing prostate cancer due to the antioxidant lycopene which is believed to inhibit prostate cancer growth and metastasis [47, 48].

Although the role of diet in prostate cancer development and progression to an aggressive disease has been extensively studied in clinical studies and preclinical studies, the underlying metabolic mechanisms responsible for the impact of dietary fat on prostate cancer remain unclear. Considering that out of the above-mentioned risk factors diet is the only modifiable one, a better understanding of the link between diet and disease progression is of great relevance for prevention and potential treatment of prostate cancer.

1.1.4. Prostate cancer screening and diagnosis

There are two commonly used methods for prostate cancer screening: the digital rectal examen (DRE) and the PSA blood test. A DRE is a test performed by a physician during which he inserts a lubricated finger into the rectum and feels the surface of the prostate for any irregularities. During a DRE, the physician assesses the posterior aspect of the peripheral zone. Although the majority of carcinomas arise from the peripheral zone, they may also develop in the transition or

central zones, which might go unnoticed by the physician. Given the fact that a DRE is not highly precise and that not every doctor has the expertise to perform the exam, it does not often detect prostate cancer at early stages [49]. PSA is a protein released by prostate tissue that is found in the blood. Levels of PSA can be raised if there is abnormal activity in the prostate such as prostate cancer, BPH, and prostatitis [50]. Although PSA testing is useful for detecting prostate cancer at early stages of the disease, controversy surrounding the use of this method for screening in people without symptoms exists based on the fact that it may identify very slow-growing prostate cancer that would not pose a threat to someone's life. Subsequently, this may lead to overdiagnosis and overtreatment, and cause side effects affecting the patient's quality of life [50]. Importantly, if a DRE or PSA test identifies an abnormality, further testing such as a magnetic resonance imaging (MRI) and a biopsy will be used to make a definitive diagnosis of prostate adenocarcinoma [51].

1.1.5. Staging and grading of prostate cancer

Tumor staging and grading are used to describe the growth and spread as well as the histology and cellular changes of cancers, which serves as the starting point for patient care in clinical oncology. Prostate cancer stages, which refers to the extent of the disease spread, are most commonly established using the tumor-node-metastasis (TNM) system developed by the American Joint Committee on Cancer (AJCC). Using this system, cancers are categorized based on tumor size and local growth (T), extend of lymph node metastases (N), and occurrence of distance metastases (M) [52]. The results of the TNM assessment are combined to determine the stage of the disease, which can be anywhere from stage I, referring to a cancer confined to the prostate, to stage IV where there is evidence of distant metastasis beyond prostate tissue [53]. Cancer grading is used by physicians to describe the histology and pathology of cancer compared to normal tissue in order to assess the aggressiveness of the disease and institute a line of treatment.

Grading for prostate cancer is established using the Gleason scoring system, which classifies tumors based on glandular architecture and cellular cytomorphology of the prostate tissue as seen under a microscope [52]. Pathologists report both a primary and secondary grades, with the primary grade being the most common histological grade and the second one representing the second most common grade of the specimen. The primary and secondary grades are assigned based on the degree of differentiation of the cells and the pattern of cell growth.

Specifically, if the cancer cells are well differentiated, they are less likely to grow and spread quickly, and will be given a low grade (1 to 3), whereas if the cancer cells are poorly differentiated and are more likely to spread quickly, a high grade will be assigned (4 or 5) [54]. In other words, the more the cancer cells look, behave, and arrange like normal cells the lower the grade number that will be assigned. The primary and secondary grade are subsequently added to come up with an overall score between 6 to 10 [54].

1.1.6. Current prostate cancer treatments

Several prostate cancer treatments have been developed to offer the best management option for patients based on the stage and aggressiveness of their disease as well as the patients' preferences and overall health, including the following:

1.1.6.1. Active surveillance

Since it was first described in 2002 [55], active surveillance was shown to be both safe and effective by many cohort studies [56-58] and has now become a standard of care for patients with low-risk prostate cancer. Active surveillance is primarily used in order to delay cancer treatment and offers the benefits of preservation of quality of life for the patient, while assuring that effective therapy will be used if required. Normally, active surveillance involves long-term follow-up with

evaluation of PSA levels, imaging, and biopsy, allowing for appropriate risk reclassification and subsequent selection of future intervention methods if necessary [59].

1.1.6.2. Surgery

The surgical line of treatment for prostate cancer involves the removal of the prostate and some surrounding lymph nodes during an operation. Many different types of surgeries have been developed for management of prostate cancer depending on the stage of the disease: 1) Radical (open) prostatectomy involves the removal of the entire prostate and the seminal vesicles as well as some surroundings lymph nodes, and is it used for treatment of localized prostate cancer. This type of surgery may include the risk of affecting sexual function and cause urinary incontinence [60]. 2) Robotic (laparoscopic) prostatectomy is a less invasive surgery than the radical prostatectomy involving the removal of the prostate gland, and it is also used to treat local prostate cancer. In general, this operation causes less pain and may shorten the recovery period, however, the side effects on sexual and urinary functions are similar to that of the radical prostatectomy [60]. 3) Bilateral orchiectomy, also called total orchiectomy, involves the removal of both testicles and is used to treat metastatic prostate cancer. The goal of this operation is to remove the main source of testosterone production, which was reported by Huggins & Hodges to increase metastatic prostate cancer over 80 years ago [61] and is now known as a main source for driving prostate cancer growth. The removal of the testicles may cause some negative psychological effects on men such as the phantom syndrome as well as uncomfortable feelings such burning or electric-shock-like sensations [62]. The use of bilateral orchiectomy has been on the decline since the 1990's and early 2000's treatment [63, 64], mainly due to the introduction of chemical castration, which is now more commonly used as a line of treatment [65]. Interestingly, it has recently been shown that orchiectomy may carry certain advantages over chemical castration, including lower rates of some

adverse side effects and reduced costs over long-term follow up [66, 67], suggesting that orchiectomy might be an underutilized, cost-effective treatment for prostate cancer patients.

1.1.6.3. Radiation therapy

Radiation therapy usually consist of a regimen of a specific number of treatments given over a set period of time during which high-energy rays are used to destroy cancer cells. The most common type of radiation treatment is the external-bean radiation therapy (EBRT), during which a machine located outside the body is used to focus a beam of x-rays on the area where the cancer is located. According to the American Society for Radiation Oncology, EBRT may be used for people with early-stage low-risk to intermediate-risk prostate cancer [68]. Intensity-modulated radiation therapy (IMRT) is a type of external-beam radiation therapy that uses CT scans to gather information about the size, shape, and location of the prostate cancer before administrating x-rays. With this technique, how much radiation is required to destroy the cancer cells can be determined ahead of time and directed directly at the disease area without damaging nearby organs. Another type of radiation treatment is brachytherapy, or internal radiation therapy, which involves the insertion of radioactive sources (seeds) directly into the prostate that will give off radiation just around the areas where they are inserted. Treatment may be given as low-dose-rate seeds, which may be left in the prostate permanently or as high-dose-rate seeds, which are usually left into the body for less than 30 min, and it is usually used for early-stage prostate cancer [69].

Recently, new radioactive substances have been approved for radiation therapy in advanced stages of prostate cancer including radium-223 dichloride (^{223}Ra) and lutetium Lu 177 vipivotide tetraxetan (^{177}Lu-PSMA-617). ^{223}Ra is an alpha-emitting radionucleotide that mimics calcium to form complexes with hydroxyapatite, resulting in its distribution to locations within the skeleton that metabolize calcium during bone creation, consequently targeting bone metastases [70], and it

is the first alpha-emitting radiopharmaceutical approved for treatment of CRPC with bone metastases and absence of visceral concerns [71]. Notably, ^{223}Ra was shown to have a favorable safety profile with minimal toxicity in phase 1 and 2 clinical studies involving patients with bone metastases [72, 73], while a phase 3 clinical study demonstrated a beneficial effect of the radionucleotide on overall survival rate, with a 30% reduction in the risk of death in patients with CRPC and bone metastases compared to placebo [74]. ^{177}Lu-PSMA-617 is a radioligand therapeutic agent that has been developed to target a specific molecule called prostate-specific membrane antigen (PSMA) that is highly expressed in cancer cells, and therefore delivers radiation directly to the PSMA-positive cancer cells [75]. The radioligand has now been approved by the FDA in June 2021 for the treatment of metastatic CRPC (mCRPC).

1.1.6.4. Hormonal therapy

Prostate cancer growth is known to be driven by male sex hormones called androgens, the most common one being testosterone. Hormonal therapy, also called androgen-deprivation therapy (ADT), is used to lower testosterone levels in the body and ultimately slow down prostate cancer growth. Luteinizing hormone-releasing hormone (LHRH) agonist and antagonist, also called gonadotropin-releasing hormone (GnRH) agonist and antagonist, have revolutionized the treatment of advanced prostate cancer by giving an alternative to surgical castration. LHRH agonist work by downregulating the GnRH receptors in the pituitary gland, herby decreasing the release of luteinizing hormone and testosterone, while LHRH antagonist work by directly inhibiting the AR receptor in the pituitary gland [76]. Although ADT has become commonly used as a therapeutic option for advanced prostate cancer, it is important to note that is comes with its lot of potential side effects, including hot flashes, fatigue, metabolic dysfunction, testosterone surges, and increased risk of cardiovascular disease [76]. Moreover, insufficiency of ADT over

time often leads to patients falling into relapse and developing mCRPC due to several mechanisms converging mostly on the AR axis. When this is the case, second-generation AR-targeted therapies may be used to overcome resistance and block androgen biosynthesis in CRPC, mCRPC, and metastatic castration-sensitive prostate cancer (mCSPC). These include the AR-inhibitors apalutamide (CRPC and mCSPC), darolutamide (CRPC), and enzalutamide (CRPC, mCRPC, mCSPC). Furthermore, abiraterone acetate, an androgen synthesis inhibitor which targets the enzyme CYP17A1, may also be used to stop adrenal glands and prostate cancer cells from producing testosterone in patients with mCRPC [77].

1.1.6.5. Chemotherapy

Chemotherapy refers to the use of drugs to destroy cancers cells by keeping them from growing and dividing, and it is usually the form of treatment used when patients develop resistance to ADT and second-generation AR-targeted therapies. Thus, chemotherapy is used to treat patients with advanced CRPC and CSPC. There are several standard drugs used for prostate cancer, and the most common one is docetaxel, which is a taxane that binds tubulin and stabilizes microtubules, inhibiting cell mitosis and leading to cancer cell apoptosis [78]. Cabazitaxel, which is microtubule inhibitor, is often used in patients who have been previously treated for mCRPC with docetaxel and have developed resistance to that drug [79]. The side effects of chemotherapy vary largely depending on the individual and the type of chemotherapy received, but oftentimes include fatigue, soreness, pain, nausea, vomiting, appetite loss, and hair loss.

1.1.6.6. Immunotherapy

Immunotherapy is a form of treatment designed to boost the body's natural defenses to fight the cancer by improving or restoring immune function. There are currently only two FDA-approved prostate cancer immunotherapies: sipuleucel-T (Provenge) and Pembrolizumab. For

people with mCRPC, vaccine therapy with sipuleucel-T may be an option. When this treatment is used, blood is first removed from the patient in a process called leukapheresis, autologous peripheral-blood mononuclear cells are separated from the blood sample and activated with a recombinant fusion protein (PA2024), and the cells are then put back into the patient where they may now actively recognize and destroy prostate cancer cells [80]. Given the fact that sipuleucel-T does not lead to lower PSA levels nor shrinking of the tumor, it may be hard to assess the effectiveness of the treatment. However, results from clinical trials have demonstrated that the use of sipuleucel-T prolonged overall survival by 4 months among men with mCRPC [80].

Immune check point inhibitors targeting T-cell molecules such as T-lymphocyte-associated protein 4 (CTL-4), programmed cell death protein 1 (PD-1), and programmed cell death protein ligand 1 (PDL-1) have recently emerged as therapies with durable responses across solid tumors [81-83]. However, this type of treatment has proven difficult for prostate cancer due to low T-cell infiltration, making it particularly resistant to immune directed therapies. Recent studies have demonstrated that a subset of pre-treated mCRPC patients respond to anti-PD-1/PDL-1 therapy, although this subset of patient represents the minority of patients (4%-20%) [84-86]. Nonetheless, Pembrolizumab, an immune checkpoint inhibitor targeting PD-1, is used after all other treatment options are exhausted. Common side effects of immunotherapy include skin reactions, diarrhea, flu-like symptoms, and weight changes.

1.1.6.7. PARP inhibitors

Poly-ADP ribose polymerase (PARP) inhibitors exploit what is known as synthetic lethality, in which two defects combined become lethal to a cell. PARP inhibitors target PARP enzymes, which are a family of enzymes that catalyze the transfer of ADP-ribose to target proteins. PARP enzymes play key roles in various cellular processes including transcription, replication,

and DNA repair [87]. As of May 2020, the FDA approved the PARP inhibitors olaparib (Lynparza) and rucaparib (Rubraca) for the treatment of prostate cancer patients. Specifically, olaparib has been approved for the treatment of mCRPC patients with homologous recombination repair gene mutations who have progressed following treatment with enzalutamide or abiraterone [87]. Rucaparib has been approved for the treatment of mCRPC patients with *BRCA1* or *BRCA2* mutations who have already been treated with ADT and chemotherapy [87]. Although not yet FDA approved, the PARP inhibitors niraparib has recently showed promising potential in men with mCRPC with DNA repair anomalies. Interim results from an ongoing clinical trial have shown that niraparib achieved a composite response rate of 65% in patients with *BRCA* mutations [88], suggesting that PARP inhibition through niraparib may soon play an important role in treatment of mCRPC patients with DNA repair mutations. Side effects of PARP inhibitors may include side effects such as fatigue, headaches and dizziness, and indigestion.

1.1.7. Clinical challenges and limitations to prostate cancer care

Despite the major progress in prostate cancer treatment modalities and survival rates in the past decades, some limitations to prostate cancer care still exist and contribute to the disease being projected as one of the leading cause of cancer-related mortality in Canadian men in 2022 [17]. One of the main clinical challenges to prostate cancer care is the acquired resistance seen manly in patients treated with ADT and AR-targeted therapy. Indeed, in many cases, deprivation of androgens initially reduces progression of prostate cancer, however, acquired resistance will develop over time and lead to mCRPC, a much more lethal form of the disease. A better understanding of the underlying mechanism driving prostate cancer to an aggressive, lethal stage could potentially leads to the development of new therapeutic strategies. Another major limitation to prostate cancer care is the lack of tools for disease stratification (indolent vs. aggressive), which

has a negative impact on accurate diagnostic determination and often leads to mismanagement of prostate cancer patients (*i.e.*, overtreatment of indolent tumors). Consequently, the development of new biomarkers for different stages of prostate cancer would increase our ability to distinguish between the indolent and aggressive forms of the disease, improving prostate cancer management.

1.2. Heterogeneity of prostate cancer and the role of MYC

1.2.1. Molecular subtypes of prostate cancer

Prostate cancer is driven by multiple genomic alterations, with distinct patterns and clinical implications. There is substantial heterogeneity among primary prostate cancers, which is evident in the spectrum of molecular alterations and their variable clinical course. Over time, an increase in the number and the severity of genomic alterations adds molecular complexity and is associated with progression of prostate cancer to a metastatic disease. Using molecular and genetic profiles to define biologically relevant categories of prostate cancer allows molecular subtyping of the disease [89, 90]. Thus, molecular subtypes of prostate cancer classify tumors based on their underlying genomic alterations and gene expression signature which over the course of the progression of the disease.

Prostate cancer can be classified into (1) clinically localized, treatment naïve prostate cancer, (2) aggressive metastatic but, hormone sensitive prostate cancer, and (3) lethal, ADT insensitive, CRPC (Figure 1-2) [89]. Clinically localized prostate cancer is defined by specific genomic alterations that occur in the early stage of the disease and may be classified in subclasses. These subclasses include the ETS positive subtypes defined by TMPRSS2-ERG fusion (40–50% of cases) [91, 92], TMPRSS-ETV1 fusion (5–10% of cases) [92, 93] and TMPRSS-ETV4 and -ETV5 (1-5% of cases) [94, 95] as well as the ETS-negative subtypes defined by SPOP mutations (6–15% of cases) [96] and FOXA1 mutations (4% of cases) [90]. Of note, *FOXA1* has been found

to be much more frequently mutated in a cohort of Chinese primary prostate cancer patients (41%) compared to the TCGA cohort (4%), which suggests that there may be ethnicity-specific patterns with regards to mutation frequency of *FOXA1* [97].

Acquisition of additional molecular alterations leads to aggressive, metastatic prostate cancer. Some of the most common genomic alterations in advanced, metastatic prostate cancer include loss of function of the tumor suppressor PTEN (40–60% of cases), loss of function of the tumor suppressor TP53 (40–60% of cases), loss of function of the tumor suppressor RB1 (28% of cases), and amplification of MYC (37% of cases), all of which are predisposed to ETS-fusion positive subclasses [90]. Of note, MYC amplification is also found in 10% of localized prostate cancer [90]. Common molecular alterations that are restricted to the ETS-negative subclasses include deletion of CDH1 (5-10% of cases) [90, 98], and SPINK1 overexpression (5–10% of cases) [90]. After the initiation of ADT for localized or metastatic disease, some patients invariably progress towards CRPC, which can be divided in distinct subtypes. Genomic alterations to the AR are the most significant alterations observed in CRPC (60% of cases) and may include AR amplification, AR mutations, AR splice variants, or other alterations resulting in ligand-independent AR activation [99, 100]. CRPC also shows a high prevalence of alterations in DDR genes including BRCA1 (2% of cases), BRCA2 (10% of cases), ATM (11% of cases), CDK12 (11% of cases), and MSH2 (3% of cases) [90, 101]. Although alterations of these genes also occur in primary prostate cancer, enrichment of these mutations in CRPC implicates them as drivers of

the CRPC phenotype [90, 101]. AR-indifferent CRPC subtypes have also been established, including NEPC (10-20% of cases) [102].

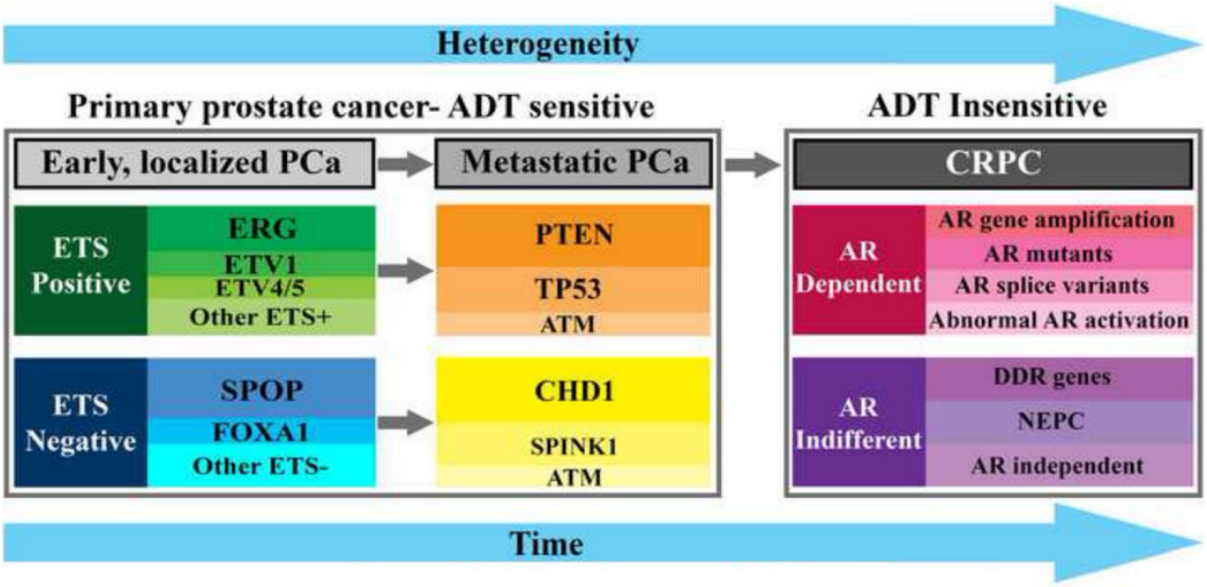

Figure 1-2. Classification of prostate cancer according to defined molecular subtypes.

Adapted from Arora & Barbieri (2018) [65]. Used with permission from Springer Nature with RightsLink®. License number 5351170754613

1.2.2. MYC in prostate cancer

The proto-oncogene c-*MYC (MYC)* has been implicated in many different types of cancer. MYC functions has a transcription factor that coordinates many biological processes such as energy metabolism and cellular proliferation [103]. In prostate cancer, MYC-overexpression is found in 10% of primary tumors and 37% of metastatic tumors and is associated with poor overall survival [104-107]. Gain of chromosome 8q and focal amplification of 8q24.21 are frequent events in primary prostate cancer linked to MYC-amplification [108]. Overexpression of MYC in prostate cancer has a significant impact on cell metabolism due to the fact that it induces a global metabolic reprograming, which in turn supports the survival and growth of cancer cells [109, 110]. Importantly, lifestyle factors such as diet may amplify the MYC transcriptional program. Indeed, Labbé *et al*. demonstrated that a diet rich in saturated fat promotes MYC-driven transcriptional

programs, even in a premalignant condition such a prostatic intraepithelial neoplasia (PIN), which highlights the importance of MYC even in the absence of genomic alterations [45]. Further, MYC overexpression in normal luminal cells of murine prostate is sufficient to initiate prostate cancer, indicating the key role of MYC in driving prostate cancer initiation [111]. Moreover, MYC overexpression has been shown to diminish the canonical AR transcriptional program and alter the AR cistrome [45]. Critically, Qiu and Boufaied *et al*. showed MYC overexpression results in the establishment of a corrupted AR transcriptional program in a murine model of prostate cancer [45]. They further showed that patients with mCRPC characterized by MYC-overexpression and low AR activity are more likely to fail to first-line next-generation AR inhibitors (*i.e*., enzalutamide or abiraterone acetate) [45], highlighting the profound impact of MYC overexpression in prostate cancer progression and treatment resistance.

1.2.3. An *in vivo* model of MYC-driven prostate cancer

A transgenic model that overexpressed human MYC in the prostate was designed by Ellwood and colleagues [111]. Specifically, they designed Lo-MYC transgenic mice and Hi-MYC transgenic mice. Lo-MYC mice express human MYC under the control of the probasin promoter. Critically, lo-MYC mice express low levels of MYC expression at 1-2 weeks of age, and MYC gene expression increases along with androgen levels as the mice mature from 4-8 weeks of age [111]. On the other hand, Hi-MYC mice express human MYC under the control of the ARR_2/probasin promoter which contains two additional androgen response elements (AREs), thus enhancing the level of MYC expression overall [111]. Importantly, Ellwood and colleagues demonstrated that MYC-overexpression results in the development of PIN in mouse as early as 2 weeks of age in Hi-MYC mice. This was largely seen in the dorsolateral and ventral lobes and eventually progressed to locally invasive adenocarcinoma at essentially 100% penetrance [111].

Since its introduction in 2003, the transgenic mouse model of MYC-driven prostate cancer has been used to study the role of MYC in a variety of processes, notably in cancer immunity, therapeutic response, fatty acid metabolism, and epigenetic regulation [112-115].

1.2.4. An *in vitro* model of MYC-driven prostate cancer

The MyC-CaP cell line was isolated from 16-month Hi-MYC transgenic mice [116]. Specifically, primary prostate cells were isolated from a prostate carcinoma and the MyC-CaP cell line was established from a single-cell derived clone [116]. Critically, the MyC-CaP cell line retains the expression of the human MYC transgene [116]. Moreover, the MyC-CaP cell line has no history of ADT or hormonal therapy and demonstrated androgen-dependent growth in soft agar *in vitro* and when engrafted *in vivo* in mice [116]. Importantly, the MyC-CaP cell line can easily be transfected and infected [116]. This makes the MyC-CaP cell line amenable to genome editing strategies.

1.3. Epigenetics regulation in prostate cancer initiation and development

1.3.1. Epigenetic dysregulation in prostate cancer: General introduction

In addition to genomic alterations, epigenetics dysregulation has been associated with prostate cancer progression [117, 118]. The term, "epigenetics," was first introduced in 1942 by Conrad Waddington to refer dynamic interactions between the genome and the environment that are involved in cell differentiation and development [119]. He defined epigenetics as heritable alterations in gene expression that are not due to changes to the nucleotide sequence [119]. More precisely, epigenetic modifications are reversible changes in gene expression that result from modifications of the chromatin structure and DNA accessibility without alteration of the cell's DNA sequence [120]. Epigenetic modifications can regulate gene expression patterns via different

mechanisms which alter the chromatin state such as DNA methylation, histone methylation, histone acetylation, and histone phosphorylation [121].

While normal cells regulate some of their functions through alteration of their epigenomes, environmental factors such as infection and inflammation may cause epigenetic dysregulation to arise and accumulate, and ultimately drive tumorigenesis [122]. For example, histone modifications, aberrant DNA methylation, and non-coding RNAs contribute to the initiation and progression of prostate cancer [122, 123]. Targeting epigenetic pathways is an emerging therapeutic strategy in prostate cancer, and identification of unique epigenetic patterns in prostate cancer cells such as specific DNA hypo- or hyper-methylation or expression of key epigenetic regulators could lead to the discovery of new diagnostic and prognostic biomarkers as well as targets for treatment of the disease [123].

1.3.2. DNA methylation

DNA methylation is catalyzed by DNA methyltransferases (DNMTS) enzymes, which transfer a methyl group from S-adenosylmethionine (SAM) to the fifth carbon position of cytosine residues in CpG dinucleotides. The covalent modification of DNA sites by methylation is a process which alters chromatin accessibility and defines regions of transcriptional activity, and it is involved in the regulation of diverse biological processes [124]. While regulation of DNA methylation is essential for mammalian development and differentiation for the control of gene expression and gene silencing, aberrant DNA hypermethylation in promoter regions of tumor suppressor genes or global DNA hypomethylation, contribute to the initiation and progression of a variety of cancers by leading to gene silencing or genomic instability, respectively [125, 126].

In prostate cancer, DNA hypermethylation within promoter regions of tumor-suppressor genes is the most characterized epigenetic modification, and is associated with genes related to

DNA repair, cell cycle, apoptosis, and cell adhesion [123, 127]. For example, hypermethylation of the tumor-suppressor *GSTP1* has been found in prostate cancer as well as in prostatic intraepithelial neoplasia and could be utilized as a biomarker for diagnosis given the fact that it is not present in normal prostatic tissue [128, 129]. Indeed Wu *et al*. demonstrated that GSTP1 hypermethylation in plasma, serum, and urine DNA has a higher specificity for prostate cancer diagnosis than serum PSA [130]. The tumor suppressor gene *CDKN2A* is an inhibitor of cyclin-dependent kinase and an important player in cell cycle processes. *CDKN2A* is frequently inactivated by promoter hypermethylation in many cancers including prostate cancer [131].

Moreover, suppression of *CDH1*, which plays an essential role in maintaining normal epithelial integrity, has been shown to correlate with the incidence of cancer [132]. Loss of *CHD1* in prostate cancer has been shown to results from hypermethylation of the *CDH1* promoter region, and its hypermethylation status is associated with tumor progression and poor overall survival [133, 134]. On the other hand, DNA hypomethylation, which refers to the demethylation of normally methylated CpG sites, is frequently observed in late stages of prostate cancer [135, 136]. For instance, *PLAU* and its receptor play important roles in tumor metastasis through degradation of extracellular matrix and several studies have shown a correlation between *PLAU* expression and cancer [137, 138]. The expression of *PLAU* is normally repressed by DNA methylation. In prostate cancer, the expression of *PLAU* is much higher than in benign prostatic tissue due to hypomethylation of the promoter region of the gene, leading to oncogenic effects [139].

1.3.3. Histone modifications

Histones are responsible for chromatin organization by folding DNA into the nucleus. There are four core histones (H2A, H2B, H3, H4) which all possess highly conserved c-terminal, and flexible N-terminal trails that can be modified through post-translation modifications. Histone

post-translation modifications serve to change chromatin structure, and aberrant histone modifications are correlated with dysregulation of the expression of a variety of important genes [140]. In cancer, aberrant histone modifications including histone methylation, histone acetylation, and histone phosphorylation can cause the inactivation of tumor suppressor genes or the activation of oncogenes, contributing to tumorigenesis [141].

1.3.3.1. Histone Acetylation

Histone acetylation is achieved by the introduction of an acetyl group to lysine residues in the N-terminal domain of core histones. Histone acetyltransferases (HATS) catalyze histone acetylation by the addition of an acetyl group from acetyl-CoA to the ε-amino group of a histone lysine residue, which neutralizes the positive charge of lysine and disrupts the interaction between the DNA and the histone tail, thereby activating transcription [142]. Histone deacetylases (HDACs) carry out deacetylation by removal an acetyl group from the N-terminal lysine residue of histone tails, which results in a change in chromatin conformational state from active to inactive and subsequently deactivate transcription [143]. Elevated levels of Histone H3 acetylation at specific regions of prostate cancer tumor samples was first stated by Cang *et al*. and have since been found to be elevated at AR binding regions, impacting androgen target genes expression [144]. Recently, super-enhancers, which are defined as clusters of enhancers with high H3K27 acetylation, have been identified to play key roles as oncogenic drivers in various cancers. In prostate cancer, overexpression of *ERG*, a key driver of metastasis, leads to the formation of super-enhancers and facilitates the transcriptional activity of genes associated with disease progression [145, 146].

1.3.3.2. Histone methylation

Histone methylation is achieved by the addition of one, two or three methyl groups from SAM to certain lysine or arginine residues in the N-terminal domains of core histones, and can associated with either open or closed chromatin [147]. Changes in DNA methylation status of histones have been reported to contribute to prostate cancer progression. For example, high levels of H3K4me2 are found to correlate with prostate cancer recurrence, while levels of H3K4me1, H3K9me2 and H3K9me3 are found to be decreased in prostate tumors compared to non-malignant tissues [148]. Moreover, H3K27me3 marks have been found to be enriched at promoter regions of tumor suppressor genes in metastatic prostate cancer [149]. The increased genomic distribution of H3K27m3 is due to the overexpression of *EZH2*, a histone methyltransferase frequently observed in prostate cancer. *EZH2* inhibitors have been shown to have antiproliferative effects in prostate cancer and multiple clinical trials are currently ongoing [150, 151]. Recently, histone H4K20 hypomethylation at the promoter regions of MYC regulated genes has been shown to be increased following MYC-overexpression, a feature that was exacerbated by saturated fat intake, and contribute to prostate cancer lethality [45]. Furthermore, the overexpression of histone demethylases such as of jumonji AT-rich interactive domain 1B (*JARID1B*)/*KDM5B, JARID1C/KDM5C* and jumonji D2 (*JMJD2*)/*JHDM3*/*KDM4* are frequently observed in prostate cancer and are involved in disease progression [152, 153].

1.3.3.3. Histone phosphorylation

Histone phosphorylation is catalyzed by protein kinases and is achieved by the addition of phosphate groups to serine, threonine or tyrosine residues in histone tails. In prostate cancer, H3T6 phosphorylation by the protein kinase PKCβ is key in inhibiting demethylation of H3K4me2 by LSD1 during AR-dependent gene activation [147]. Furthermore, increased levels of H3T6 as well

as H3T11 phosphorylation are positively correlated with high Gleason scores [154, 155]. Importantly, inhibition of PKN1, which is responsible for H3T11 phosphorylation, was shown to decrease prostate cancer cell proliferation [156].

1.3.4. Chromatin remodeling

Chromatin writers, erasers, readers and remodelers play crucial roles in governing chromatin structure through post-translational modifications (PTMs) [157]. Chromatin writers (*i.e.*, HATS) add PTMs to histones while chromatin erasers (*i.e.*, HDACs) remove specific PTMs from histones. Chromatin-remodeling proteins modulate DNA-histone interaction, they change chromatin conformation, and they increase or decrease the binding of functional DNA-regulating protein complexes. Chromatin readers (*i.e.*, switch/sucrose-nonfermentable; SWI/SNF)) recognize either specific PTMs or a combination of PTMs and histone variants and direct a particular transcriptional outcome. The specific recognition of PTMs such as methylation, acetylation, and phosphorylation by readers recruits various components of the nuclear signaling network to chromatin, mediating fundamental biological processes such as gene transcription, DNA replication, DNA-damaged response and chromatin remodeling [158]. Critically, readers of methylation marks bind to this PTM through an aromatic cage, typically formed by two to four aromatic residues [158]. In many complexes, the aromatic rings are positioned perpendicular to each other, surrounding the fully extended side chain of the methylated lysine or arginine, and the mono-, di- or trimethylated state is selected by the exact composition and size of the pocket [158]. For example, a small pocket size can preclude interaction with a higher methylation state owing to steric hindrance, whereas a larger pocket selects for a higher methylation state as the necessary contacts are possible only with the bulkier methylammonium group [158]. In a similar manner as readers of methylation marks, readers of phosphorylation and acetylation marks recognize specific

phosphorylation or acetylation states based on the composition and size of their binding pocket, which is driven by complex bonding activity [158]. Since the chromatin state largely dictates whether a transcription factor or other chromatin-associated proteins can access the DNA, chromatin readers, writers, eraser, and remodelers play crucial roles in regulating gene expression.

Several chromatin-modulating proteins have been found to be involved in prostate cancer progression. For instance, the bromodomain protein 4 (BRD4) is a chromatin reader which regulates gene transcription by recognizing and binding to active H3K27ac [159]. BRD4 has been reported to be involved in androgen receptor signaling and progression of prostate cancer [160, 161]. Indeed, BRD4 can promote the transcriptional activities of oncogenic factors in prostate cancer by physically interacting with the N-terminal domain of androgen receptor (AR), which is a crucial element of the AR signaling pathway [160, 161]. The SWI/SNF chromatin remodeler complex has also been shown to play a role in prostate cancer. Namely, the SWI/SNF complex is a cofactor of the AR and contributes to AR-driven prostate cancer progression [162-165]. Furthermore, the SWI/SNF complex maintains core enhancer circuitry in prostate cancer cells, and targeting the SWI/SNF complex for proteasomal degradation has been shown to reduce tumour growth in a mouse model of CRPC [166]. Moreover, chromatin remodeling factor CHD1 is recurrently deleted in primary prostate tumours. Loss of CDH1 results in a plastic epigenetic state that permits reprogramming of the AR cistrome, ultimately contributing to prostate cancer progression [167, 168].

1.3.5. Epigenetic regulation in prostate cancer: clinical implications

Targeting epigenetic regulators has been shown to be an effective way to suppress prostate cancer growth. Namely, the transcription factor *AR* is the most established therapeutic target for prostate cancer. Targeting androgen signaling via ADT is the first line of treatment for prostate

cancer. When resistance to ADT arises, second-generation anti-androgen drugs such as enzalutamide, abiraterone, apalutamide, and darolutamide are used to inhibit AR signaling [169-172]. However, while these treatments are initially effective, resistance ultimately occurs. New strategies blocking continued AR signaling are currently being investigated [173, 174]. Inhibition of the enhancer of zeste homolog 2 (EZH2) has also shown to suppress prostate cancer cell proliferation and invasion *in vivo* as well as *in vitro* [150, 175-177]. EZH2 is a critical component of the polycomb repressive complex 2 (PRC2), which is an essential chromatin modifier that represses the transcription of target genes through trimethylation of lysine 27 on histone 3 (H3K27me3) [178, 179], and has been shown to play critical roles in prostate cancer metastasis [180-182]. Different types of EZH2 inhibitors have been developed, and there are a number of clinical trials for drugs targeting EZH2 in different types of cancer that are currently ongoing. Namely, the embryonic ectoderm development protein (EED) is another component of PCR2 and is essential for the histone methyltransferase activity of PCR2 because it directly binds to H3K27me3. The EED inhibitor MAK683/EED226 is currently being evaluated in a phase 1/2 clinical trial for advanced malignancies including prostate cancer [183]. Critically, MAK683/EED226 selectively binds to the domain of EED that interacts with H3K27me3, leading to a conformational change in the EED binding pocket and preventing interactions between EED and EZH2 [183]. Another EZH2 inhibitor is CPI-1205, which is a potent, selective, and cofactor-competitive inhibitor of wild type and mutant EZH2 catalytic activity. CPI-1205 has demonstrated anti-proliferative effects in prostate cancer and is currently being evaluated in a phase 1/2 clinical trial for castration-resistant prostate cancer [184, 185]. The selective inhibitor PF-06821497, which inhibits the histone lysine methyltransferase (HMT) of EZH2 is also currently under evaluation in

a phase 1 clinical trial in patients with CRPC [185, 186]. These data suggest that inhibition of histone methyltransferases may be a promising approach to target prostate cancer progression.

Proteins of the BET bromodomain family are epigenetic readers that bind to acetylated histones through their bromodomains to affect gene transcription, and they localize at sites of enhancers of various oncogenes to promote prostate cancer tumorigenesis and progression [187]. BET proteins regulate transcription by recognizing and binding to acetylated lysine residues via their two bromodomains, BD1 and BD2 [188], and they have been linked to AR signaling activation by promoting AR-mediated chromatin accessibility [189, 190]. Numerous BET inhibitors have been developed over the past decade, many of which have demonstrated antitumor effects in prostate cancer preclinical models [191-194]. A phase 1 clinical trial investigating the BET inhibitor GSK525762 in combination with abiraterone or enzalutamide in CRPC is currently ongoing [195]. Recently, a phase 1b/2a clinical trial investigating the combination of the BET inhibitor PLX2853 with abiraterone as well as a phase 2 clinical trial combining enzalutamide with the BET inhibitor ZEN003694 have been launched, both in men with CRPC [195]. Importantly, this suggests that chromatin remodeling-related genes may be targeted to suppress prostate cancer metastasis.

Moreover, the histone acetyltransferases p300 and CBP, which are highly homologous, are known to regulate key genes in prostate cancer including AR target genes [196]. Several groups have developed inhibitors to target one or both of those histone acetyltransferases because of their role in prostate cancer. For example, Lasko *et al*. demonstrated that treatment with the catalytic inhibitor A-485 blocked AR signaling and growth of AR-dependent CRPC xenografts *in vivo* [196]. Further, Liu *et al*. demonstrated that inhibition of p300/CBP by A-485 in combination with anti-PD-L1 antibodies increased T-cell infiltration in tumors and augmented the tumor immune

response in a syngeneic model of prostate cancer [197]. Clinical trials on p300/CBP histone acetyltransferase inhibitors in prostate cancer have recently begun. Namely, a phase 1/2 clinical trial of the p300/CBP inhibitor CCS1477 in combination with abiraterone or enzalutamide as well as a phase 1 clinical trial with the p300/CBP inhibitor FT-7051 are currently ongoing, both in mCRPC patients [195]. Together, these data suggest that combining histone acetyltransferase inhibitors with immunotherapy may be a promising approach to enhance the activity of immunotherapy in prostate cancer.

Epigenetic mechanisms play a key in prostate cancer progression and targeting epigenetic-related genes has been shown to reduce prostate cancer progression and improve prostate cancer therapies. A better understanding of the specific epigenetic expression patterns that allow prostate cancer to thrive may enable the identification of potentially targetable key epigenetic regulators which support prostate cancer progression.

1.4. The development of CRISPR/Cas9 screening and its use in cancer research

1.4.1. The CRISPR system: RNA-guided defense in bacteria

The Clusters of Regulatory Interspaced Short Palindromic Repeats (CRISPRs) and their CRISPR-associated (Cas) protein are currently in the spotlight of fundamental research. The first CIRSPRs were first reported over 30 years ago [198] in *Escherichia coli* in the course of an experiment analysing the gene responsible for isozyme conversion of alkaline phosphatase. At the time, researchers lacked the tools to predict the biological function of these repetitive sequences, hence, it was not until the mid 2000s, when three independent research groups discovered sequence similarity between the spacer regions of CRISPRs and sequences of bacteriophages and plasmids [199-201], that the function of these CRISPRs as an adaptive immune system came to light. In

parallel, several genes typically located nearby the CRISPR arrays in the bacterial chromosome, which are referred to as CRISPR-associated (Cas) genes, were identified as being strictly associated with the repetitive sequences and work together to constitute an acquired immunity [202]. The immunization process of the CRISPR/Cas bacterial system begins when a bacterium is invaded with genetic elements from a phage or a plasmid. Following exposure to the foreign genetic material, short fragments of the foreign DNA are integrated into the CRIPSR spacer arrays, thereby providing a record of previous infection that enables the host to recognize and prevent future invasion [203, 204]. Subsequently, the CRISPR locus is transcribed into precursor-CRISPR transcripts which are then enzymically processed into mature CRISPR RNAs (crRNAs) that include a copy of the integrated bits of viral DNA together with a piece of the CRISPR array repeat sequence. These individual mature crRNA units then associate with a Cas protein to form a crRNA-effector complexes, which will be able to interrogate the cell looking for DNA targets that have the same sequence. Importantly, a short conserved sequence (2-5bp) known as protospacer adjacent motif (PAM) located in close proximity to the crRNA target is essential for the crRNA-Cas complex to bind to the target sequence and generate a double-strand break, resulting in the degradation of the viral DNA [205]. To summarize, the CRISPR/Cas system works as a defense mechanism allowing bacteria and archaea to respond quickly and effectively to foreign material, resembling the RNA-interference (RNAi) mechanism which serves to destroy viral RNA molecules in eukaryotes [206].

A number of CRISPR-Cas systems have been discovered since it was first identified as an immune mechanism in bacteria and they are grouped into two classes (I & II), which are subdivide into distinct types (I-VI) and 33 subtypes [207] according to the classification of CRISPR-Cas loci (**Figure 1-3**). The classification of the CRISPR-Cas system is based on Cas protein and effector

module composition. The class 1 CRISPR-Cas9 systems, which include types I, III, IV and 18 subtypes, are composed of effector modules with multiple Cas proteins that form the crRNA-Cas complex and work together in the binding and cleaving of the target sequence. More precisely, the different class 1 CRISPR-Cas9 systems can be distinguished into different types and subtypes based on differential clustering of the effector proteins Cas3 (sometimes fused to Cas2), Cas5, Cas6, Cas7, Cas8, Cas10 and Cas11 [207, 208]. On the other hand, the class II CRISPR-Cas systems which include type II, V, VI, and 17 subtypes, have a single, multi-domain Cas protein (Cas9, Cas12, or Cas13) that form the crRNA complex and combine all activities required for interference, analogous to the multi-Cas complex of class I systems. The different types and subtypes of class 2 CRISPR-Cas systems can be differentiated based on the mechanisms of pre-crRNA processing. For example, in type VI and subtype V-A, the effector protein encompasses the pre-crRNA processing RNase activity, whereas in type II and in many type V subtypes, the processing activity is performed by RNase III rather than a Cas enzyme [209, 210]. The classification of the many CRISPR-Cas systems encompasses the most abundant types and subtypes that are currently known; however, it is likely that the continued investigation of bacterial and archaeal CRISPR-Cas defense mechanisms will shine a light on new functionally and evolutionary interesting variants.

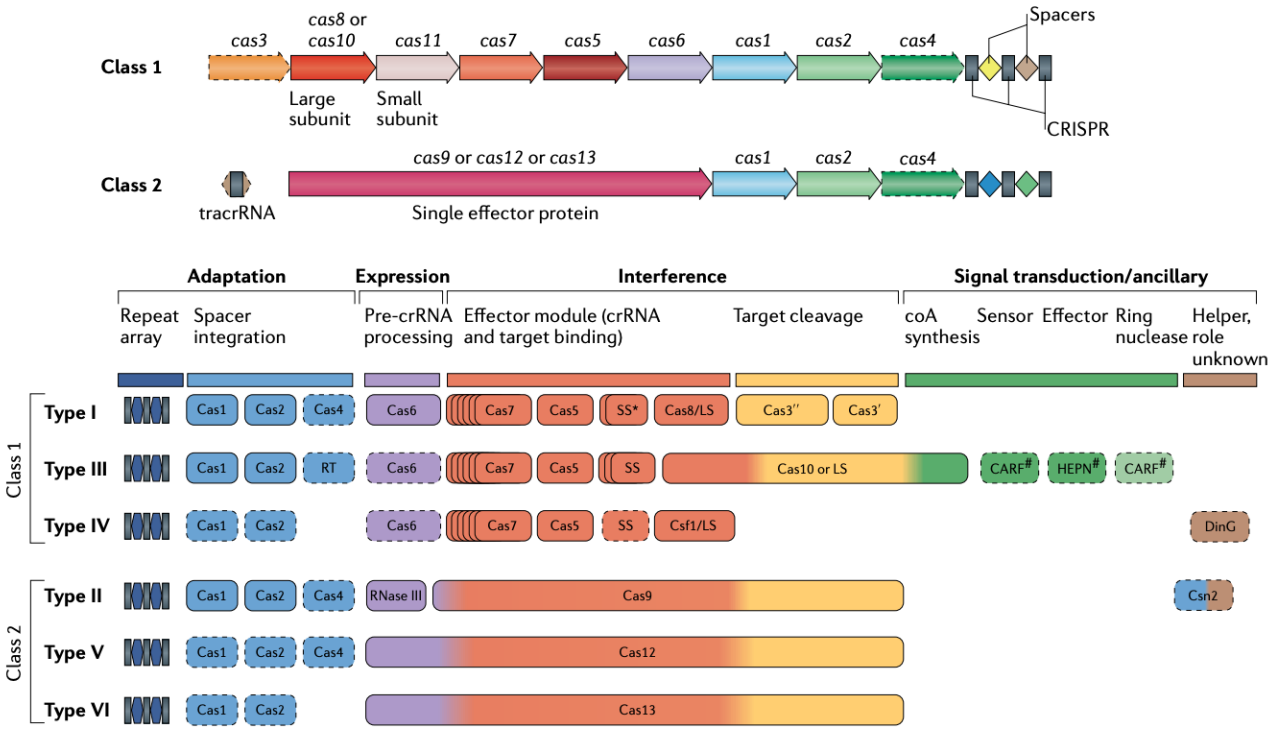

Figure 1-3. Classes of CRISPR/Cas systems and their modular organization.

Class 1 CRISPR-Cas systems have effector modules composed of multiple Cas proteins that form a crRNA-binding complex and include types I, III, and IV. Class 2 CRISPR-Cas systems have a single, multidomain crRNA-binding protein that is functionally analogous to the entire class 1 effector complex, and include types II, V, and VI. Adapted from Makarova et al. (2020) [124]. Used with permission from Springer Nature with RightsLink®. License number 5337220199481

1.4.2. The CRISPR/Cas9 technology: A revolution in genome editing

The field of genome engineering was revolutionized in 2012 when Jennifer Doudna and Emmanuelle Charpentier discovered that they could harness the function of the Cas9 endonuclease from the type II bacterial CRISPR system as a genetic editing tool [211]. Indeed, their work demonstrated that the Cas9 protein constitute of family of enzymes that can be programmed with guide RNA engineered as a single transcript to introduce site-specific double-stranded breaks in target DNA sequences. More precisely, the dual trans-activating crRNA (tracrRNA):crRNA complex was engineered as a single guide RNA (sgRNA) with the 20-nucleotide sequence at the

5’ end determining the DNA target site and the double-stranded structure at the 3’ end of the guide sequence capable of binding Cas9, creating a simple two-component system capable of targeting and cleaving any target DNA sequence adjacent to a PAM sequence. Further, by designing five different chimeric guide RNAs targeting a portion of the gene encoding the green-fluorescent protein (GFP), which all efficiently programmed Cas9 to cleave the plasmid at the correct target site, Doudna and Charpentier established that the design of chimeric guide RNAs is universally applicable [211], thereby raising the exciting possibility of developing a simple, versatile RNA-guided genome editing technology which can be used to easily delete, insert, or modify the expression of genes. Shortly after the discovery of the CRISPR/Cas9 system as a potential tool for genome engineering, three studies published in 2013 demonstrated that the new technology could be efficiently used to edit the genome of human cells including human embryonic kidney cells, chronic myelogenous leukemia cells and induced pluripotent stem cells, as well as in mouse cells [212-214]. In the following years, the CRISPR/Cas9 technology was increasingly taken advantage of in the field of genome engineering in many different areas of research. Namely, the CRISPR/Cas9 system has been shown to be potentially useful to prevent and combat antibiotic-resistant bacteria [215], for the treatment of viral infections such as HIV [216], and in preventing genetic conditions such as Duchenne Muscular Dystrophy [217]. Further, genome-wide CRISPR libraries have been constructed and used for the systematic investigation of genes associated with specific phenotypes [218] as well as for drug screening [219]. The use of CRISPR/Cas9 has also been widely explored for cancer therapy [220] and clinical trials have been initiated for genome editing in humans [221, 222]. Altogether, the numerous and continuously increasing clinical and next-generation research applications of the CRISPR/Cas9 technology indicates the robustness of the technology as a tool for correcting genetic diseases and improving cell therapies.

1.4.3. Different CRISPR/Cas 9 screening formats and designs

Over the years of exploring the different possibilities of screening offered by the CRISPR/Cas9 technology, many different screening formats and strategies have been developed and optimized. The two most widely used CRISPR screening formats are the arrayed and pooled formats. In an arrayed screen, a different sgRNA together with the other CRISPR reagents, which include an envelope plasmid and a packaging plasmid, are added to each well of a multi-well plate separately [223]. In this type of screen, the target of the sgRNA in each separate well is already known, allowing for easy correlation between phenotype to genotype. On the other hand, in the pooled screening format, a sgRNA library is synthesized and transfected into a pool of cells, introducing various genetic perturbations [224, 225]. Depending on the genetic perturbation occurring following the transfection, the cells will either be positively selected (*e.g.*, increased proliferation rate) or negatively selected (*e.g.*, decreased proliferation rate or cell death). If the cells are positively selected, it means that the genetic manipulation works in favor or the cell and allows it to survive and proliferate at a faster rate. On the other hand, if the cells are negatively selected, it means that the cells are depleted from the pool following the genetic perturbation, hinting that the targeted genomic regions are essential for cell survival and proliferation [226]. While arrayed screening allows for a clear phenotype-to-genotype correlation, pooled screening offers the advantage of being less expensive and laborious and can be used for *in vivo* studies [224].

Moreover, there are several different CRISPR/Cas9 screening strategies that can be harnessed depending on the goal of the experiment, including CRISPR knockout (CRISPR KO), CRISPR interference (CRISPRi) and CRISPR activation (CRISPRa) (**Figure 1-4**). Using the CRISPR KO strategy, an active Cas9 is used along with sgRNAs to target a site near a PAM

sequence and generate a double-stranded break in the DNA. The double-strand break will trigger the non-homologous end-joining repair (NHEJ) DNA repair mechanism to be activated. The NHEJ mechanism is a quick, error-prone process that links two DNA ends and often leads to insertions or deletions into the target site, ultimately causing frameshift mutations [227]. The CRISPR KO screens generate the complete knockout of the target genes and are thereby useful for the investigation of gene essentiality in specific cell types and for the identification of new drug targets [228]. In contrast, the CRISPRi and CRISPRa screening strategies are based on the use of a catalytically dead Cas9 (dCas9), which lacks cleaving activity but retains its ability to bind to a DNA target sequence. CRISPRi uses a dCas9 to recruit repressor domains (*e.g.*, KRAB) and targets the promoter or protein-coding region of the target gene to repress transcription, while CRISPRa uses dCas9 to recruit enhancer domains (*e.g.*, VP64 or VPR) to target promoter regions and upregulate transcription [229]. CRISPRi and CRISPRa can increase or decrease levels of gene expression respectively, and can be used to define relationships between the extent of phenotypic effects and the levels of a gene product [230].

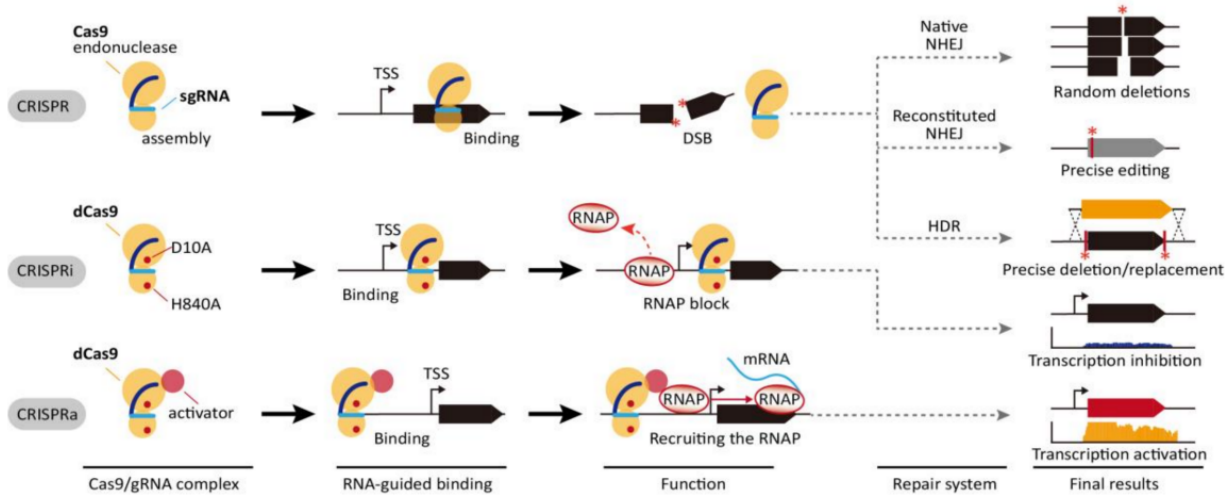

Figure 1-4. Different CRISPR/Cas9 screening strategies.

The CRISPR/Cas9 KO system (depicted CRISPR) generates double-stranded breaks in the DNA sequence and ultimately knocks out the expression of the target gene. Double-stranded breaks formed by CRISPR/Cas system can be repaired by the error prone NHEJ repair pathway, resulting in the formation of randomly sized deletions, or by the HDR repair pathway, resulting in gene deletion or replacement via homologous template. CRISPRi and CRISPRa utilize a dCas9 to recruit repressors or activators and generate knockdown or activation of the target genes, respectively. Adapted from Cho *et al*. (2018) under the terms of the Creative Commons Attribution-NonCommercial 4.0 International License as described at http://creativecommons.org/licenses/by-nc/4.0/

1.4.4. CRISPR/Cas9 screening in prostate cancer research

CRISPR/Cas9 screening has been widely applied to many areas of cancer research and has allowed the identification of various key oncogenes and new druggable targets. CRISPR/Cas9 screening have also been used in cancer to investigate synthetic lethalities and mechanisms of drug resistance and drug susceptibility. For example, Lei *et al*. identified CDK12 as being conservatively required for prostate cancer cells using an *in vitro* CRISPR/Cas9 KO screen which included sgRNAs targeting protein kinases (*i.e.,* kinome-scale CRISPR/Cas9 KO screen) [231]. They further showed that suppression of CDK12 by the covalent inhibitor THZ531 led to antiproliferative effects, highlighting the validity CDK12 as a druggable target for prostate cancer. Similarly, using an *in vitro* CRISPR/Cas9 KO screen which included sgRNAs targeting the coding

regions of the genome (*i.e.,* genome-wide CRISPR/Cas9 KO screen), Palit *et al*. demonstrated that the loss of the co-repressor *TLE3* confers resistance to the AR antagonists apalutamide and enzalutamide [232]. Along the same lines, Das *et al*. performed genome-scale CRISPRi screens in metastatic prostate cancer models to identify genes required for cellular proliferation or survival [233]. They demonstrated that *KIF4* and *WDR62* promote aggressive prostate cancer phenotype both *in vitro* and *in vivo*. Using an opposite technique, Chen *et al*. performed a genome-wide *in vitro* CRISPRa screen to identify vulnerabilities of metformin-resistant prostate cancer [234]. They discovered that the activation of many genes, including ECE1, ABCA12, BPY2, EEF1A1, RAD9A, and NIPSNAP1 contributed to *in vitro* resistance to metformin in prostate cancer cells.

One of the advantages of CRISPR/Cas9 screening is that it can readily be used for *in vivo* experiments. Thus, new potential drug targets and novel genes with oncogenic or tumor-suppressive functions can be identified in a model which more closely recapitulates tumor microenvironment. Ye *et al*., applied the genome-wide CRISPR/Cas9 KO screening strategy to investigate the effect of editing GPRC6A, a G-protein coupled receptor that is a master regulator of energy metabolism, on prostate cancer growth and progression *in vivo* [235]. Their study demonstrated that GPRC6A deficiency in a PC-3 xenograft mouse model of prostate cancer leads to significant impaired tumor growth [235], indicating a key role of GPRC6A in prostate cancer progression. Moreover, Riedel *et al*. utilized a genome-wide *in vivo* CRISPR/Cas9 KO screening strategy to investigate the role of *FOS* in prostate cancer [236]. They demonstrated that *FOS* deficiency in *PTEN*-deficient prostate cancer drives the progression of the disease.

To summarize, the CRISPR/Cas9 system has been widely used in prostate cancer research for the identification of oncogenes, tumor-suppressor genes and synthetic lethalities both *in vitro* and *in vivo*. Thus, the CRISPR/Cas9 system is a highly efficient and relatively simple tool that

may be used to identify new essential and potentially therapeutically targetable mechanisms in cancer.

1.4.5. Limitations of the CRISPR/Cas9 genome editing technology

Despite the overwhelming excitement surrounding the CRISPR/Cas9 system as a tool for genome editing, there are limitations associated with the use of this technology. The most important limitation of the system is the off-target effects resulting in non-specific cuts in the DNA, leading to unwanted gain-of-function or loss-of-function mutations, and ultimately creating false positive or false negative results, respectively [222]. Some researchers have attempted to alleviate the off-target effects by modifying the length of the sgRNAs, either by using truncated sgRNAs [237] or by adding two guanines at the 5' end [238], by delivering a purified Cas9 protein [239], or by decreasing the concentration of the Cas9 endonuclease [240]. Although these approaches have been shown to decrease off-target effects, they come with the disadvantage of reducing on target effects. Other limitations of the CRISPR/Cas9 technology include the size of the catalytic window, which is about 4-5 nucleotides, resulting in low specificity and efficiency, and the requirement of the PAM sequence for DNA cleavage, limiting the potential target sequences [241, 242]. Furthermore, as the cells are dividing during genome editing, genetic mosaicism may become a potential limitation due to the fact that daughter cells could potetially not carry the CRISPR-induced modifications [243]. Moreover, the recent significant advances in the CRISPR/Cas9 field of research introduced concerns regarding the safe and ethical use of the technology, and there is currently an ongoing debate in the scientific community on how to use this genome editing technology responsibly without hindering the benefits of potential novel discoveries [244]. Of note, despite the limitations of the CRIPSR/Cas9 system, this method of screening has been shown to outperform other existing genome-editing platforms such as Zinc-

finger nucleases (ZFNs) [245], transcription activator-like effector nucleases (TALENs) [245] and RNA interference (RNAi) [246], by providing higher screening sensitivity, higher data reproducibility, lower noise, and less off-target effects.

1.5. Research objectives

1.5.1. Rationale

Chromatin integrity and accessibility for transcriptional regulation are central features altered in prostate cancer progression. Epigenetic modifications alter chromatin structure and DNA accessibility. The proto-oncogene *MYC* is a well-known epigenetic and transcriptional regulator which controls 10-15% of the human genome [103]. Thereby, when deregulated, *MYC* is known to drive hallmarks of cancer. Notably, MYC-overexpression induces global metabolic reprograming events which support cancer cell survival and growth [247, 248]. Furthermore, MYC plays a central role in prostate cancer transcriptional reprogramming and is a key driver of prostate cancer tumorigenesis and progression. It has been shown that MYC interacts with epigenetic modifying factors such as histone acetyltransferases, histone methyltransferases, and chromatin-modifying complexes, to remodel chromatin structure and modify DNA accessibility [249]. While MYC is known to interact with epigenetic co-factors to alter chromatin accessibility, the role of epigenetic regulators in MYC-driven transcriptional reprograming which drives prostate cancer progression remains elusive.

1.5.2. Hypothesis

We hypothesize that in the context of MYC-overexpression, prostate cancer cells are dependent on the expression of key epigenetic regulators for survival and growth.

1.5.3. Objectives

1) Design and amplify custom CRISPR/Cas9 sgRNA libraries targeting epigenetic regulators;

2) Identify epigenetic dependencies in a MYC-driven prostate cancer model *in vitro*;
3) Define the molecular basis of epigenetic dependencies in MYC-driven prostate cancer.

1.5.4. Research design and methods

Our experimental design is articulated around the use of two custom CRISPR/Cas9 sgRNA KO libraries that are specifically designed to target 1,343 genes, mostly epigenetic-related and highly expressed in cancer settings, in addition to 500 positive control genes and 500 negative control genes. A murine model of MYC-driven prostate cancer referred to as the MyC-CaP cell line was used to carry out *in vitro* CRISPR/Cas9 KO screen using our two libraries. These tools allowed us to investigate the role of epigenetic modifications in the context of MYC-driven prostate cancer.

1.5.5. Contribution to the advancement of knowledge

We hope that by unrevealing the molecular basis of MYC-driven prostate cancer we can identify novel therapeutically targetable epigenetic-related mechanisms that can be exploited to treat prostate cancer patients with MYC-overexpressing tumors. We hope that our basic findings can be translated into personalized medicine treatments, ultimately improving prostate cancer patients care and treatment plans and potentially reducing the overall burden of prostate cancer in the population.

Chapter 2. Methods

2.1. Synthesis of custom CRISPR/Cas9 KO libraries

Custom CRSIPR/Cas9 KO libraries targeting 1,343 murine genes were created. Of note, both the murine c-*Myc* gene and the human c-*MYC* transgene are included as target genes in our custom CIRISPR/Cas9 KO libraries. The targeted genes include epigenetic factors such as chromatin readers, writers, erasers, remodelers, and transcription factors that are known to be highly expressed in cancer settings. In total, each gene is targeted by 10 independent sgRNAs, separated into two libraries (5 sgRNAs - library A; 5 sgRNAs - library B). Each library contains negative control genes including *PPP1R12C* (187 sgRNAs), *GT(ROSA)26SOR* (39 sgRNAs), and *COL1A1* (274 sgRNAs), and positive control genes including 50 different *RPS* and *RPL* genes (10 sgRNAs per positive control gene), for a total of 500 negative control sgRNAs and 500 positive control sgRNAs. In total, each library contains 7,715 sgRNAs. The sgRNAs were designed by the laboratory of Dr. X. Shirley Liu (Harvard University). The sgRNA flanked by complementary sequence to the site of insertion into LentiGuide-Puro vector (52963, Addgene) were synthesized as oligonucleotides (GTGGAAAGGACGAAACACCG-NNNNNNNNNNNNNNNNNNN-GTTTTAGAGCTAGAAATAGCAAGTTAAAATAAGG) through the DNA synthesis platform CustomArray Inc. (Bothell, WA, USA).

2.2. Cloning of sgRNA libraries

The sgRNA pools were PCR amplified (T100 Thermal Cycler; 621BR08810, Bio-Rad) using a high-fidelity DNA polymerase (Q5 High-Fidelity DNA Polymerase; M0491L, New England BioLabs) and the Array_F and Array_R primers (Invitrogen, Purity: Desalted). Settings

and primers are listed in **Table 1** and **Table 2** respectively. PCR reaction products were column purified using the Monarch PCR and DNA Cleanup Kit (T1030S, New England BioLabs) according to manufacturer's instruction. To confirm correct oligo size (~150 bp), the PCR purified oligo libraries were run onto a 2% (wt/vol) agarose gel and DNA quality was verified using BioDrop μLITE (80-3006-51, Montreal Biothech Inc.). The LentiGuide-Puro vector was digested with BsmBI-V2 (R0580, New England BioLabs) overnight at 55°C, followed by dephosphorylation using Antarctic Phosphatase (M0289S, New England BioLabs) for 1 h at 37°C. The digested and dephosphorylated vector was gel purified on a 1% (wt/vol) agarose gel using Monarch DNA Gel Extraction Kit (T1020S, New England BioLabs) according to manufacturer's instruction. The gel extracted DNA was further purified using the Beckman Coulter AMPURE XP kit (NC9959336, ThermoFisher Scientific) following manufacturer's instructions and DNA quality was verified using BioDrop μLITE (80-3006-51, Montreal Biothech Inc.). Gibson assembly reaction was performed to clone oligo libraries into the digested vector backbone at a ratio of 1:5 (backbone vs oligo), using the 2X Gibson Assembly Master Mix (E2611S, New England BioLabs) at 50°C for 1 h. The products were purified using Beckman Coulter AMPURE XP kit (NC9959336, ThermoFisher Scientific), following manufacturer's instructions, and DNA quality was checked using BioDrop μLITE (80-3006-51, Montreal Biothech Inc.). To verify that the oligo libraries were successfully inserted into the backbone, we performed PCR reactions (T100 Thermal Cycler; 621BR08810, Bio-Rad) using hU6 as a forward primer with different sgRNAs as reverse primers. Primers and settings are listed in **Table 2** and **Table 3**, respectively. The PCR amplified Gibson products were run onto a 2% (wt/vol) agarose gel to verify that the intended sgRNA sequences were amplified, and thus, present in the Gibson product. The Gibson assembly products from each library were transformed into electrocompetent cells (Endura™

ElectroCompetent Cells; 60242-2, Lucigen Corporation) using Gene Pulser Xcell (617BR1-05531, Bio-Rad) and the optimal electroporation settings (10 uF, 600 ohms, 1800 volts) suggested for Endura™ ElectroCompetent Cells. Following electroporation, bacteria were recovered by incubation at 37°C for 1 h in Recovery Medium (provided with Endura™ ElectroCompetent Cells) before being platted on a pre-warm 245 mm LB agar plate containing 100 µg/mL of carbenicillin (20871-10, Cerdarlane Labatories) and incubated at 37°C overnight. Bacteria were scrapped off the plates the following day and DNA was extracted using the PureLink™ Expi Endotoxin-Free Maxi Plasmid Purification Kit (A31231, ThermoFisher Scientific). For quality control purposes, our amplified sgRNA libraries were sequenced using the MiSeq Reagent Micro Kit v2 (300-cycles; MS-103-1002, Illumina).

Table 1. sgRNA PCR amplification settings.

Cycle Number	Denature	Anneal	Extend
1	98°C, 30s		
10	98°C, 30s	70°C, 30s	72°C, 30s
11			72°C, 2min

Table 2. List of primers.

Primer Name	Purpose	Sequence
Array_F	PCR amplification of sgRNA libraries	TAACTTGAAAGTATTTCGATTTCTTGGCTTT ATATATCTTGTGGAAAGGACGAAACACCG
Array_R	PCR amplification of sgRNA libraries	ACTTTTTCAAGTTGATAACGGACTAGCCTTA TTTTAACTTGCTA TTTCTA GCTCTAAAAC

hU6	PCR amplification of Gibson product	GAGGGCCTATTTCCCATGATT
Smad2	PCR amplification of Gibson product	TAGTAGGAGACAGTTCAGC
Runx1	PCR amplification of Gibson product	AGGAGTACCTTGAAAGCGA
Ctcf	PCR amplification of Gibson product	CCATATTTACAACCTGCAA
Erg1	PCR amplification of Gibson product	TCGCCTTCTCATTATTCAG

Table 3. Gibson product PCR amplification settings.

Cycle Number	Denature	Anneal	Extend
1	95°C, 3min		
34	95°C, 30s	45°C, 30s	72°C, 1min
35			72°C, 5min

2.3. Cell culture

MyC-CaP (CRL-3255™, ATCC) and HEK293-FT (Kindly provided by Dr. Michel L. Tremblay, McGill University) cells were cultured in a humidified incubator at 37˚C with 5% CO_2. MyC-CaP cells were maintained in Rosewell Park Memorial Institute Medium (RPMI; 350-015-CL, Wisent) while HEK293-FT cells were maintained in Dulbecco's Modified Eagle Medium (DMEM; 319-015-CL, Wisent), and both media were supplemented with 10% fetal bovine serum

(FBS; 12483020, Life Technologies) and 1% HyCloneTM penicillin/streptomycin (SV30010, Fisher Scientific).

2.4. Generation of MyC-CaP Cas9 stable cell line and clones

The MyC-CaP Cas9 stable cell line was generated by transducing MyC-CaP cells using the LentiCas9-Blast construct (52962, Addgene), followed by antibiotic selection using blasticidine (ANT-BL-1, Cerdarlane Labatories). Resistant single cells were then individually plated in 96-well plates to select monoclonal lines. Monoclonal lines were characterized using Western blots, Cas9 activity assays, and proliferation assays.

2.5. Protein extraction

Cells were collected, washed with Dulbecco's phosphate-buffered saline (D-PBS; 311-425-CL, Wisent), and pelleted by centrifugation. Cells were lysed on ice with homemade radioimmunoprecipitation assay (RIPA) buffer (50 mM Tris-HCl, 150 mM NaCl, 1 mM EDTA, 0.1% w/v SDS, 1% w/v sodium deoxycholate, and 1% v/v Triton X-100) containing fresh protease inhibitor (A32955, ThermoFisher Scientific) for 30 min, followed by centrifugation at 16 000 x *g* at 4˚C for 30 min. Following centrifugation, protein lysates were collected and quantified with the Pierce BCA protein assay (A53225, ThermoFisher Scientific).

2.6. Western blotting

Equal amounts of protein were mixed with 4x Laemmli buffer (1610747, Bio-Rad) and boiled at 95℃ for 5 min. The samples were loaded on a 10% Tris-glycine SDS-polyacrylamide gel and transferred to nitrocellulose blotting membranes (1704271, Bio-Rad) using the Trans-Blot®

Turbo™ Transfer System (1704150EDU, Bio-Rad) following manufacturer's instructions. To validate that the transfer was successful, the membrane was stained with Ponceau Red (BP103-10, ThermoFisher Scientific). The membrane was blocked using 5% milk TBS-T (Tris-buffer saline solution with 0.1% Tween 20) for 1 h at room temperature. The membrane was then incubated overnight at 4˚C with primary antibodies for CAS9 (65832S, Cell Signaling Technology) diluted at 1:1,000 and GAPDH (2118S, Cell Signaling Technology) diluted at 1:5,000 in 5% bovine serum albumin (BSA) solution. The following day, the membranes were washed with TBS-T, incubated for 1 h at room temperature with secondary goat anti-rabbit antibodies diluted at 1:5,000 in 5% milk, and washed again with TBS-T. Clarity Western ECL substrate (1705061, Bio-Rad) was prepared according to the manufacturer's instruction and added to the membranes, and images were taken using the ChemiDoc™ Imaging System (12003153, Bio-Rad).

2.7. Cas9 activity assay

To assess the functionality of Cas9, the MyC-CaP Cas9 clones (2,000,000 cells/well) were transfected on 12-well plates with the vector pKLV2-U6gRNA5(gBFP)-PGKGFP2ABFP-W (67984, Addgene), which contains both GFP and blue fluorescent protein (BFP), as well as a sgRNA targeting BFP using Lipofectamine™ 2000 Transfection Reagent (11668019, ThermoFisher Scentific) following the manufacturer's recommended protocol. The MyC-CaP wild-type (WT) cell line was used as a positive control. Fluorescent imaging of the transfected cells was performed using a Motorized Inverted Research Microscope IX81 (3B02967, Olympus). Images were collected using a 10X/0.3 objective and analyzed using the ImageJ software.

2.8. Proliferation assay

The MyC-CaP Cas9 clones as well as the MyC-CaP WT cell line were seeded in a 96-well plate (1000 cells/well) using standard cell culture medium and placed in the IncuCyte® S3 live-cell analysis system (Sartorius, Essen Bioscience). Images of the whole well were taken using 4x phase contrast lens, every 6 h for 4 days and each condition was run in 6 replicates. Images were analyzed with the Basic Analyzer software (Version v2018B) provided with the IncuCyte®. Confluency of the cells at different time points were normalized to the initial confluency time point. An unpaired *t*-test was performed to compare the means of two unmatched groups using the GraphPad Prism 8 software (version 8.0.2).

2.9. Lentiviral library production and MOI determination

Lentiviruses were produced using HEK293-FT cells. Cells were seeded (3,000,000 cells/dish) in 10 cm Petri dishes using standard cell culture media and incubated overnight at 37℃, such that they would be at a confluence of about 80% at the time of transfection. For each 10 cm petri dish, the packaging plasmid psPAX2 (12260, Addgene), the envelop plasmid pMD2.G (12259, Addgene), and the sgRNA plasmid were co-transfected at a ~1:1:1 ratio in HEK293-FT cells using X-tremeGENE™ HP DNA Transfection Reagent (6366546001, Roche) following the manufacturer's recommended protocol. Twenty-four hours after transfection, the cell culture media was removed and replaced with DMEM supplemented with 10% FBS, 1% HyCloneTM penicillin/ streptomycin, and 1% BSA. Cells were incubated for another 24 h, lentiviruses were then harvested and concentrated using the Lenti-X™ Concentrator (631232, Cerdarlane Labatories) according to the manufacturer's instructions. The lentiviruses were resuspended in standard cell culture media and stored as aliquots at -80℃.

To determine the multiplicity of infection (MOI) of the lentiviruses, reverse transductions using different dilutions of the lentiviruses were performed on the MyC-CaP cell line. Precisely, 500 µl or 1 mL of lentivirus was combined with 6,000,000 cells and 8 µg/mL of EMD Millipore™ Polybrene Infection/Transfection Reagent (TR1003G, ThermoFisher Scientific) and plated onto 15 cm Petri dishes in duplicates. The following day, cell culture media was removed and replaced with either RPMI containing 10% FBS, 1% HyCloneTM penicillin/streptomycin, and 25 µg/mL of puromycin (450-162-XL, Wisent), or standard cell culture media. After 48 h, time after which all uninfected cells should be dead, cells were harvested and counted using the Hausser Scientific Bright-Line™ Phase Hemacytometer (02-671-6, ThermoFisher Scientific). The percentage of infected cells was determined by dividing the number of cells that were infected (plate with puromycin) by the total number of cells (plate without puromycin) and multiplying by 100 (*i.e.*, (infected cells/total cells) x 100). The volume of each lentivirus required to achieve an MOI of 0.3 was determined using the percentage of infected cells from each dilution series (*i.e.*, percentage of infected cells/30% x volume of lentivirus used).

2.10. Puromycin kill curve of MyC-CaP cells (48 h)

MyC-CaP cells were seeded (30,000 cells/well) in a 96-well plate and incubated overnight at 37℃. Increasing concentration of puromycin ranging from 0 µg/mL to 100 µg/mL were added to the cells and phase images were collected every 4 h for 48 h using the IncuCyte® S3 live-cell analysis system. The Basic Analyzer software (Version v2018B) provided with the IncuCyte® was used to determine the concentration of puromycin required to kill all cells within 48 h following selection. The concentration of puromycin required to kill all uninfected cells within 48

h was further validate using MyC-CaP cells (6,000,000 cells/dish) in a 15 cm Petri dish, which is the format used for antibiotic selection during the *in vitro* CRISPR/Cas9 KO screens.

2.11. Library transduction and selection

MyC-CaP Cas9 cells were reverse transduced (6,000,000 cells/dish) in 15 cm Petri dishes using 8 μg/mL of EMD Millipore™ Polybrene Infection/Transfection Reagent and the lentiviral sgRNA library at an MOI of 0.3. The number of plates was determined to ensure a 500x coverage of our sgRNA library according to a MOI of 0.3. Twenty-four hours following the reverse transduction, optimal puromycin concentration (25 μg/mL) for selection was added to fresh cell culture media. Forty-eight hours following puromycin selection, the cells were collected, and aliquots were frozen at -80℃. The aliquots of cells collected 48 h following puromycin selection represent the control samples at day 0 (T0). The cells were re-seeded (2,000,000 cells/dish) in two separate 15 cm Petri dishes, they were collected again every time they were about 80%-90% confluent, and aliquots of cells were frozen at each harvest. The number of cell doublings was calculated at each harvest by dividing the natural logarithm of 2 (ln (2)) by the growth rate (gr) of the cells (ln (number of cells at time of harvest/number of cells seeded)/number of days). Selection in an *in vitro* CRISPR/Cas9 KO screen should be performed over a period of time which allows for the Kos to develop in all the alleles of each sgRNA's target gene and for the cells to exhibit a subsequent phenotype (depletion or enrichment), while avoiding over-selection so as not to induce biases in sgRNA representation. The selection in our *in vitro* CRISPR/Cas9 KO screens went on for 18 days (T18), time at which the cells had reached 19 doubling cycles. The day 0 (T0) samples were used as the control sample and the day 11 (T11) samples, time at which the cells had reached

12 doubling cycles [250, 251], were used as the experimental timepoint for the analysis of the results.

2.12. Genomic DNA (gDNA) extraction

The gDNA extraction was performed as described by Chen and colleagues [224]. Cell pellets ($4x10^6$ cells) were lysed using a homemade lysis buffer (50 mM Tris, 50 mM EDTA, 1% SDS, pH 8) and 25 µg/ml Proteinase K (P6556-10MG, Sigma-Aldrich) at 55℃ overnight. The lysate was then treated with 10 mg/mL RnaseA (From Monarch Genomic DNA Purification kit; T3010S, New England BioLabs) at 37℃ for 30 min. Samples were cooled on ice before adding pre-chilled 7.5M ammonium acetate (A2706-100ML, Sigma-Aldrich) and centrifuged at 4,000 x *g* for 10 min. The supernatant was transferred to new tubes and DNA was precipitated with 500 µl of isopropanol and centrifuged a second time at 4,000 x *g* for 10 min. gDNA pellets were washed with 70% ethanol, air-dried for 10 to 30 min, and resuspended into 40 µl of 1X TE buffer (From Monarch Genomic DNA Purification kit). To fully resuspend the DNA, samples were incubated at 65℃ for 1 h and at room temperature overnight. Genomic DNA concentration was measured using BioDrop µLITE (80-3006-51, Montreal Biothech Inc.). Library amplification in preparation for Next-Generation Sequencing (NGS) was performed by using a two-step PCR method. The first round of PCR was performed for purification purposes. Settings and primers are listed in **Table 4** and **Table 5**, respectively. Indices and sequencing adapters were added in the second round of PCR. PCR settings and primers and indices are listed in **Table 6** and **Table 7**, respectively. The libraires were sequenced using the NextSeq 500/550 Mid Output Kit v2.5 (150 Cycles) (20024904, Illumina).

Table 4. Library amplification PCR settings (First round).

Cycle Number	Denature	Anneal	Extend
1	98°C, 30s		
25	98°C, 10s	66°C, 30s	72°C, 27s
26			72°C, 2min

Table 5. Library amplification primers (First round).

Primer Name	Sequence
V2.1-F1	GAGGGCCTATTTCCCATGATTC
V2.1-R1	GTTGCGAAAAAGAACGTTCACGG

Table 6. Library amplification PCR settings (Second round).

Cycle Number	Denature	Anneal	Extend
1	98°C, 30s		
10	98°C, 10s	55°C, 30s	66°C, 17s
11			66°C, 5min

Table 7. Library amplification primers and indexes (Second round).

Library Sample	Forward Primer	i5 index	Reverse primer	i7 index
Library A T0-1	D501-F pool	TATAGCCT	D701-R	CGAGTAAT
Library A T0-2	D501-F pool	TATAGCCT	D702-R	TCTCCGGA
Library A T0-3	D501-F pool	TATAGCCT	D703-R	AATGAGCG
Library A T0-4	D501-F pool	TATAGCCT	D704-R	GGAATCTC

Library A T11-1	D501-F pool	TATAGCCT	D705-R	TTCTGAAT
Library A T11-1	D501-F pool	TATAGCCT	D706-R	ACGAATTC
Library A T11-2	D501-F pool	TATAGCCT	D707-R	AGCTTCAG
Library A T11-3	D501-F pool	TATAGCCT	D708-R	GCGCATTA
Library A T11-4	D501-F pool	TATAGCCT	D709-R	CATAGCCG
Library B T0-1	D501-F pool	TATAGCCT	D710-R	TTCGCGGA
Library B T0-2	D501-F pool	TATAGCCT	D711-R	GCGCGAGA
Library B T0-3	D501-F pool	TATAGCCT	D712-R	CTATCGCT
Library B T0-4	D501-F pool	TATAGCCT	D713-R-TKOv3	GATTATTC
Library B T11-1	D501-F pool	TATAGCCT	D714-R-TKOv3	AGCCGCAT
Library B T11-2	D501-F pool	TATAGCCT	D715-R-TKOv3	CTGATTAA
Library B T11-3	D501-F pool	TATAGCCT	D701-R	CGAGTAAT

2.13. Bioinformatics

Reads from Illumina sequencing was trim at both ends with the software Cutadapt to extract the 19 bases sgRNA sequences. Samples from both library A and B was analyzed separately using MAGeCK (version v0.5.9.2) to count and normalize for sequencing depth. Gene essentiality was tested with MAGeCK Robust Rank Analysis (RRA) algorithm with a list of negative controls. We also combine MAGeCK sgRNA fold change from both set to calculate a Z-score using the

mean (m) and standard deviation (s) of the negative controls “z <- (x-m)/s”. Then, for each gene, a Kolmogorov-Smirnov (KS) test was performed by comparing the z-scores of sgRNAs targeting a gene with the z-scores of negative controls. Finally, *P*-value from KS test was adjusted for false discovery rate (FDR) using Benjamini-Hochberg (BH) method. Significant genes were finally compared to the DepMap Public 22Q1 common essential gene list. MAGeCKFlute (version 1.12.0) was used for downstream analysis (*e.g.*, overrepresentation analysis (ORA) and Gene Set Enrichment Analysis (GSEA)). Volcano plots was generated using EnhancedVolcano R package (version 1.10.0) and Venn diagrams using VennDiagram R package (version 1.7.1).

Chapter 3. Results

3.1. Cloning of custom sgRNA CRISPR/Cas9 KO libraries

The custom sgRNA CRISPR/Cas9 KO libraries were amplified using PCR. The success of the reaction was confirmed by running the PCR-amplified libraries on agarose gel (**Figure 3-1A**). Restriction digestion using the enzyme BSM1 was performed on the lentiviral vector LentiGuide-Puro to cut in two specific sites on the plasmid (**Supplementary Figure 4-1**). Following dephosphorylation and purification, the success of the digestion was confirmed by agarose gel (**Figure 3-1B**). The PCR amplified libraries were inserted into the digested and purified vector using a Gibson Assembly reaction. Since there is a possibility that the PCR amplified libraries did not get properly inserted into the vector, we verified the success of the reaction by performing a PCR reaction of the Gibson Assembly using hU6 as a forward primer combined with some of the sgRNAs from the sgRNA libraries as reverse primers (Ctcf, Erg1, Smad2, Runx1). The PCR results showed amplification for each of the sgRNA used as primers in both Gibson products (**Figure 3-1C**), confirming the presence of sgRNAs into the vector. Next, the Gibson Assembly products were amplified using electroporation and DNA was extracted from the bacteria and sent for Next-Generation-Sequencing (NGS) for quality control. Our amplified libraries have a mean sequencing coverage of 249 per sgRNA, meaning that each sgRNA has a representation of approximately 250x in our final amplified libraries, while the ideal coverage is anywhere between 100x-1000x (**Figure 3-2A**) [252]. Furthermore, the distribution of sequencing reads per sgRNAs (**Figure 3-2B-D**) of our amplified libraries demonstrated the evenness of the representation of each sgRNA in our libraries. Importantly, an even distribution of the sgRNAs means that each target gene in our libraries will be targeted by approximately the same number of sgRNAs, avoiding

potential biases in gene depletion or enrichment related to differential representation of sgRNAs. Overall, these results demonstrate a high and even coverage of the sgRNAs and genes in our amplified libraries, confirming the high quality of our amplified libraries to be used in our CRIPSR/Cas9 screening experiments.

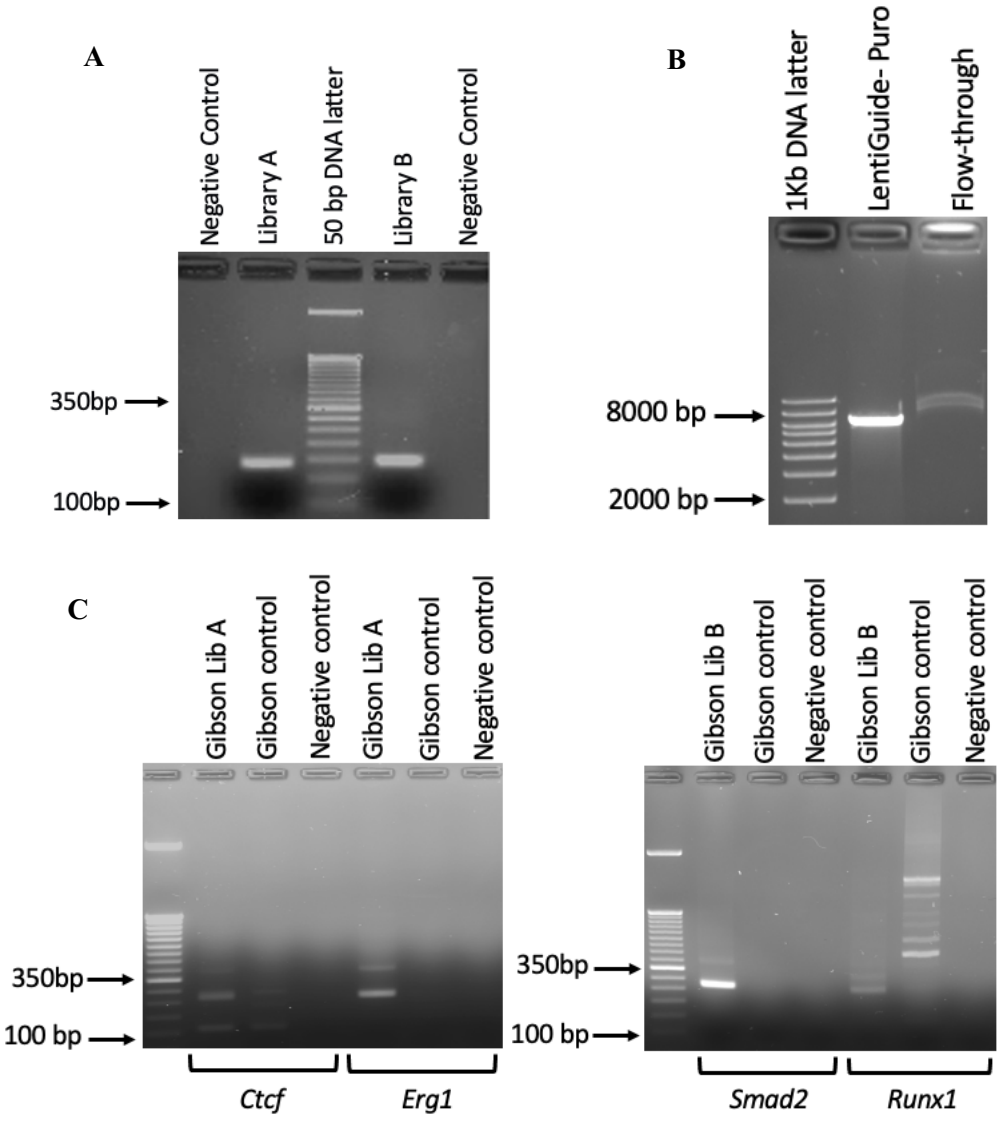

Figure 3-1. Library A and library B PCR amplification and Gibson Assembly.

A. Agarose gel electrophoresis of custom sgRNA CRISPR/Cas9 KO library A and library B following PCR amplification. The oligos are ~150 bp in size. **B**. Agarose gel electrophoresis of vector LentiGuide puro following digestion with enzyme BSMB1. The non-digested plasmid is ~10,100 bp, and the BSMB1 cutting sites span ~1,900 bp, therefore the digested plasmid should be ~8,200 bp. **C**. Agarose gel electrophoresis of Gibson library A (*left panel*) using sgRNA *Ctcf* and *Erg1* as primers and Gibson library B (*right panel*) using sgRNA *Smad2* and *Runx1* as primers. The expected size for each of the sgRNA amplification is ~250 bp. The multiple bands are due to amplification arising from non-specific binding of the primers to the DNA sequence.

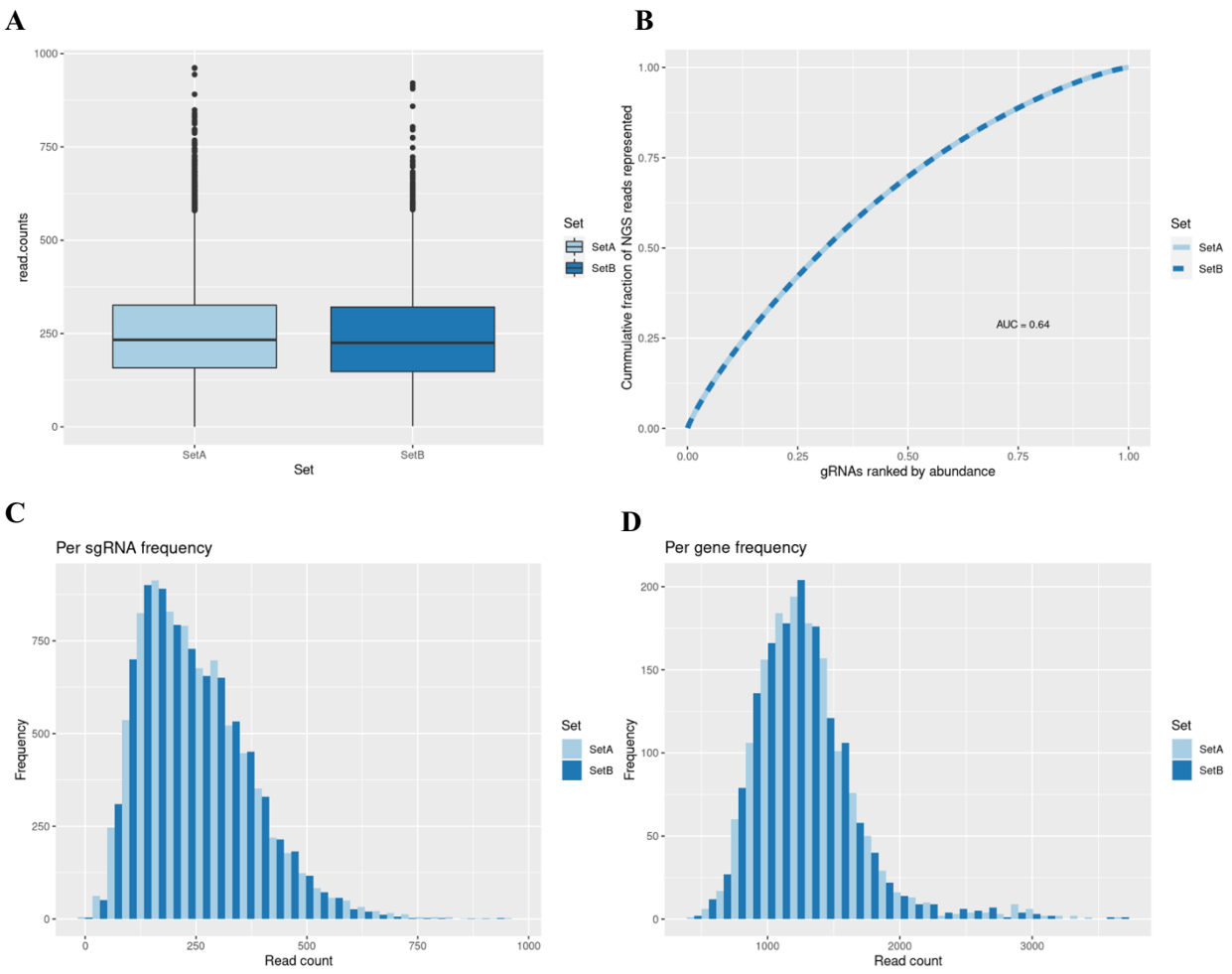

Figure 3-2. NGS of amplified sgRNA CRIPSR/Cas9 KO libraries.

A. The amplified sgRNA libraries were sequenced on a MiSeq using 75 cycles of a Micro kit V2 in single read mode. Sequencing results gave 2,429,474 reads for library A (setA) and 2,319,748 reads for library B (setB). The mean sequencing coverage is 249 per sgRNA. **B**. Lorenz curve showing the distribution of sequencing reads of sgRNAs over the gene library. This curve ranks sgRNA by abundance. Ideally, each sgRNA is represented at the same frequency, so the fraction of sequencing reads represented would increase at a constant rate and produce a diagonal line with an Area Under the Curve (AUC) of 0.5. An AUC of 0.64 is close to perfect uniformity, meaning that the amplification was successful. **C**. Histogram representing the frequency of read counts per sgRNA. **D**. Histogram representing the frequency of read counts per gene represented in the libraries.

3.2. Cas9-expressing clone generation and characterization

We selected the MyC-CaP cell line for our *in vitro* model of MYC-driven prostate cancer. The MyC-CaP cell line was originally isolated from 16-month-old Hi-MYC transgenic mice and it retains the expression of the human MYC transgene [253]. Importantly, the MyC-CaP cell line has no history of ADT or hormonal therapy prior to its isolation, expresses AR uniformly, and demonstrates hormone-dependent growth in soft agar *in vitro* [253]. In order to conduct the *in vitro* CRISPR/Cas9 KO screens, a MyC-CaP Cas9-expressing cell line was generated. The MyC-CaP Cas9 cell line was created by transducing the cells with the pLentiCas9-Blast construct, followed by antibiotic selection to eliminate all the cells that were not transduce and thus do not express Cas9. To ensure homogeneous expression of Cas9 in our cell line, Cas9-expressing monoclonal cell lines were generated from the MyC-CaP Cas9 pool. Subsequently, the monoclonal cell lines that were generated were characterized to select which one was going to be used for the CRIPSR/Cas9 screen. A Western Blot of the MyC-CaP Cas9 clones was performed to validate the expression of Cas9 (**Figure 3-3A**). The MyC-CaP Cas9 clones all had different levels of Cas9 protein expression, with the clone MyC-CaP Cas9 E2 having the highest level of Cas9 protein expression (**Figure 3-3A**). Further, an antibody against MYC was also used to validate its expression in the MyC-CaP Cas9 clones. All the MyC-CaP Cas9 clones expressed MYC at the same level (**Figure 3-3A**). Next, a proliferation assay was performed on the MyC-CaP Cas9 clones to verify the proliferation rates compared to the MyC-CaP WT cell line (**Figure 3-3B**). The proliferation rate of the clone MyC-CaP Cas9 E2 clone was the most similar to the MyC-CaP WT cell line (**Figure 3-3B, supplementary Figure 4-2).** To ensure that Cas9 is active in the MyC-CaP Cas9 clones and maintains its ability to cut at a target site, a Cas9 activity assay was performed. A vector expressing GFP and BFP, as well as a sgRNA targeting BFP was used to

transfect the MyC-CaP Cas9 clones and the MyC-CaP WT cell line (**Figure 3-3C**). Upon transfection, the infected cells should all express GPF, and if Cas9 is functional, in the MyC-CaP Cas9 clones, they should not express BFP, as there is an integrated sgRNA targeting that sequence in the vector. The MyC-CaP WT cell line expressed both GFP and BFP, confirming the success of the transfection (**Figure 3-3C)**. Of the MyC-CaP Cas9 clones, B1, B8, and E2 did not express BFP, while F12 showed expression of BFP (**Figure 3-3C)**. The expression of BFP in the MyC-CaP Cas9 F12 suggest that Cas9 is not functional, which might be due to mutations [254]. Based on the results from the Western Blot, the proliferation assay, and the Cas9 activity assay, the MyC-CaP Cas9 E2 clone was selected for the *in vitro* CRISPR/Cas9 KO screen.

Prior to starting the *in vitro* CRISPR/Cas9 KO screen, a fresh MyC-CaP Cas9 E2 clone was thawed and subjected to re-characterization. The freshly thawed MyC-CaP Cas9 E2 clone still expressed Cas9 at a high level (**Supplementary Figure 4-3A**), proliferated similarly to the MyC-CaP WT cell line (**Supplementary Figure 4-3B**), and had a functionally active Cas9 (**Supplementary Figure 4-3C**). Thus, we successfully generated a monoclonal MyC-CaP cell line which expressed a functionally active Cas9 and proliferates similarly to its parental counterpart that is suitable for an *in vitro* CRISPR/Cas9 KO screen.

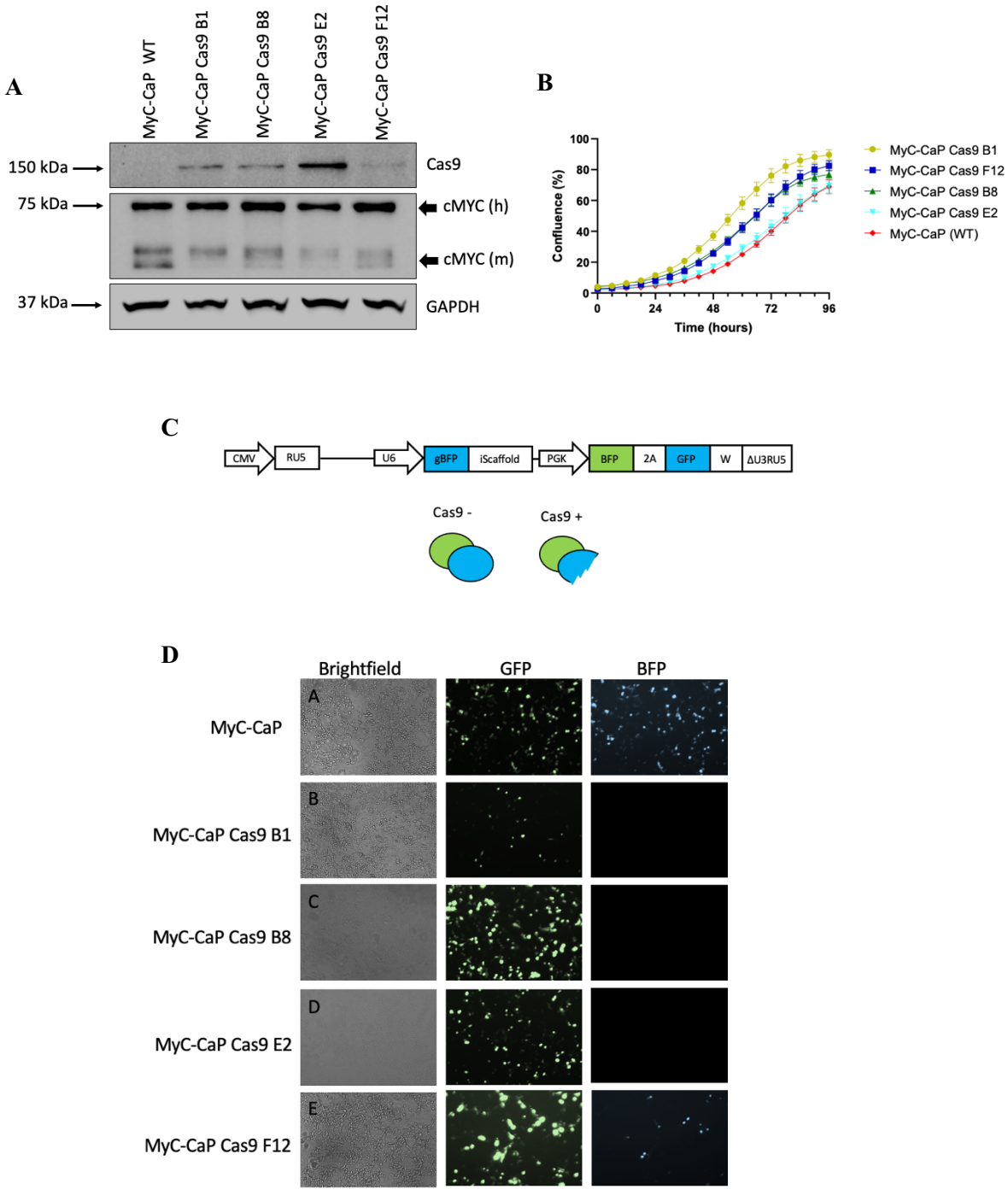

Figure 3-3. MyC-CaP Cas9 clones characterization.

A. Western Blotting was performed on MyC-CaP Cas9 clones to validate the expression of MYC and Cas9. MYC was evenly expressed across the different clones while Cas9 was only highly expressed in the clone E2. **B**. Proliferation assay of the MyC-CaP Cas9 clones and MyC-CaP WT

cell line. The clone E2 proliferated the most similarly to the WT cell line. Data represents mean ± SD. **C**. Schematic representing the vector used for the Cas9 activity assay (pKLV2-V6g-RNA5(gBFP)-PG-KGFP2ABFP-W). The vector contains both GFP and BFP, and a sgRNA targeting BFP. Upon transfection, MyC-CaP Cas9 clones should not express BFP is Cas9 is active in the cells. **D**. Cas9 activity results of the MyC-CaP Cas9 clones. The MyC-CaP WT cell line was used as a positive control for the expression of GFP and BFP. The clones B1, B8, and E2 showed no expression of BFP. The clone F12 showed signs of BFP expression, suggesting the non-functionality of Cas9.

3.3. *In vitro* MyC-CaP CRISPR/Ca9 KO screen result: Quality control

In order to perform the *in vitro* CRISRP/Cas9 KO screen, we first produced lentiviruses with our amplified CRISPR/Cas9 sgRNA libraries using HEK293-FT cells. The MyC-CaP Cas9 E2 monoclonal cell line was then transduced with our lentivirus library A and lentivirus library B in two independent experiments. The infected cells were subjected to a 48 h puromycin selection. Following the antibiotic selection, the cells were harvested, and aliquots were kept as the day 0 (T0) control samples before re-seeding the cells. The cells were harvested and re-seeded again each time they were confluent, and aliquots of the cells were kept at each harvest. Importantly, the number of ell doubling was calculated at each harvest. The *in vitro* CRISPR/Cas9 KO screen went on for 18 days, time at which the cells had reached a total of 19 doublings. For the analysis of the *in vitro* CRISPR/Cas9 KO screen, we used the day 0 (T0) samples as the control samples and the day 11 (T11) samples as the experimental samples, time at which the cells had reached 12 doublings. The genomic DNA was extracted from the cells of each sample from both time points (library A T0, n=4, library A T11, n=4, library B T0, n=3, library T11, n=3) and was sent for NGS. Using NGS, we can assess the sgRNA composition of each of the samples. The sgRNA composition of the experimental samples (T11) were compared to the sgRNA composition of the control samples (T0), allowing us assess depletion or enrichment of the sgRNAs following the KO of their target gene.

The *in vitro* CRISPR/Cas9 KO screen results were analyzed using the MAGeCK-VISPR algorithm. The sequencing quality control analysis revealed a sequencing depth of 200x and mapping ratio between 83% to 89% for each of the samples sequenced in from both libraries (**Figure 3-4A**), confirming the quality of the sequencing. In all of the control (T0) and experimental (T11) samples from both libraries, all of the sgRNAs originally included in our

libraries were sequenced at least once, except for 1 or 2 sgRNAs from library A and 1 sgRNA from library B (**Figure 3-4B**), meaning that the entirety of our libraries was present in the screen, with the exception of a couple sgRNAs. Furthermore, the Gini index was used to assess the evenness of sgRNA read counts within our samples. The low Gini index scores for all of our samples revealed a homogeneous distribution of the sgRNA read counts across the target genes in each sample for both library A and library B (**Figure 3-4C**). Next, a Principal Component Analysis (PCA) was used to observe trends and clusters amongst the samples of from the control time point (T0) and the experimental time point (T11). If our screens were experimentally successful, the T0 samples replicates should cluster together, while the T11 samples replicates should form a separate cluster. Indeed, the experimental samples (T11) should have a different representation of sgRNAs than the control samples (T0) due to depletion or enrichment of certain sgRNAs following selection. As expected, the PCA generated two distinct clusters between the control time point samples (T0) and the experimental time point samples (T11) of both libraries (**Figure 3-4D**), demonstrating a highly different distribution of sgRNAs and confirming the quality of our screens. Further, the dropout of our positive and negative control genes was assessed using sgRNA read counts. The positive control genes were all depleted from our experimental samples while the negative control genes were not depleted (**Figure 3-4E**). Altogether, the sequencing control analysis results indicate that the *in vitro* MyC-CaP CRISPR/Cas9 KO screens were experimentally successful and validate the robustness of the results obtained.

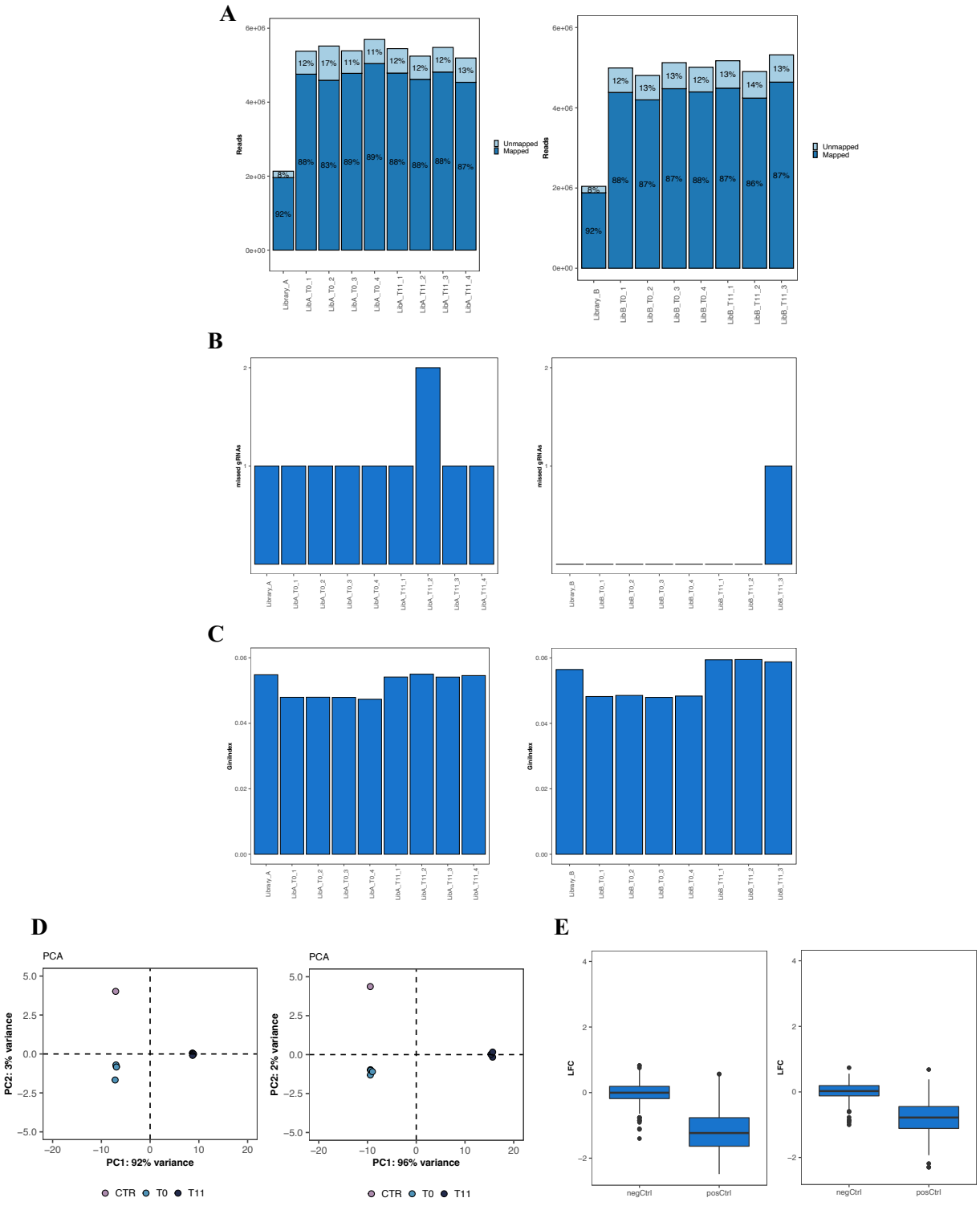

Figure 3-4. Sequencing Control of *in vitro* MyC-CaP CRISPR/Cas9 KO screens with library A and library B.

The library A and Library B samples represent the original libraries prior to the screen, the T0 samples represent the control time point and the T11 samples represent the experimental time point. **A**. Sequencing depth and mapping ratio of all samples in library A (*left panel*) and library B (*right panel*). A sequencing dept of 200x and mapping ratio of 83-89% was obtained. **B**. Bar graph representing the number of missed sgRNAs per sample in library A (*left panel*) and library B (*right panel*). **C**. Gini index representing distribution of sgRNAs across samples in library A (*left panel*) and library B (*right panel*). **D**. Sample-to-sample variance visualized using a PCA in library A (*left panel*) and library B (*right panel*). **E**. Box plot representing the dropout of our control genes according to Log Fold Change (LFC) between the experimental endpoint samples (T11) vs the control samples (T0).

3.4. *In vitro* CRISPR/Ca9 KO screen identifies epigenetic dependencies in MYC-driven prostate cancer

The *in vitro* MyC-CaP CRISPR/Cas9 KO screen results were analyzed in terms of sgRNA depletion or enrichment using the MAGeCK Robust-Rank Analysis (RRA) algorithm comparing our experimental endpoint samples (T11) to our initial time point samples (T0). Genes are depleted in a pool CRISPR/Cas9 KO screen if upon their knockout, cells either cannot survive, or will proliferate at a lower rate. Thus, genes that are significantly depleted confer a growth advantage. On the other hand, genes are enriched in a CRIPSR/Cas9 KO screen if upon their knockout, cells proliferate at a greater rate. Therefore, genes that are significantly enriched have tumor-suppressive functions. The RRA of our *in vitro* MyC-CaP CRISPR/Cas9 KO screens revealed a number of genes that are significantly depleted or enriched (P-value ≤ 0.05) in both libraries. For library A, 182 genes were significantly depleted, and 80 genes were significantly enriched (**Figure 3-5A**). For library B, 193 genes were significantly depleted, and 111 genes were significantly enriched (**Figure 3-5A**). To look further into which kind of biological pathways the hits from the screens are associated with, we performed ORA and GSEAs of the genes significantly depleted of enriched in library A and in library B (**Figure 3-5B-C**). The ORAs and GSEAs revealed vulnerabilities associated with a diverse set of epigenetic-related pathways, including histone acetylation, histone H4 acetylation, histone binding, histone H3K9 methylation, histone methyltransferase, and chromatin remodeling complex (**Figure 3-5B-C**). This suggest that a large number of genes that were significantly depleted or enriched in our screens are associated with histone acetylation, histone methylation, and chromatin remodeling.

Next, we compared the hits from library A and library B, and we found 100 genes that were significantly depleted or enriched in both libraries (**Figure 3-6A**). Based on the fact that our two

libraries target the same set of genes with different combinations of sgRNAs, we conclude that the genes that were significant in both libraries are the most robust hits from our experiments. Interestingly, the depleted genes that are common to both libraries include some well-known transcription factors that play central roles in prostate cancer initiation, development, and progression such as the human transgene *MYC*, *Ar,* and *Foxa1* [106, 247, 255-257] (**Figure 3-6B-C**). Of note, the discovery that *MYC* was depleted in our screens suggest that the MyC-CaP cell line relies on the continuous overexpression of MYC for proliferation and survival. Moreover, our results validate the role of *Ar* and *Foxa1* as key players in MYC-overexpressing prostate cancer cellular proliferation and survival. Other transcription factors which have been previously demonstrated to have an impact on prostate cancer progression including *Gata3* [258] and *Fosl1* [259-261] were also found to confer a growth advantage in our MyC-CaP prostate cancer cell line (**Figure 3-6B-C**). Moreover, The Methyltransferases *Mettl1* and *Setd8* were both significantly depleted in our screens (**Figure 3-6B-C**). *Mettl1* acts as a methyltransferase for a subset of internal N(7)-methylguanosine sites (m^7G) in mRNA [262], while *Setd8* is found as the only known lysine mono-methyltransferase in mammalian cells to produce H4K20me1, which plays a critical role in in chromatin compaction, gene regulation and cell-cycle progression [263]. The chromatin remodeling factor *Rbbp7,* which chaperones chromatin remodeling proteins to their nuclear histone substrates including HATS and HDACs [264], was also found to be depleted in our screen (**Figure 3-6B-C**) and thus, is essential for MYC-driven prostate cancer cells proliferation or survival.

Moreover, the well-known tumor-suppressor *Pten* and *Rb1* were significantly enriched in both libraries (**Figure 3-6B-C**). Loss of *PTEN* is highly frequent in primary and metastatic prostate tumors while the loss of *RB1* is associated with high number of CRPC [265, 266]. Our screen

revealed that the loss of *Pten* and *Rb1* in MYC-driven prostate cancer cells allows them to thrive and proliferate, validating their role as key tumor-suppressors in a MYC-overexpressing context. The histone chaperone *Hira* and the lysine-specific demethylase *Kdm3b* were also both significantly enriched in our screens (**Figure 3-6B-C**). The HIRA complex deposits H3.3 at euchromatin regions such as promoters, enhancers, and gene regulatory regions, and is involved in cellular senescence [267]. *KDM3B* catalyzes demethylation of H3K9me1 and H3K9me2, resulting mostly in the activation of gene transcription [268]. The result from our screen suggests that the epigenetic-related genes *Hira* and *Kdm3b* have tumor-suppressive functions in MYC-driven prostate cancer cells.

To summarize, our results validate the role of well-established prostate cancer oncogenes and tumor-suppressor genes our MYC-driven prostate cancer model. Moreover, our results pinpoint towards different epigenetic regulators as being key players in prostate cancer cells survival or proliferation in a MYC-overexpressing context, confirming that MYC-driven prostate cancer is dependent upon epigenetic-related mechanism to thrive and grow.

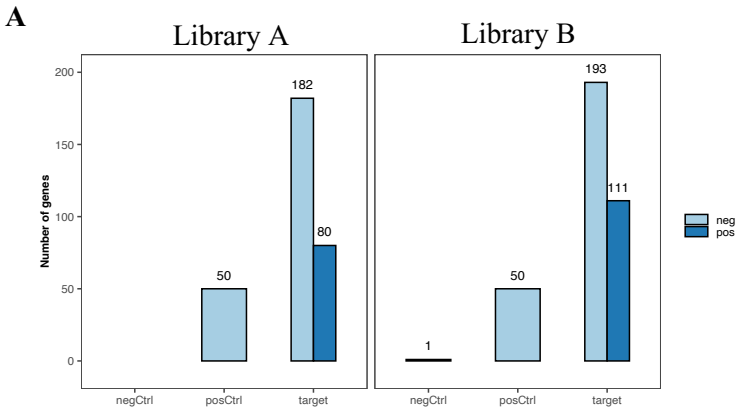
A
Library A
Library B
Number of genes
200
150
100
50
0
182
80
50
193
111
50
1
neg
pos
negCtrl
posCtrl
target

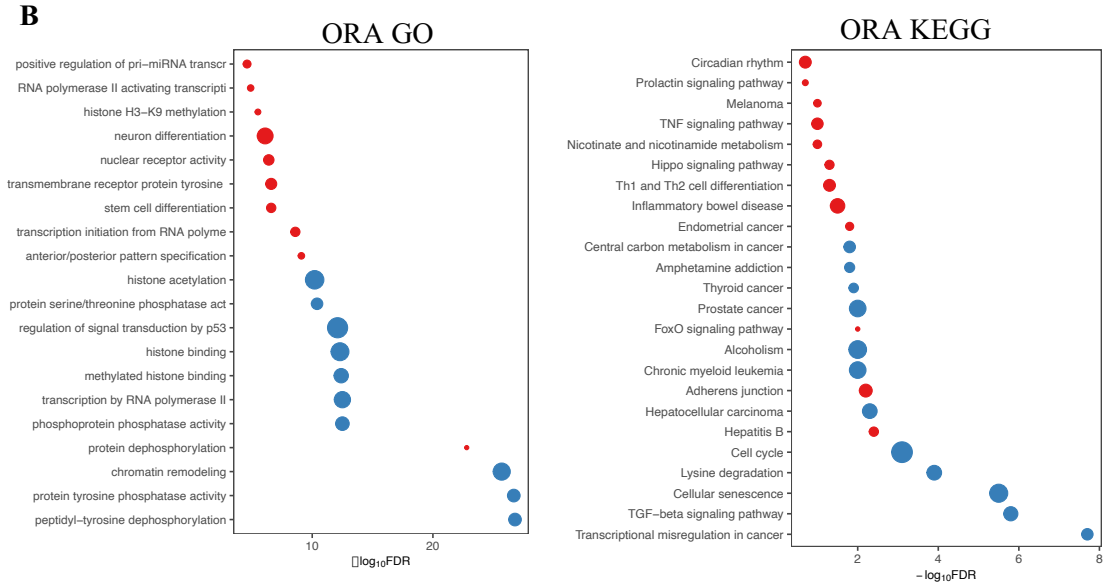
B
ORA GO
positive regulation of pri−miRNA transcr
RNA polymerase II activating transcripti
histone H3−K9 methylation
neuron differentiation
nuclear receptor activity
transmembrane receptor protein tyrosine
stem cell differentiation
transcription initiation from RNA polyme
anterior/posterior pattern specification
histone acetylation
protein serine/threonine phosphatase act
regulation of signal transduction by p53
histone binding
methylated histone binding
transcription by RNA polymerase II
phosphoprotein phosphatase activity
protein dephosphorylation
chromatin remodeling
protein tyrosine phosphatase activity
peptidyl−tyrosine dephosphorylation
10
20
log10FDR
ORA KEGG
Circadian rhythm
Prolactin signaling pathway
Melanoma
TNF signaling pathway
Nicotinate and nicotinamide metabolism
Hippo signaling pathway
Th1 and Th2 cell differentiation
Inflammatory bowel disease
Endometrial cancer
Central carbon metabolism in cancer
Amphetamine addiction
Thyroid cancer
Prostate cancer
FoxO signaling pathway
Alcoholism
Chronic myeloid leukemia
Adherens junction
Hepatocellular carcinoma
Hepatitis B
Cell cycle
Lysine degradation
Cellular senescence
TGF−beta signaling pathway
Transcriptional misregulation in cancer
2
4
6
8
−log10FDR

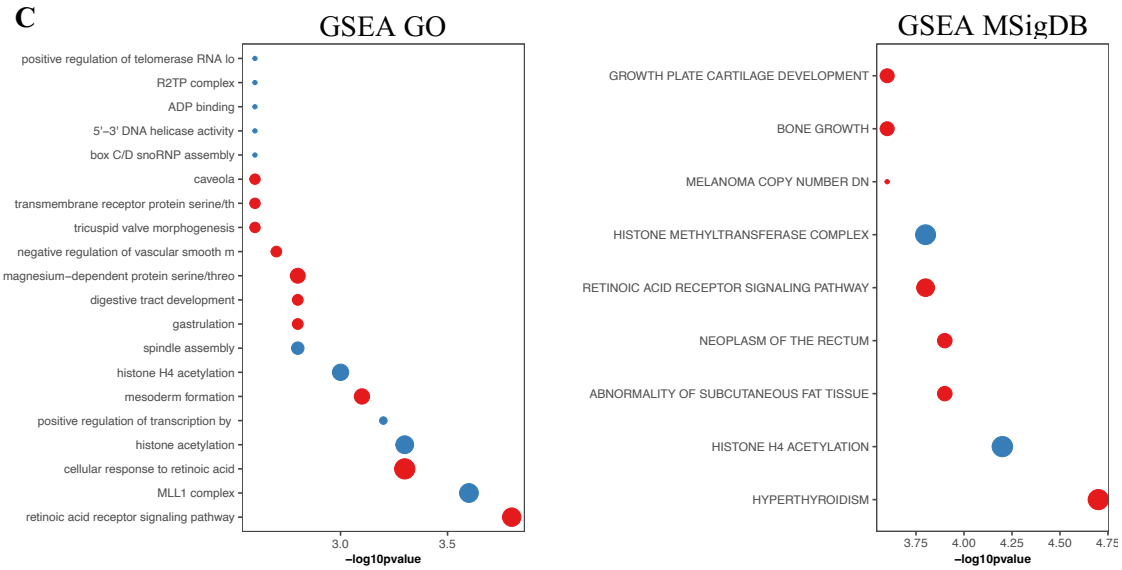
C
GSEA GO
positive regulation of telomerase RNA lo
R2TP complex
ADP binding
5'−3' DNA helicase activity
box C/D snoRNP assembly
caveola
transmembrane receptor protein serine/th
tricuspid valve morphogenesis
negative regulation of vascular smooth m
magnesium−dependent protein serine/threo
digestive tract development
gastrulation
spindle assembly
histone H4 acetylation
mesoderm formation
positive regulation of transcription by
histone acetylation
cellular response to retinoic acid
MLL1 complex
retinoic acid receptor signaling pathway
3.0
3.5
−log10pvalue
GSEA MSigDB
GROWTH PLATE CARTILAGE DEVELOPMENT
BONE GROWTH
MELANOMA COPY NUMBER DN
HISTONE METHYLTRANSFERASE COMPLEX
RETINOIC ACID RECEPTOR SIGNALING PATHWAY
NEOPLASM OF THE RECTUM
ABNORMALITY OF SUBCUTANEOUS FAT TISSUE
HISTONE H4 ACETYLATION
HYPERTHYROIDISM
3.75
4.00
4.25
4.50
4.75
−log10pvalue

Figure 3-5. MyC-CaP *in vitro* CRISPR/Cas9 KO screen significantly enriched and depleted genes in library A and B.

A. Number of genes that were significantly enriched or depleted (*P*-value ≤ 0.05) in library A (*left panel*) and library B (*right panel*). **B.** ORA of genes that are significantly depleted (blue dots) or enriched (red dots; *P*-value ≤ 0.05) in library A and library B using GO (*left panel*) and KEGG (*right panel*). **C**. GSEA of genes that are significantly depleted (blue dots) or enriched (red dots) (*P*-value ≤ 0.05) in both library A and B using GO (*left panel*) of MSigDB (*right panel*).

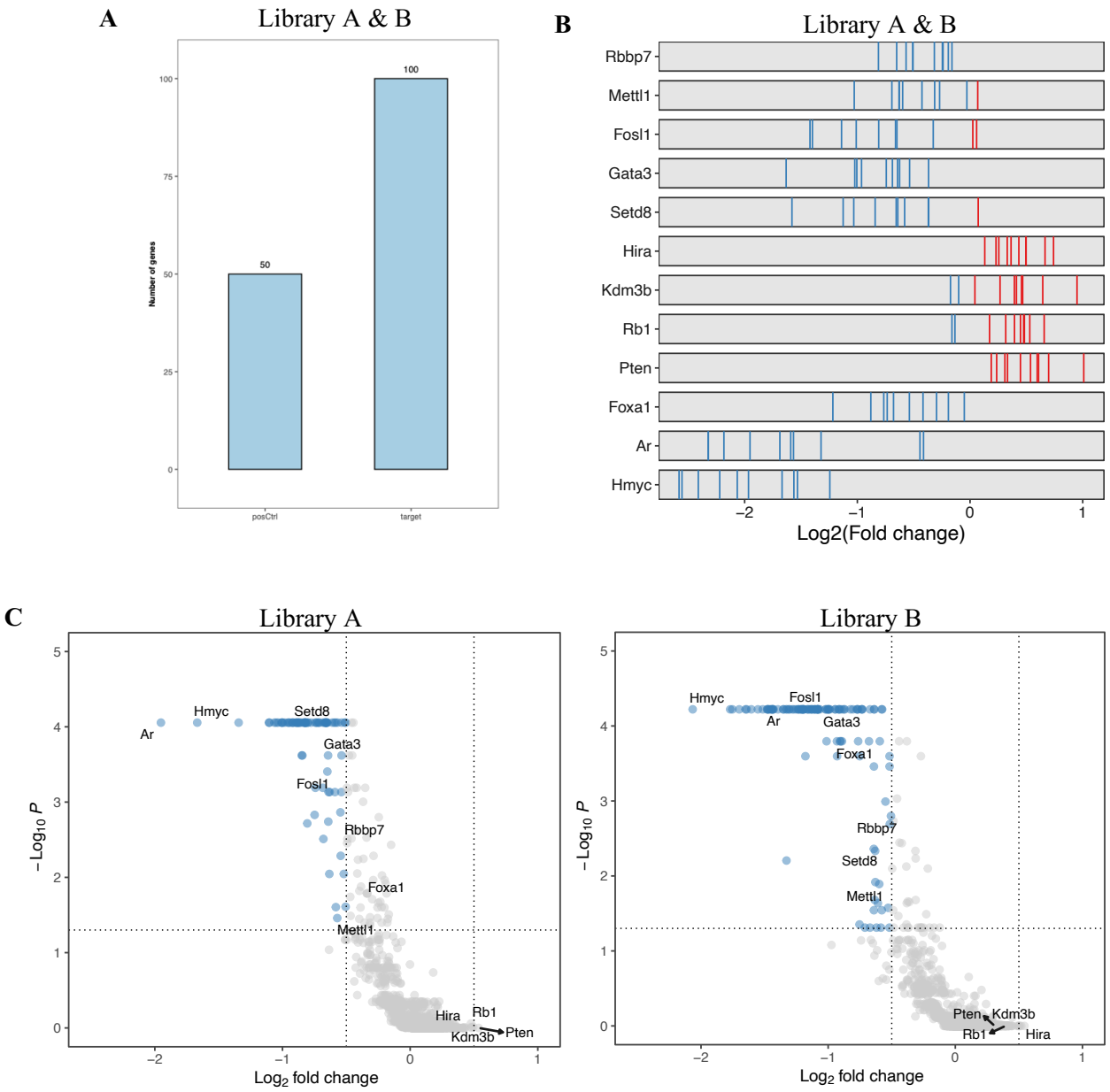

Figure 3-6. Significantly depleted or enriched genes from the MyC-CaP in vitro CRISPR/Cas9 KO screen common in both library A and B.

A. Number of genes that were significantly depleted or enriched (*P*-value ≤ 0.05) common in both library A and library B. **B**. sgRNA rank view of example genes significantly depleted (blue lines) or enriched (red lines) from both library A and B. **C**. Volcano plots depicting the significantly depleted (blue dots) or significantly enriched genes according to the $\log_2$ fold change (FC > 1) and *P*-value (< 0.05) in library A (*left panel*) and library B (*right panel*) obtained using MAGeCK RRA. The highest possible Log_{10} *P*-value based on our experimental design is 4.2.

3.5. Identification of epigenetic dependencies specific to MYC-driven prostate cancer

To assess the specificity of the genes that confer a growth advantage in our MYC-driven model of prostate cancer cells, we compared our significant genes from both libraries to the DepMap public 22Q1 common essential gene lists. We identified 30 genes that were not commonly essential across human cancer cell lines, including *MYC*, *Ar, Foxa1*, *Gata3*, *Fosl1*, and *Rbbp7* (**Figure 3-7A and Supplementary Figure 4-4A**). Next, we compared our significant hits from both libraries to the DepMap public 22Q1 essential gene lists of different prostate cancer cell lines (22Rv1, LNCaP, DU-145, VCaP, BPH1, P4E6). We identified 8 genes as not commonly essential across prostate cancer cell lines, including *MYC*, *Sp110*, *H2ax*, *Terf2*, *Uhrf1*, *Polr2a*, *Dcaf1*, and *Kmt5a* (**Figure 3-7B-C and Supplementary Figure 4-4B**. We next overlapped the DepMap common essential gene lists of human cancer cell lines with the DepMap common essential gene lists of the prostate cancer cell lines to identify genes that were not commonly essential in either category. We identified 6 genes as being non-commonly essential across human cancer cell lines and human prostate cancer cell lines, including *MYC*, *Sp110*, *Terf2*, *Uhrf1*, *Polr2a*, and *Dcaf1* (**Figure 3-7A**). Again, *Uhrf1*, which plays a role in maintaining DNA methylation and is involved in chromatin remodeling [269], and *Dcaf1,* which is a component of E3 ubiquitin-protein ligase complexes and is involved in H2A phosphorylation [270], were identified as being not commonly essential across cancer cell lines.

To summarize, analysis of our results revealed that a number of genes which were identified as conferring a growth advantage our MYC-driven prostate cancer model are not commonly essential across human cancer cell lines, indicating the specificity of their oncogenic functions to prostate cancer. Furthermore, we identified genes that were essential in the MyC-CaP

cell line, while they were not found to be essential in other prostate cancer cell lines, thus suggesting that they are essential specifically in the MyC-CaP prostate cancer cell line. Importantly, we identified epigenetic-related genes as being specifically essential to MyC-CaP prostate cancer cells proliferation and survival, indicating epigenetic dependencies in MYC-driven prostate cancer growth.

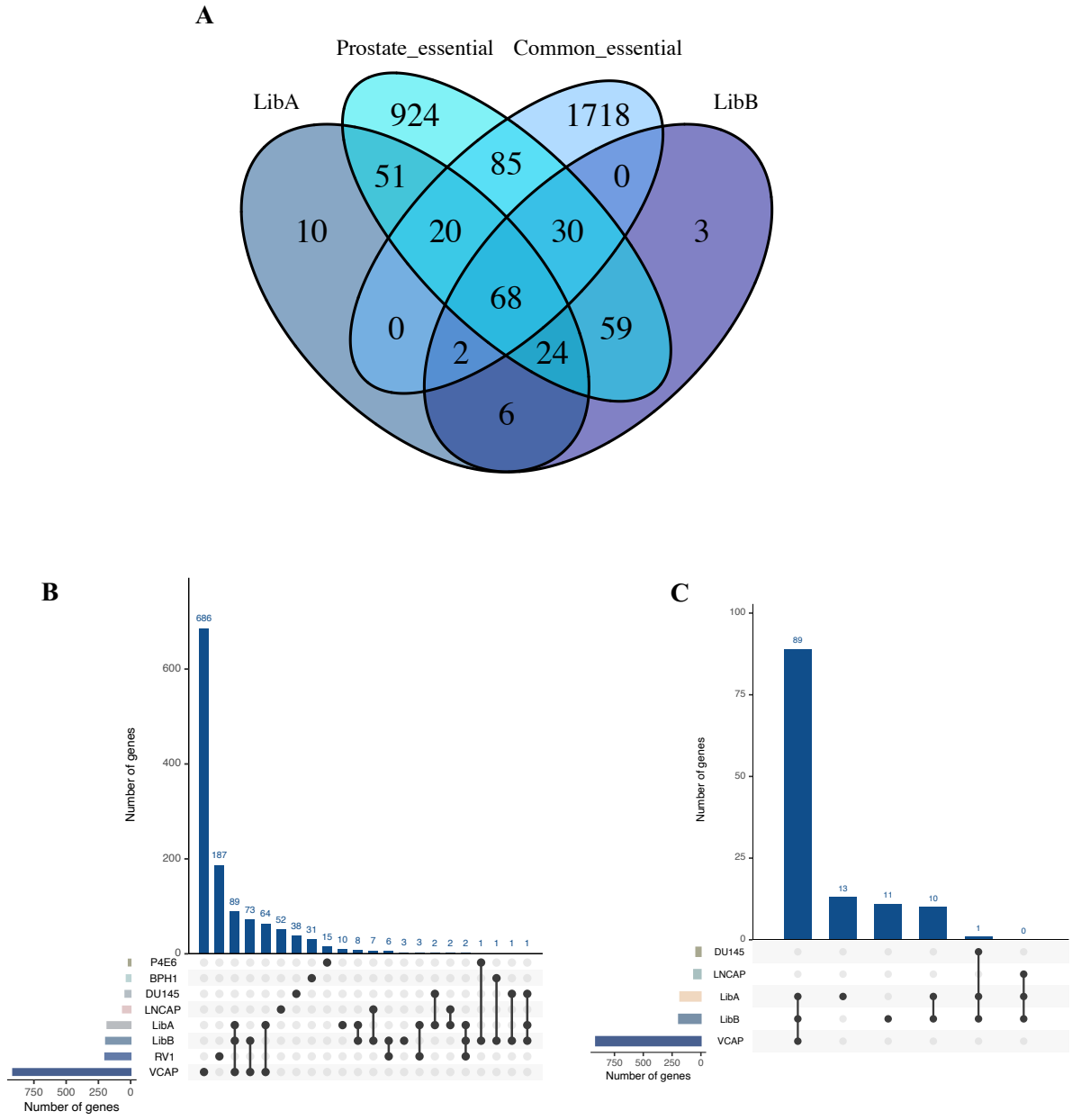

Figure 3-7. Overlap of significant hits from *in vitro* MyC-CaP CRIPSR/Cas9 KO screen with different human cancer cell lines.

A. Venn diagram showing the overlap of significantly depleted genes in our screen with essential genes identified in other human cancer cell lines and other human prostate cancer cell lines. **B**. Upset plot showing the number of identified genes in the *in vitro* MyC-CaP CRISPR/Cas9 KO screen that overlap with common essential genes of each prostate cancer cell lines (P4E6, BPH1, DU145, LNCaP, VCaP) found using DepMaP. **C**. Upset plot showing the number of identified

genes in the *in vitro* MyC-CaP CRISPR/Cas9 KO screen that overlap with common essential genes of each prostate cancer cell lines with a focus on the DU145, LNCaP, and VCaP cell lines.

Chapter 4. Discussion

4.1. Summary of results

We hypothesized that prostate cancer cells are dependent on the expression of key epigenetic regulators for survival and growth in the context of MYC-overexpression. To test this hypothesis, we performed *in vitro* CRISPR/Cas9 KO screens in a MYC-overexpressing prostate cancer cell line. First, we designed and amplified two custom CRISPR/Cas9 sgRNA libraries which targets genes mostly focused on epigenetic processes. Importantly, our CRISPR/Cas9 sgRNA libraries were successfully amplified and there was a homogenous representation of the sgRNAs in the amplified product (**Figures 3-1 & 3-2**). We performed *in vitro* CRISPR/Cas9 KO screening in the MyC-CaP cell line using the amplified library products targeting epigenetic-related genes in two independent experiments. The lentiviral libraries were transduced into the cells at a low MOI (0.3), ensuring that each cell only receive one CRISPR targeting sequence (sgRNA). Therefore, if the target gene is essential for the survival or proliferation of the cell, there will be a significant depletion of that sgRNA in the pool of cell overtime as Cas9 cuts the target sequence. On the other hand, a significant increase in the representation of a sgRNA indicates that the target gene has anti-proliferative functions. Our *in vitro* CRISPR/Cas9 KO screens identified many genes that were significantly depleted or enriched in library A and in library B (**Figure 3-5 & 3-6**). The genes that were significantly depleted in both library A and library B were genes that are essential for the proliferation or survival of prostate cancer cells, while the ones which are significantly enriched in both libraries have anti-proliferative effects on prostate cancer cells in the context of MYC-driven prostate cancer specifically. Notably, a number of genes that were significantly depleted or enriched were associated with histone modification and chromatin

remodeling (**Figure 3-5**). The genes that were significantly depleted or enriched in both libraries included some well-known oncogenes (*MYC*, *Ar*, *Fooxa1*) and tumor suppressor genes (*Pten*, *Rb1*), as well epigenetic-related genes (*Gata3*, *Fosl1*, *Mettl1*, *Setd8*, *Rbbp7*, *Hira*, *Kdm3b*) (**Figure 3-6**). Furthermore, by comparing our data to the DepMap common essential gene lists of human cancer cell lines and to the DepMap common essential gene lists of the prostate cancer cell lines, we identified epigenetic related genes that were non-essential across human cancer cell lines (*MYC*, *Ar, Foxa1*, *Gata3*, *Fosl1*, and *Rbbp7*), epigenetic-related genes that were non-essential across prostate cancer cell lines (*MYC*, *H2ax*, *Uhrf1*, *Dcaf1*, and *Kmt5a*), as well as epigenetic-related genes that were non-essential in either category (*MYC*, *Uhrf1*, and *Dcaf1*) (**Figure 3-7**). Because these hits were significantly depleted in both libraries in our *in vitro* CRISPR/Cas9 KO screen and are non-commonly essential across human cancer cell lines and human prostate cancer cell lines, our results suggest that these genes are essential in MYC-driven prostate cancer cellular proliferation. Further investigation is required to confirm their specificity to a MYC-overexpressing context of prostate cancer.

To summarize, the results of our *in vitro* CRISPR /Cas9 KO screens support our hypothesis that MYC-driven prostate cancer is dependent upon specific epigenetic-related genes for cellular proliferation. Indeed, the KO of specific epigenetic regulators in our MYC-overexpressing prostate cancer cell line resulted in the slower proliferation rates or death of the cells. Moreover, a number of genes that are essential for cellular proliferation appear to be specific to the MYC-overexpressing context of prostate cancer. Altogether, our results reveal potential epigenetic dependencies of MYC-driven prostate cancer cellular proliferation. Additional experiments and analysis are required to validate the epigenetic dependencies, and to identify their role in MYC-induced transcriptional and metabolic reprogramming.

4.2. Generation of custom CRISPR/Cas9 sgRNA libraries and MyC-CaP Cas9 clones

To study the role of epigenetic regulators in MYC-overexpressing prostate cancer growth, we designed custom CRISPR/Cas9 sgRNA libraries that specifically target epigenetic-related genes such as transcription factors, and chromatin readers/writers/eraser/remodelers. We opted for the MyC-CaP cell line for our CRISPR/Cas9 KO screens, which is a murine model of MYC-driven prostate cancer. The MyC-CaP cell line is unchallenging to maintain in culture and is compliant to gene editing strategies (see **section 1.2.3**).

In order to conduct our CRISPR/Cas9 KO experiments, we generated a MyC-CaP Cas9 stable cell line. Cas9 expression is required for the target sequence to be cleaved during CRISPR/Cas9 screening. To ensure uniform expression of Cas9 and avoid cleaving biases, we generated MyC-CaP Cas9-expressing clones from our MyC-CaP Cas9 stable cell line. To account for possible differential transfection efficiency amongst the stable pool and to select the MyC-CaP Cas9 clone that was going to be used for our experiments and, we characterized the clones based on the expression of Cas9, functionality of Cas9, and proliferation rates. We did observe some differential expression of Cas9 in our MyC-CaP Cas9 clones. While the MyC-CaP Cas9 E2 clone expresses Cas9 at high levels, the MyC-CaP Cas9 F12 clone expresses Cas9 at very low levels (**Figure 3-3A**). Further, Cas9 functionality also differed amongst the MyC-CaP Cas9 clones. Namely the MyC-CaP Cas9 F12 clone showed lower efficacy of Cas9 cleaving (**Figure 3-3D**), although this may be allotted to a lower expression of the Cas9 protein. Nonetheless, ensuring that Cas9 is functional in Cas9-expressing cell lines is critical to ensure proper experimental completion of a CRISPR/Cas9 KO screen. The Cas9 transfection also seemed to affect the proliferation behavior of the cells. For example, the MyC-CaP Cas9 B1 clone, the MyC-CaP Cas9

B8 clone, and the MyC-CaP Cas9 F12 clone proliferate at higher rates than the MyC-CaP parental cell line (**Figure 3-3B & Supplementary Figure 4-2A-D**). By generating and characterizing single-cell derived MyC-CaP Cas9 clones from our MyC-CaP Cas9 stable cell line, we ensured that the clone selected for our *in vitro* CRISPR/Cas9 KO screen had uniform expression of an enzymatically functional Cas9 protein while also proliferating similarly to its unedited parental counterpart.

4.3. Validation of the role of key oncogenes and tumor-suppressor genes in MYC-driven prostate cancer

Our results revealed epigenetic regulators which are essential for prostate cancer cell proliferation and survival in a MYC-overexpressing context. Some of the hits from our screens including *MYC*, *Ar, Foxa1, Pten* and *Rb1* are genes that have already been established as playing key role in prostate cancer progression [106, 247, 255-257, 265, 266]. While MYC overexpression has been shown to be sufficient to initiate prostate cancer [111], the results from our screen indicate that continued overexpression of MYC is required for the proliferation or survival of the MyC-CaP cell line. The ligand-inducible transcription factor *AR* is a critical player in the development and maintenance of normal prostatic tissue, and a driver of CRPC [255]. Although the AR and MYC are both central players in prostate cancer, the interplay between the two transcription factors remains widely unexplored. Interestingly, Qiu *et al*. recently demonstrated that MYC-overexpression contributes to tumor initiation and progression by disrupting the AR transcriptional program [271]. The results from our screen demonstrate that *AR* expression confers a growth advantage in MYC-driven prostate cancer, further indicating a crucial link between the AR and MYC-overexpression. The pioneer transcription factor *FOXA1* is well-characterized in prostate

cancer and is known to play a key role in disease progression [256, 257]. FOXA1 is recruited to sites with H3K4me1 or H3K4me2 marks and is required to decondense the chromatin at these sites, making them accessible to other transcription factors, such as the AR [257]. The *FOXA1* gene is recurrently mutated in The Cancer Genome Atlas (TCGA)'s characterization of 333 primary prostate cancers, and *FOXA1* mutations define a molecular subtype of the disease [272]. Indeed, FOXA1 plays a key role in AR-dependent prostate cancer progression mainly due to its ability to modulate the AR cistrome. Pomerantz *et al*., demonstrated that there is an extensive overlap in FOXA1 and AR binding at tumor-associated AR binding sites [273]. They further showed that transduction of FOXA1 in an immortalize prostate cell line reprogrammed the AR cistrome to resemble that of a of prostate tumor sites [273], linking FOXA1 to AR reprogramming and demonstrating its capacity as a pioneer transcription factor during tumorigenesis. Moreover, Qiu *et al*. demonstrated a link between FOXA1, the AR and MYC [271]. Indeed, they showed that MYC-overexpression results in a significant increase of AR binding sites, and that these binding sites are predominantly associated with FOXA1. Critically, FOXA1 occupancy was increased at AR-gained binding sites in MYC-transformed prostate tissues compared to wild-type tissues [271]. Thus, the results from our *in vitro* CRISPR/Cas9 KO screens are in line with what is known about the role of these transcription factors in prostate cancer and further indicates a link between the AR and MYC, as well as between FOXA1 and MYC.

Moreover, our results also indicate a key role of the well-known tumor suppressors *Pten* and *Rb1* in MYC-driven prostate cancer. Loss of *PTEN* is found in approximately 30% of primary tumors and up to 70% of metastatic cancers [100, 265], while loss of *RB1* is found in up to 45% of CRPC [100, 274]. Our screen revealed that the loss *Pten* and *Rb1* in MYC-driven prostate cancer cells allow them to thrive and proliferate, validating their role as key tumor-suppressors in a MYC-

overexpressing context of prostate cancer. Altogether, our results are in agreement with previous studies and validate the role of these epigenetic regulators in the context of MYC-overexpressing prostate cancer.

4.4. Epigenetic dependencies of MYC-driven prostate cancer cellular proliferation and survival

Furthermore, the results from our screen identified new key epigenetic regulators that are essential in the context of MYC-driven prostate cancer. For example, the transcription factor *Gata3* was significantly depleted in our screens. *Gata3* inactivation in *Pten*-deficient tissue has been previously shown to accelerate tumor progression [258]. However, the KO of *Gata3* in the MyC-CaP cell line resulted in slower proliferation rates or cell death, indicating a differential role of *Gata3* in different molecular contexts of prostate cancer. The transcription factor *Fosl1* was another one of the significantly depleted genes in our screens. Previous studies have demonstrated that *FOSL1* promotes prostate cancer progression [259-261]. For instance, Luo and colleagues demonstrated that *FOSL1* can promote the occurrence and progression of prostate cancer by altering the epithelial-mesenchymal transition process of the cells [259]. Specifically, transwell experiments demonstrated that *FOSL1* could enhance prostate cancer metastasis while *in vivo* experiments demonstrated that *FOSL1* promotes an accelerated progression of prostate cancer [259]. In line with previous reports, our results demonstrate that *Fosl1* plays an oncogenic role in MYC-driven prostate cancer. The Methyltransferases *Mettl1* and *Setd8* were both significantly depleted in our screens. *METTL1* is responsible for mediating the formation of N(7)-methylguanine (m^7G) and regulating RNA translation , and upregulation of *METTL1* expression has been shown to promote oncogenic activity [275-277].For example, overexpression of *METTL1*

has been shown to promote tumor proliferation in in hepatocellular carcinoma, liver cancer and colon cancer [275-277]. Along the same lines, our screen indicates that *Mettl1* confers a growth advantage in MYC-overexpressing prostate cancer cells. Similarly, *SETD8* has been shown to be involved in different types of cancers [278-280]. *SETD8* is found as the only known lysine mono-methyltransferase in mammalian cells to produce H4K20me1, which plays a critical role in in chromatin compaction, gene regulation and cell-cycle progression [263]. Interestingly, *SETD8* was recently suggested to play a role in mediating MYC-driven medulloblastoma tumorigenesis [280]. Moreover, global chromatin profiling of tumors from mice overexpressing the *c-MYC* transgene in the prostate epithelium revealed that the H4K20 mark was significantly affected compared to WT mice [45]. In line with previous studies, our results indicate a key role of *Setd8* in MYC-overexpressing prostate cancer proliferation, which further suggest a specific role of *Setd8* in MYC-induced prostate cancer growth. The chromatin remodeling factor *RBBP7* chaperones chromatin remodeling proteins to their nuclear histone substrates including HATS and HDACs and plays conflicting roles in tumor progression in different types of cancer [264, 281]. *RBBP7* has demonstrated co-suppressive functions in prostate cancer cell lines when the tumor suppressor *HNF1B* is present [177]. Our results suggest that *Rbbp7* confers a growth advantage in MYC-overexpressing prostate cancer cells, thus indicating a potential context-dependent role of *Rbbp7* in prostate cancer. *UHRF1* and *DCAF1* are protein-coding genes which are involved in epigenetic remodeling. *UHRF1* encodes a member of a subfamily of RING-finger type E3 ubiquitin ligases (Ubiquitin-Like-Containing PHD And RING Finger Domains Protein 1) which acts as a key epigenetic regulator by bridging DNA methylation and chromatin modification [282]. Specifically, it binds hemi-methylated DNA at replication forks and recruits DNMT1 methyltransferase to ensure faithful propagation of the DNA methylation patterns through DNA replication [282]. In

addition, it recognizes and binds H3K9me3 and H3R2me0 respectively, and recruits chromatin proteins [282]. Babbio *et al*. reported that *UHRF1* is frequently overexpressed in human prostate tumours and has an important role in prostate cancer pathogenesis and progression [283]. They also reported that *UHRF1* expression was negatively correlated with several tumour suppressor genes. Similarly, to of *UHRF1*, *DCAF1* encodes for a component of E3 ubiquitin-protein ligase complexes (VPRBP) which is involved in various biological processes including histone modification [284]. *DCAF1* has been shown to phosphorylate histone H2A at T120 and to be associated with elevated levels of H2AT120 in prostate cancer tissues [285]. Interestingly, *DCAF1* has also been implicated in controlling the transcriptional activity of the tumor suppressor p53 [286]. For example, Kim *et al*. demonstrated that *DCAF1* interacts with p53 and is recruited to the promoters of p53 target genes, functioning to block transcriptional activation via acetylation of histone-H3 tails [286]. In line with these studies, our data shows that knockdown of *Uhrf1* and *Dcaf1* leads to a decrease in cellular proliferation in MYC-driven prostate cancer, which may be due, in part, to the reactivation of tumor-suppressor genes.

Moreover, the histone chaperone *Hira* and the lysine-specific demethylase *Kdm3b* were both significantly enriched in our screens. The HIRA complex deposits H3.3 at euchromatin regions such as promoters, enhancers, and gene regulatory regions, and is involved in cellular senescence and carcinogenesis [267, 287]. Cellular senescence is a tumor suppressive mechanism, and our result demonstrate that *Hira* has tumor suppressive functions in MYC-induce cellular proliferation, indicating a potential link between HIRA and cancer cells cellular senescence in a MYC context. *KDM3B* catalyzes demethylation of H3K9me1 and H3K9me2, resulting mostly in the activation of gene transcription [268]. *KDM3B* has recently been shown to act as an important player for proliferation of AR-expressing androgen-independent CRPC cells (LNCaP-abl and

LNAI) [288]. However, the results from our screens demonstrate that *Kdm3b* maintains tumor-suppressive functions in our androgen-dependent MYC-driven prostate cancer cells (MyC-CaP), suggesting that the role of *Kdm3b* in prostate cancer growth may by context-dependent.

Altogether, the results from our *in vitro* CRISPR/Cas9 KO screen demonstrates that epigenetic regulators are key in maintaining prostate cancer cellular proliferation in a MYC-overexpressing context. MYC-overexpression has been shown to give rise to global metabolic reprograming events which support cancer cell proliferation and growth [247, 248]. Epigenetic remodeling relies on metabolites as substrates and cofactors, therefore, MYC dysregulation may result in dependency to epigenetic regulators due to global metabolic reprograming. Further experiments are required to validate and characterize epigenetic dependencies in MYC-induced prostate cancer growth.

4.5. Clinical implications of epigenetic dependencies in MYC-driven prostate cancer

Studies have demonstrated that targeting epigenetic regulators is an effective way to supress prostate cancer growth. For example, targeting the methyltransferase *METTL1,* leading to impaired expression of m^7G transfer RNAs (tRNAs), has been shown to suppress tumor growth in various xenograft models including glioblastoma multiforme, liposarcoma, melanoma, and acute myeloid leukemia [262, 289]. Moreover, knockdown of *UHRF1* has been shown to reduce proliferation of prostate cancer cells and result in the reactivation of several tumour suppressor genes [283]. Recently, Poulose *et al.* showed that the protein encoded by *DCAF1*, VPRBP, is co-regulated by the AR at the transcript level and by O-GlcNAc transferase at the protein level, and that VPRBP

knockdown in prostate cancer cells let to a significant decrease in cell proliferation and increased p53 recruitment to the chromatin [290].

Moreover, drugs have targeting epigenetic regulators have been developed for the treatment of several types of cancer. For instance, *AR* is the most established therapeutic target for prostate cancer and targeting the AR signaling axis via ADT is currently the first line of treatment for patients with the disease. However, resistance to ADT usually arises, after which patients are usually treated with second-generation anti-androgen drugs. Although second-generation AR-targeting drugs are initially effective, resistance ultimately occurs, highlighting the need for new therapeutic strategies blocking continued AR-signaling. Other epigenetic-targeting drugs such EZH2 inhibitors [183, 184], BET inhibitors [195], and p300/CPB inhibitors [195] are currently undergoing clinical trials for the treatment of prostate cancer and have shown promising therapeutic effects. Notwithstanding, these epigenetic-targeting drugs are not sufficient on their own to supress prostate cancer growth, but rather, they are combined with other drugs (*e.g.*, abiraterone, enzalutamide) in order to achieve optimal therapeutic benefits. Keeping that into considering, it is unlikely that any of the epigenetic targets identified in our *in vitro* CRISPR/Cas9 KO screens will work as single-agent therapy but instead could be coupled with other therapeutic strategies to treat patients with MYC-driven prostate cancers. For instance, it has been shown that a diet rich in saturated fat enhances MYC-driven prostate cancer growth through amplification of a MYC transcriptional signature [45]. Notably, a fundamental feature of epigenetic modifications is its reliance on substrates or cofactors obtained from the diet. Therefore, epigenetic-targeted therapy could be combined with precision nutrition strategies to treat prostate cancer patients. Altogether, a better understanding of the role of epigenetic regulators in prostate cancer

progression, could lead to the development of new therapeutic strategies and improve prostate cancer treatment.

4.6. Limitations of the study and potential future experiments

While the experiment completed to date points to several interesting key epigenetic regulators in MYC-driven prostate cancer, much work still needs to be done to validate and characterize epigenetic dependencies. The most significant limitation associated with our experiment is possible false positive and false negative hits resulting from off-target effects from non-specific cuts in the DNA. To address this issue, validation of the candidate genes will be necessary. Validation can be done by performing arrayed *in vitro* CRISPR/Cas9 KO screens for each of the selected candidate genes. For instance, performing arrayed *in vitro* CRISPR/Cas9 KO screens using separate sets of sgRNAs targeting some promising candidates such *Gata3, Fosl1, Mettl1, Setd8, Rbbp7, Uhrf1*, and *Dcaf1* will enable a direct assessment of genotype-phenotype effects and validate the role of these candidate genes as essential in MYC-driven prostate cancer cellular proliferation. Another limitation of our study is that biases may arise throughout a CRISPR/Cas9 KO screen due to differential sgRNA cutting efficiency. To overcome this issue, combinations of sgRNAs that are different from the original screen may be used for subsequent screening, which will also further validate our candidate genes.

Moreover, once the hits from our screens have been validated, further experiments can be performed to characterize the candidate genes. In order to do so, we could begin by generating candidate genes-KO MyC-CaP stable cell lines. Validation of the genome edit can be done by PCR and Western Blot (if an antibody is available). Next, several *in vitro* experiments can be performed to determine the role of the candidate genes in different biological processes. For example, if the

candidate gene that we select is found to be involved cell cycle regulation and cellular metabolism, cell cycle analysis and mitochondrial stress tests comparing the MyC-CaP WT cell line to the candidate gene-KO MyC-CaP stable cell line could be performed to assess the role of the candidate gene in these pathways. Next, to further characterize the candidate genes and the effects of their KO on the MYC-induced transcriptional reprograming, we could perform ATAC-seq on the candidate gene-KO MyC-CaP stable cell line as well as the MyC-CaP WT cell line to identify regions with high chromatin plasticity specific to the candidate gene-KO and their underlying DNA binding motifs. DNA binding motif analyses of highly plastic chromatin region will enable the identification of transcription factors likely to contribute to the preservation of a defined transcriptional program. In this line, we could also carry out RNA-seq on the candidate gene-KO MyC-CaP stable cell line as well as the MyC-CaP WT cell line followed by GSEA analyses to determine the cellular transcriptional program characteristic to the candidate genes KO. Additionally, based on the known role of the candidate genes or their impact on the epigenetic landscape, we could perform ChIP-seq for relevant histone marks specific to the candidate gene KO using again the candidate gene-KO MyC-CaP stable cell line as well as the MyC-CaP WT cell line. This would allow us to establish the landscape of *in vitro* epigenetic dependencies in MYC-driven prostate cancer.

According to our results, the epigenetic-related genes *Uhrf1* and *Dcaf1* seem to be essential specifically in the MyC-CaP prostate cancer cell line. Experiments that would allow the comparison between MYC-overexpressing and MYC-null contexts could be performed to assess the specificity of these epigenetic regulators to a MYC-overexpressing context of prostate cancer. For example, generation of stable MYC KO prostate cancer cell lines and subsequent *in vitro*

CRISPR/Cas9 KO screening would enable the investigation of the candidate gene in both contexts and the assessment of their specificity to MYC-induced prostate cancer cellular proliferation.

While *in vitro* CRISPR screening in cancer cells is useful to identify genes essential to cellular proliferation, it fails to recapitulate the physiological environment of cancer. In order to identify unique epigenetic dependencies that may be left uncovered by *in vitro* screening and to better recapitulate complex cellular interactions, we could perform an *in vivo* CRISPR/Cas9 KO screen. Taking advantage of the small-scale of our custom CRISPR/Cas9 sgRNA libraries, we could transduce MyC-CaP cells with our libraries, harvest the cells following antibiotic selection and inject them into mice. Importantly, this would allow to explore the effect of knocking-out specific epigenetic regulators on tumor growth and identify *in vivo* epigenetic dependencies in a MYC-overexpressing context.

The epigenetic landscape is intimately linked to metabolite availability and dietary intake of specific nutrients may enhance certain epigenetic signature. Interestingly, Labbé *et al*. demonstrated that MYC-driven transformation of the murine prostate results in hypomethylation of H4K20, which was further enhanced by a high-fat diet [45]. They further demonstrated that the MYC-transcriptional signature was amplified in high-fat diet-fed Hi-MYC mice, providing a potential link between diet, epigenetic modifications, and the regulation of oncogenic programs. Given that fundamental feature of epigenetic remodeling is its reliance on substrates or cofactors obtained from the diet and along with the evidence that a high-fat diet amplifies the MYC-transcriptional signature, it would be interesting to investigate the effect of a diet rich in saturated fat on epigenetic dependencies in a MYC-overexpressing context. In this line of thought, we could perform *in vivo* CRISPR/Cas9 KO screens where infected MyC-CaP cells will be injected into mice fed either a diet rich in saturated fat or a control diet. This could allow us to investigate the

effect of a diet rich in saturated fat on MYC-driven prostate cancer and potentially identify diet-dependent epigenetic-dependencies.

4.7. Conclusions and future perspectives

The results presented in this study are favorable regarding the role of epigenetic regulators in MYC-driven prostate cancer growth. In addition to reinforcing the role of already-established oncogenes and tumor-suppressor genes, our results revealed new potential epigenetic dependencies of MYC-overexpressing prostate cancer cellular proliferation. Future studies will focus on validating and characterizing the role of epigenetic regulators in MYC-driven prostate cancer. We hope that by elucidating the epigenetic expression patterns necessary for MYC-driven prostate cancer to thrive, we can identify novel therapeutically targetable epigenetic mechanisms.

REFERENCES

1. Cunha, G.R., et al., *Development of the human prostate.* Differentiation, 2018. **103**: p. 24-45.
2. Coakley, F.V. and H. Hricak, *Radiologic anatomy of the prostate gland: a clinical approach.* Radiol Clin North Am, 2000. **38**(1): p. 15-30.
3. McNeal, J.E., *The zonal anatomy of the prostate.* Prostate, 1981. **2**(1): p. 35-49.
4. McNeal, J.E., et al., *Zonal distribution of prostatic adenocarcinoma. Correlation with histologic pattern and direction of spread.* Am J Surg Pathol, 1988. **12**(12): p. 897-906.
5. Lee, J.J., et al., *Biologic differences between peripheral and transition zone prostate cancer.* Prostate, 2015. **75**(2): p. 183-90.
6. Ittmann, M., *Anatomy and Histology of the Human and Murine Prostate.* Cold Spring Harb Perspect Med, 2018. **8**(5).
7. Huang, Y.H., Y.Q. Zhang, and J.T. Huang, *Neuroendocrine cells of prostate cancer: biologic functions and molecular mechanisms.* Asian J Androl, 2019. **21**(3): p. 291-295.
8. Kurita, T., et al., *Role of p63 and basal cells in the prostate.* Development, 2004. **131**(20): p. 4955-64.
9. Goldstein, A.S., et al., *Identification of a cell of origin for human prostate cancer.* Science, 2010. **329**(5991): p. 568-71.
10. Wang, Z.A., et al., *Luminal cells are favored as the cell of origin for prostate cancer.* Cell Rep, 2014. **8**(5): p. 1339-46.
11. di Sant'Agnese, P.A., *Neuroendocrine cells of the prostate and neuroendocrine differentiation in prostatic carcinoma: a review of morphologic aspects.* Urology, 1998. **51**(5A Suppl): p. 121-4.
12. Spetsieris, N., et al., *Neuroendocrine and Aggressive-Variant Prostate Cancer.* Cancers (Basel), 2020. **12**(12).
13. Xie, Y., S. Ning, and J. Hu, *Molecular mechanisms of neuroendocrine differentiation in prostate cancer progression.* Journal of Cancer Research and Clinical Oncology, 2022. **148**(7): p. 1813-1823.
14. Wang, H.T., et al., *Neuroendocrine Prostate Cancer (NEPC) progressing from conventional prostatic adenocarcinoma: factors associated with time to development of NEPC and survival from NEPC diagnosis-a systematic review and pooled analysis.* J Clin Oncol, 2014. **32**(30): p. 3383-90.
15. Sung, H., et al., *Global Cancer Statistics 2020: GLOBOCAN Estimates of Incidence and Mortality Worldwide for 36 Cancers in 185 Countries.* CA Cancer J Clin, 2021. **71**(3): p. 209-249.
16. LeBlanc, A.G., A. Demers, and A. Shaw, *Recent trends in prostate cancer in Canada.* Health Rep, 2019. **30**(4): p. 12-17.
17. Brenner, D.R., et al., *Projected estimates of cancer in Canada in 2022.* Cmaj, 2022. **194**(17): p. E601-e607.
18. Gandaglia, G., et al., *Epidemiology and Prevention of Prostate Cancer.* Eur Urol Oncol, 2021. **4**(6): p. 877-892.
19. Matrana, M.R. and B. Atkinson, *Screening for prostate cancer: the debate continues.* J Adv Pract Oncol, 2013. **4**(1): p. 16-21.

20. Patel, A.R. and E.A. Klein, *Risk factors for prostate cancer.* Nat Clin Pract Urol, 2009. **6**(2): p. 87-95.
21. Barber, L., et al., *Family History of Breast or Prostate Cancer and Prostate Cancer Risk.* Clin Cancer Res, 2018. **24**(23): p. 5910-5917.
22. Bostwick, D.G., et al., *Human prostate cancer risk factors.* Cancer, 2004. **101**(10 Suppl): p. 2371-490.
23. Bratt, O., *Hereditary prostate cancer: clinical aspects.* J Urol, 2002. **168**(3): p. 906-13.
24. Bratt, O., *Hereditary Prostate Cancer: Clinical Aspects.* The Journal of Urology, 2002. **168**(3): p. 906-913.
25. Madersbacher, S., et al., *The influence of family history on prostate cancer risk: implications for clinical management.* BJU Int, 2011. **107**(5): p. 716-721.
26. Ren, Z.J., et al., *First-degree family history of breast cancer is associated with prostate cancer risk: a systematic review and meta-analysis.* BMC Cancer, 2019. **19**(1): p. 871.
27. Rantapero, T., et al., *Inherited DNA Repair Gene Mutations in Men with Lethal Prostate Cancer.* Genes (Basel), 2020. **11**(3).
28. Gillanders, E.M., et al., *Combined genome-wide scan for prostate cancer susceptibility genes.* J Natl Cancer Inst, 2004. **96**(16): p. 1240-7.
29. Das, S., et al., *Bringing Prostate Cancer Germline Genetics into Clinical Practice.* J Urol, 2019. **202**(2): p. 223-230.
30. Zhen, J.T., et al., *Genetic testing for hereditary prostate cancer: Current status and limitations.* Cancer, 2018. **124**(15): p. 3105-3117.
31. Yap, T.A., et al., *The DNA Damaging Revolution: PARP Inhibitors and Beyond.* Am Soc Clin Oncol Educ Book, 2019. **39**: p. 185-195.
32. Das, S., et al., *Bringing Prostate Cancer Germline Genetics into Clinical Practice.* Journal of Urology, 2019. **202**(2): p. 223-230.
33. Pomerantz, M.M., et al., *The association between germline BRCA2 variants and sensitivity to platinum-based chemotherapy among men with metastatic prostate cancer.* Cancer, 2017. **123**(18): p. 3532-3539.
34. Rawla, P., *Epidemiology of Prostate Cancer.* World J Oncol, 2019. **10**(2): p. 63-89.
35. Gupta, S., et al., *Prostate Cancer: How Young is too Young?* Curr Urol, 2017. **9**(4): p. 212-215.
36. Siegel, R.L., K.D. Miller, and A. Jemal, *Cancer statistics, 2020.* CA Cancer J Clin, 2020. **70**(1): p. 7-30.
37. Hur, J. and E. Giovannucci, *Racial differences in prostate cancer: does timing of puberty play a role?* Br J Cancer, 2020. **123**(3): p. 349-354.
38. Martin, D.N., A.M. Starks, and S. Ambs, *Biological determinants of health disparities in prostate cancer.* Curr Opin Oncol, 2013. **25**(3): p. 235-41.
39. Freedland, S.J. and W.B. Isaacs, *Explaining racial differences in prostate cancer in the United States: sociology or biology?* Prostate, 2005. **62**(3): p. 243-52.
40. Layne, T.M., et al., *Prostate cancer risk factors in black and white men in the NIH-AARP Diet and Health Study.* Prostate Cancer Prostatic Dis, 2019. **22**(1): p. 91-100.
41. Shimizu, H., et al., *Cancers of the prostate and breast among Japanese and white immigrants in Los Angeles County.* Br J Cancer, 1991. **63**(6): p. 963-6.
42. Fujita, K., et al., *Obesity, Inflammation, and Prostate Cancer.* J Clin Med, 2019. **8**(2).
43. Darcey, E. and T. Boyle, *Tobacco smoking and survival after a prostate cancer diagnosis: A systematic review and meta-analysis.* Cancer Treat Rev, 2018. **70**: p. 30-40.

44. Darlington, G.A., et al., *Prostate cancer risk and diet, recreational physical activity and cigarette smoking.* Chronic Dis Can, 2007. **27**(4): p. 145-53.
45. Labbé, D.P., et al., *High-fat diet fuels prostate cancer progression by rewiring the metabolome and amplifying the MYC program.* Nat Commun, 2019. **10**(1): p. 4358.
46. Higdon, J.V., et al., *Cruciferous vegetables and human cancer risk: epidemiologic evidence and mechanistic basis.* Pharmacol Res, 2007. **55**(3): p. 224-36.
47. Gann, P.H., et al., *Lower prostate cancer risk in men with elevated plasma lycopene levels: results of a prospective analysis.* Cancer Res, 1999. **59**(6): p. 1225-30.
48. Peisch, S.F., et al., *Prostate cancer progression and mortality: a review of diet and lifestyle factors.* World J Urol, 2017. **35**(6): p. 867-874.
49. Naji, L., et al., *Digital Rectal Examination for Prostate Cancer Screening in Primary Care: A Systematic Review and Meta-Analysis.* Ann Fam Med, 2018. **16**(2): p. 149-154.
50. Ilic, D., et al., *Prostate cancer screening with prostate-specific antigen (PSA) test: a systematic review and meta-analysis.* Bmj, 2018. **362**: p. k3519.
51. Eklund, M., et al., *MRI-Targeted or Standard Biopsy in Prostate Cancer Screening.* N Engl J Med, 2021. **385**(10): p. 908-920.
52. Telloni, S.M., *Tumor Staging and Grading: A Primer.* Methods Mol Biol, 2017. **1606**: p. 1-17.
53. Schatten, H., *Brief Overview of Prostate Cancer Statistics, Grading, Diagnosis and Treatment Strategies.* Adv Exp Med Biol, 2018. **1095**: p. 1-14.
54. Kweldam, C.F., G.J. van Leenders, and T. van der Kwast, *Grading of prostate cancer: a work in progress.* Histopathology, 2019. **74**(1): p. 146-160.
55. Choo, R., et al., *Feasibility study: watchful waiting for localized low to intermediate grade prostate carcinoma with selective delayed intervention based on prostate specific antigen, histological and/or clinical progression.* J Urol, 2002. **167**(4): p. 1664-9.
56. Klotz, L., et al., *Long-term follow-up of a large active surveillance cohort of patients with prostate cancer.* J Clin Oncol, 2015. **33**(3): p. 272-7.
57. Bul, M., et al., *Active surveillance for low-risk prostate cancer worldwide: the PRIAS study.* Eur Urol, 2013. **63**(4): p. 597-603.
58. Scott, E., et al., *Intermediate and longer-term outcomes from a prospective active-surveillance program for favorable-risk prostate cancer. Tosoian JJ, Mamawala M, Epstein JI, Landis P, Wolf S, Trock BJ, Carter HB.J Clin Oncol. 2015 Oct 20;33(30):3379-85. [Epub 2015 Aug 31]. doi: 10.1200/JCO.2015.62.5764.* Urol Oncol, 2017. **35**(3): p. 121-122.
59. Klotz, L., *Active surveillance in intermediate-risk prostate cancer.* BJU Int, 2020. **125**(3): p. 346-354.
60. Hoffman, K.E., et al., *Patient-Reported Outcomes Through 5 Years for Active Surveillance, Surgery, Brachytherapy, or External Beam Radiation With or Without Androgen Deprivation Therapy for Localized Prostate Cancer.* Jama, 2020. **323**(2): p. 149-163.
61. Huggins, C. and C.V. Hodges, *Studies on prostatic cancer: I. The effect of castration, of estrogen and of androgen injection on serum phosphatases in metastatic carcinoma of the prostate. 1941.* J Urol, 2002. **168**(1): p. 9-12.
62. Selvi, I. and H. Basar, *Subcapsular orchiectomy versus total orchiectomy and LHRH analogue in the treatment of hormone-sensitive metastatic prostate cancer: a different*

perspective in evaluation of the psychosocial effects. Support Care Cancer, 2020. **28**(9): p. 4313-4326.
63. Thomsen, F.B., et al., *Gonadotropin-releasing Hormone Agonists, Orchiectomy, and Risk of Cardiovascular Disease: Semi-ecologic, Nationwide, Population-based Study.* Eur Urol, 2017. **72**(6): p. 920-928.
64. Krahn, M., et al., *Androgen deprivation therapy in prostate cancer: are rising concerns leading to falling use?* BJU Int, 2011. **108**(10): p. 1588-96.
65. Garje, R., et al., *Utilization and Outcomes of Surgical Castration in Comparison to Medical Castration in Metastatic Prostate Cancer.* Clin Genitourin Cancer, 2020. **18**(2): p. e157-e166.
66. Weiner, A.B., et al., *Surgical versus Medical Castration for Metastatic Prostate Cancer: Use and Overall Survival in a National Cohort.* J Urol, 2020. **203**(5): p. 933-939.
67. Sun, M., et al., *Comparison of Gonadotropin-Releasing Hormone Agonists and Orchiectomy: Effects of Androgen-Deprivation Therapy.* JAMA Oncol, 2016. **2**(4): p. 500-7.
68. Bekelman, J.E., et al., *Clinically Localized Prostate Cancer: ASCO Clinical Practice Guideline Endorsement of an American Urological Association/American Society for Radiation Oncology/Society of Urologic Oncology Guideline.* J Clin Oncol, 2018. **36**(32): p. 3251-3258.
69. Kamran, S.C. and A.V. D'Amico, *Radiation Therapy for Prostate Cancer.* Hematol Oncol Clin North Am, 2020. **34**(1): p. 45-69.
70. Den, R.B., L.A. Doyle, and K.E. Knudsen, *Practical guide to the use of radium 223 dichloride.* Can J Urol, 2014. **21**(2 Supp 1): p. 70-6.
71. Gallicchio, R., et al., *Radium-223 for the treatment of bone metastases in castration-resistant prostate cancer: when and why.* Tumori, 2019. **105**(5): p. 367-377.
72. Nilsson, S., et al., *First clinical experience with alpha-emitting radium-223 in the treatment of skeletal metastases.* Clin Cancer Res, 2005. **11**(12): p. 4451-9.
73. Nilsson, S., et al., *Bone-targeted radium-223 in symptomatic, hormone-refractory prostate cancer: a randomised, multicentre, placebo-controlled phase II study.* Lancet Oncol, 2007. **8**(7): p. 587-94.
74. Parker, C., et al., *Alpha emitter radium-223 and survival in metastatic prostate cancer.* N Engl J Med, 2013. **369**(3): p. 213-23.
75. Keam, S.J., *Lutetium Lu 177 Vipivotide Tetraxetan: First Approval.* Mol Diagn Ther, 2022: p. 1-9.
76. Van Poppel, H. and P.A. Abrahamsson, *Considerations for the use of gonadotropin-releasing hormone agonists and antagonists in patients with prostate cancer.* Int J Urol, 2020. **27**(10): p. 830-837.
77. Yin, L. and Q. Hu, *CYP17 inhibitors--abiraterone, C17,20-lyase inhibitors and multi-targeting agents.* Nat Rev Urol, 2014. **11**(1): p. 32-42.
78. Barata, P.C. and A.O. Sartor, *Metastatic castration-sensitive prostate cancer: Abiraterone, docetaxel, or….* Cancer, 2019. **125**(11): p. 1777-1788.
79. de Bono, J.S., et al., *Prednisone plus cabazitaxel or mitoxantrone for metastatic castration-resistant prostate cancer progressing after docetaxel treatment: a randomised open-label trial.* Lancet, 2010. **376**(9747): p. 1147-54.
80. Kantoff, P.W., et al., *Sipuleucel-T immunotherapy for castration-resistant prostate cancer.* N Engl J Med, 2010. **363**(5): p. 411-22.

81. Wolchok, J.D., et al., *Overall Survival with Combined Nivolumab and Ipilimumab in Advanced Melanoma.* N Engl J Med, 2017. **377**(14): p. 1345-1356.
82. Motzer, R.J., et al., *Nivolumab plus Ipilimumab versus Sunitinib in Advanced Renal-Cell Carcinoma.* N Engl J Med, 2018. **378**(14): p. 1277-1290.
83. Reck, M., et al., *Pembrolizumab versus Chemotherapy for PD-L1-Positive Non-Small-Cell Lung Cancer.* N Engl J Med, 2016. **375**(19): p. 1823-1833.
84. Hansen, A.R., et al., *Pembrolizumab for advanced prostate adenocarcinoma: findings of the KEYNOTE-028 study.* Annals of Oncology, 2018. **29**(8): p. 1807-1813.
85. Tucker, M.D., et al., *Pembrolizumab in men with heavily treated metastatic castrate-resistant prostate cancer.* Cancer Medicine, 2019. **8**(10): p. 4644-4655.
86. Antonarakis, E.S., et al., *Pembrolizumab for Treatment-Refractory Metastatic Castration-Resistant Prostate Cancer: Multicohort, Open-Label Phase II KEYNOTE-199 Study.* Journal of Clinical Oncology, 2020. **38**(5): p. 395-405.
87. GREWAL, K., K. GREWAL, and I.A. TABBARA, *PARP Inhibitors in Prostate Cancer.* Anticancer Research, 2021. **41**(2): p. 551-556.
88. Saad, F., et al., *Niraparib with androgen receptor-axis-targeted therapy in patients with metastatic castration-resistant prostate cancer: safety and pharmacokinetic results from a phase 1b study (BEDIVERE).* Cancer Chemother Pharmacol, 2021. **88**(1): p. 25-37.
89. Arora, K. and C.E. Barbieri, *Molecular Subtypes of Prostate Cancer.* Current Oncology Reports, 2018. **20**(8): p. 58.
90. Abeshouse, A., et al., *The Molecular Taxonomy of Primary Prostate Cancer.* Cell, 2015. **163**(4): p. 1011-1025.
91. Tomlins, S.A., et al., *ETS gene fusions in prostate cancer: from discovery to daily clinical practice.* Eur Urol, 2009. **56**(2): p. 275-86.
92. Tomlins, S.A., et al., *Recurrent fusion of TMPRSS2 and ETS transcription factor genes in prostate cancer.* Science, 2005. **310**(5748): p. 644-8.
93. Hermans, K.G., et al., *Truncated ETV1, fused to novel tissue-specific genes, and full-length ETV1 in prostate cancer.* Cancer Res, 2008. **68**(18): p. 7541-9.
94. Kumar-Sinha, C., S.A. Tomlins, and A.M. Chinnaiyan, *Recurrent gene fusions in prostate cancer.* Nat Rev Cancer, 2008. **8**(7): p. 497-511.
95. Rubin, M.A., C.A. Maher, and A.M. Chinnaiyan, *Common gene rearrangements in prostate cancer.* J Clin Oncol, 2011. **29**(27): p. 3659-68.
96. Barbieri, C.E., et al., *Exome sequencing identifies recurrent SPOP, FOXA1 and MED12 mutations in prostate cancer.* Nat Genet, 2012. **44**(6): p. 685-9.
97. Li, J., et al., *A genomic and epigenomic atlas of prostate cancer in Asian populations.* Nature, 2020. **580**(7801): p. 93-99.
98. Liu, W., et al., *Identification of novel CHD1-associated collaborative alterations of genomic structure and functional assessment of CHD1 in prostate cancer.* Oncogene, 2012. **31**(35): p. 3939-48.
99. Grasso, C.S., et al., *The mutational landscape of lethal castration-resistant prostate cancer.* Nature, 2012. **487**(7406): p. 239-43.
100. Taylor, B.S., et al., *Integrative genomic profiling of human prostate cancer.* Cancer Cell, 2010. **18**(1): p. 11-22.
101. Abida, W., et al., *Prospective Genomic Profiling of Prostate Cancer Across Disease States Reveals Germline and Somatic Alterations That May Affect Clinical Decision Making.* JCO Precision Oncology, 2017(1): p. 1-16.

102. Parimi, V., et al., *Neuroendocrine differentiation of prostate cancer: a review.* Am J Clin Exp Urol, 2014. **2**(4): p. 273-85.
103. Dang, C.V., *MYC on the path to cancer.* Cell, 2012. **149**(1): p. 22-35.
104. Kumar, A., et al., *Substantial interindividual and limited intraindividual genomic diversity among tumors from men with metastatic prostate cancer.* Nat Med, 2016. **22**(4): p. 369-78.
105. *The Molecular Taxonomy of Primary Prostate Cancer.* Cell, 2015. **163**(4): p. 1011-25.
106. Gurel, B., et al., *Nuclear MYC protein overexpression is an early alteration in human prostate carcinogenesis.* Mod Pathol, 2008. **21**(9): p. 1156-67.
107. Sato, H., et al., *Fluorescence in situ hybridization analysis of c-myc amplification in stage TNM prostate cancer in Japanese patients.* Int J Urol, 2006. **13**(6): p. 761-6.
108. Labbé, D.P. and M. Brown, *Transcriptional Regulation in Prostate Cancer.* Cold Spring Harb Perspect Med, 2018. **8**(11).
109. Hsieh, A.L., et al., *MYC and metabolism on the path to cancer.* Seminars in Cell & Developmental Biology, 2015. **43**: p. 11-21.
110. Stine, Z.E., et al., *MYC, Metabolism, and Cancer.* Cancer Discovery, 2015. **5**(10): p. 1024-1039.
111. Ellwood-Yen, K., et al., *Myc-driven murine prostate cancer shares molecular features with human prostate tumors.* Cancer Cell, 2003. **4**(3): p. 223-38.
112. Singh, K.B., et al., *A novel metabolic function of Myc in regulation of fatty acid synthesis in prostate cancer.* Oncogene, 2021. **40**(3): p. 592-602.
113. Hempel Sullivan, H., et al., *Differential mast cell phenotypes in benign versus cancer tissues and prostate cancer oncologic outcomes.* The Journal of Pathology, 2021. **253**(4): p. 415-426.
114. Burkhart, D.L., et al., *Evidence that EZH2 Deregulation is an Actionable Therapeutic Target for Prevention of Prostate Cancer.* Cancer Prev Res (Phila), 2020. **13**(12): p. 979-988.
115. Simons, B.W., et al., *PSMA expression in the Hi-Myc model; extended utility of a representative model of prostate adenocarcinoma for biological insight and as a drug discovery tool.* Prostate, 2019. **79**(6): p. 678-685.
116. Watson, P.A., et al., *Context-Dependent Hormone-Refractory Progression Revealed through Characterization of a Novel Murine Prostate Cancer Cell Line.* Cancer Research, 2005. **65**(24): p. 11565-11571.
117. Ruggero, K., et al., *Epigenetic Regulation in Prostate Cancer Progression.* Curr Mol Biol Rep, 2018. **4**(2): p. 101-115.
118. Kgatle, M.M., et al., *Prostate Cancer: Epigenetic Alterations, Risk Factors, and Therapy.* Prostate Cancer, 2016. **2016**: p. 5653862.
119. Waddington, C.H., *The epigenotype. 1942.* Int J Epidemiol, 2012. **41**(1): p. 10-3.
120. Berdasco, M. and M. Esteller, *Aberrant epigenetic landscape in cancer: how cellular identity goes awry.* Dev Cell, 2010. **19**(5): p. 698-711.
121. Frame, F.M. and N.J. Maitland, *Epigenetic Control of Gene Expression in the Normal and Malignant Human Prostate: A Rapid Response Which Promotes Therapeutic Resistance.* Int J Mol Sci, 2019. **20**(10).
122. Dawson, M.A., *The cancer epigenome: Concepts, challenges, and therapeutic opportunities.* Science, 2017. **355**(6330): p. 1147-1152.

123. Conteduca, V., et al., *Epigenetics in prostate cancer: clinical implications.* Translational Andrology and Urology, 2021. **10**(7): p. 3104-3116.
124. Baylin, S.B., *DNA methylation and gene silencing in cancer.* Nat Clin Pract Oncol, 2005. **2 Suppl 1**: p. S4-11.
125. Kim, M. and J. Costello, *DNA methylation: an epigenetic mark of cellular memory.* Exp Mol Med, 2017. **49**(4): p. e322.
126. Wang, G., et al., *Genetics and biology of prostate cancer.* Genes Dev, 2018. **32**(17-18): p. 1105-1140.
127. Jasek, K., et al., *DNA Methylation Status in Cancer Disease: Modulations by Plant-Derived Natural Compounds and Dietary Interventions.* Biomolecules, 2019. **9**(7): p. 289.
128. Brooks, J.D., et al., *CG island methylation changes near the GSTP1 gene in prostatic intraepithelial neoplasia.* Cancer Epidemiol Biomarkers Prev, 1998. **7**(6): p. 531-6.
129. Nakayama, M., et al., *GSTP1 CpG island hypermethylation as a molecular biomarker for prostate cancer.* J Cell Biochem, 2004. **91**(3): p. 540-52.
130. Wu, T., et al., *Measurement of GSTP1 promoter methylation in body fluids may complement PSA screening: a meta-analysis.* Br J Cancer, 2011. **105**(1): p. 65-73.
131. Jerónimo, C., et al., *A quantitative promoter methylation profile of prostate cancer.* Clin Cancer Res, 2004. **10**(24): p. 8472-8.
132. Vleminckx, K., et al., *Genetic manipulation of E-cadherin expression by epithelial tumor cells reveals an invasion suppressor role.* Cell, 1991. **66**(1): p. 107-19.
133. Quinn, D.I., S.M. Henshall, and R.L. Sutherland, *Molecular markers of prostate cancer outcome.* Eur J Cancer, 2005. **41**(6): p. 858-87.
134. Li, L.C., et al., *Methylation of the E-cadherin gene promoter correlates with progression of prostate cancer.* J Urol, 2001. **166**(2): p. 705-9.
135. Yegnasubramanian, S., et al., *DNA hypomethylation arises later in prostate cancer progression than CpG island hypermethylation and contributes to metastatic tumor heterogeneity.* Cancer Res, 2008. **68**(21): p. 8954-67.
136. Florl, A.R., et al., *Coordinate hypermethylation at specific genes in prostate carcinoma precedes LINE-1 hypomethylation.* Br J Cancer, 2004. **91**(5): p. 985-94.
137. Ma, J., et al., *Overexpression of forkhead box M1 and urokinase-type plasminogen activator in gastric cancer is associated with cancer progression and poor prognosis.* Oncol Lett, 2017. **14**(6): p. 7288-7296.
138. Jaiswal, R.K., A.K. Varshney, and P.K. Yadava, *Diversity and functional evolution of the plasminogen activator system.* Biomed Pharmacother, 2018. **98**: p. 886-898.
139. Hagelgans, A., et al., *Deregulated expression of urokinase and its inhibitor type 1 in prostate cancer cells: role of epigenetic mechanisms.* Exp Mol Pathol, 2013. **94**(3): p. 458-65.
140. Kouzarides, T., *Chromatin modifications and their function.* Cell, 2007. **128**(4): p. 693-705.
141. Baylin, S.B. and P.A. Jones, *Epigenetic Determinants of Cancer.* Cold Spring Harb Perspect Biol, 2016. **8**(9).
142. Tollefsbol, T.O., *Chapter 1 - Epigenetics of Human Disease*, in *Epigenetics in Human Disease*, T.O. Tollefsbol, Editor. 2012, Academic Press: San Diego. p. 1-6.
143. Struhl, K., *Histone acetylation and transcriptional regulatory mechanisms.* Genes Dev, 1998. **12**(5): p. 599-606.

144. Jia, L., et al., *Genomic androgen receptor-occupied regions with different functions, defined by histone acetylation, coregulators and transcriptional capacity.* PLoS One, 2008. **3**(11): p. e3645.
145. Babu, D. and M.J. Fullwood, *Expanding the effects of ERG on chromatin landscapes and dysregulated transcription in prostate cancer.* Nat Genet, 2017. **49**(9): p. 1294-1295.
146. Adamo, P. and M.R. Ladomery, *The oncogene ERG: a key factor in prostate cancer.* Oncogene, 2016. **35**(4): p. 403-414.
147. Sugiura, M., et al., *Epigenetic modifications in prostate cancer.* Int J Urol, 2021. **28**(2): p. 140-149.
148. Ellinger, J., et al., *Global levels of histone modifications predict prostate cancer recurrence.* Prostate, 2010. **70**(1): p. 61-9.
149. Chen, Z., et al., *Histone modifications and chromatin organization in prostate cancer.* Epigenomics, 2010. **2**(4): p. 551-60.
150. Varambally, S., et al., *The polycomb group protein EZH2 is involved in progression of prostate cancer.* Nature, 2002. **419**(6907): p. 624-9.
151. Bryant, R.J., et al., *EZH2 promotes proliferation and invasiveness of prostate cancer cells.* Prostate, 2007. **67**(5): p. 547-56.
152. Xiang, Y., et al., *JARID1B is a histone H3 lysine 4 demethylase up-regulated in prostate cancer.* Proc Natl Acad Sci U S A, 2007. **104**(49): p. 19226-31.
153. Duan, L., et al., *KDM4/JMJD2 Histone Demethylase Inhibitors Block Prostate Tumor Growth by Suppressing the Expression of AR and BMYB-Regulated Genes.* Chem Biol, 2015. **22**(9): p. 1185-96.
154. Metzger, E., et al., *Phosphorylation of histone H3T6 by PKCbeta(I) controls demethylation at histone H3K4.* Nature, 2010. **464**(7289): p. 792-6.
155. Metzger, E., et al., *Phosphorylation of histone H3 at threonine 11 establishes a novel chromatin mark for transcriptional regulation.* Nat Cell Biol, 2008. **10**(1): p. 53-60.
156. Baumgart, S.J. and B. Haendler, *Exploiting Epigenetic Alterations in Prostate Cancer.* Int J Mol Sci, 2017. **18**(5).
157. Gillette, T.G. and J.A. Hill, *Readers, writers, and erasers: chromatin as the whiteboard of heart disease.* Circ Res, 2015. **116**(7): p. 1245-53.
158. Musselman, C., et al., *Perceiving the epigenetic landscape through histone readers.* Nature structural & molecular biology, 2012. **19**: p. 1218-27.
159. Sengupta, D., et al., *Disruption of BRD4 at H3K27Ac-enriched enhancer region correlates with decreased c-Myc expression in Merkel cell carcinoma.* Epigenetics, 2015. **10**(6): p. 460-6.
160. Urbanucci, A., et al., *Androgen Receptor Deregulation Drives Bromodomain-Mediated Chromatin Alterations in Prostate Cancer.* Cell Rep, 2017. **19**(10): p. 2045-2059.
161. Asangani, I.A., et al., *Therapeutic targeting of BET bromodomain proteins in castration-resistant prostate cancer.* Nature, 2014. **510**(7504): p. 278-82.
162. Huang, Z.-Q., et al., *A role for cofactor–cofactor and cofactor–histone interactions in targeting p300, SWI/SNF and Mediator for transcription.* The EMBO Journal, 2003. **22**(9): p. 2146-2155.
163. Marshall, T.W., et al., *Differential requirement of SWI/SNF for androgen receptor activity.* J Biol Chem, 2003. **278**(33): p. 30605-13.
164. Link, K.A., et al., *BAF57 governs androgen receptor action and androgen-dependent proliferation through SWI/SNF.* Mol Cell Biol, 2005. **25**(6): p. 2200-15.

165. Jin, M.L., Y.W. Kim, and K.W. Jeong, *BAF53A regulates androgen receptor-mediated gene expression and proliferation in LNCaP cells.* Biochemical and Biophysical Research Communications, 2018. **505**(2): p. 618-623.
166. Xiao, L., et al., *Targeting SWI/SNF ATPases in enhancer-addicted prostate cancer.* Nature, 2022. **601**(7893): p. 434-439.
167. Augello, M.A., et al., *CHD1 Loss Alters AR Binding at Lineage-Specific Enhancers and Modulates Distinct Transcriptional Programs to Drive Prostate Tumorigenesis.* Cancer Cell, 2019. **35**(4): p. 603-617.e8.
168. Zhang, Z., et al., *Loss of CHD1 Promotes Heterogeneous Mechanisms of Resistance to AR-Targeted Therapy via Chromatin Dysregulation.* Cancer Cell, 2020. **37**(4): p. 584-598.e11.
169. Fizazi, K., et al., *Darolutamide in Nonmetastatic, Castration-Resistant Prostate Cancer.* N Engl J Med, 2019. **380**(13): p. 1235-1246.
170. Smith, M.R., et al., *Apalutamide Treatment and Metastasis-free Survival in Prostate Cancer.* N Engl J Med, 2018. **378**(15): p. 1408-1418.
171. de Bono, J.S., et al., *Abiraterone and increased survival in metastatic prostate cancer.* N Engl J Med, 2011. **364**(21): p. 1995-2005.
172. Scher, H.I., et al., *Increased survival with enzalutamide in prostate cancer after chemotherapy.* N Engl J Med, 2012. **367**(13): p. 1187-97.
173. Liu, C., et al., *ARVib suppresses growth of advanced prostate cancer via inhibition of androgen receptor signaling.* Oncogene, 2021. **40**(35): p. 5379-5392.
174. Melnyk, J.E., et al., *Targeting a splicing-mediated drug resistance mechanism in prostate cancer by inhibiting transcriptional regulation by PKCβ1.* Oncogene, 2022. **41**(11): p. 1536-1549.
175. Ren, G., et al., *Polycomb protein EZH2 regulates tumor invasion via the transcriptional repression of the metastasis suppressor RKIP in breast and prostate cancer.* Cancer Res, 2012. **72**(12): p. 3091-104.
176. Sellers, W.R. and M. Loda, *The EZH2 polycomb transcriptional repressor--a marker or mover of metastatic prostate cancer?* Cancer Cell, 2002. **2**(5): p. 349-50.
177. Wang, J., et al., *HNF1B-mediated repression of SLUG is suppressed by EZH2 in aggressive prostate cancer.* Oncogene, 2020. **39**(6): p. 1335-1346.
178. Margueron, R. and D. Reinberg, *The Polycomb complex PRC2 and its mark in life.* Nature, 2011. **469**(7330): p. 343-9.
179. Au, S.L., et al., *EZH2-Mediated H3K27me3 Is Involved in Epigenetic Repression of Deleted in Liver Cancer 1 in Human Cancers.* PLoS One, 2013. **8**(6): p. e68226.
180. Chang, C.J. and M.C. Hung, *The role of EZH2 in tumour progression.* Br J Cancer, 2012. **106**(2): p. 243-7.
181. Koyanagi, M., et al., *EZH2 and histone 3 trimethyl lysine 27 associated with Il4 and Il13 gene silencing in Th1 cells.* J Biol Chem, 2005. **280**(36): p. 31470-7.
182. Chen, H., S.W. Tu, and J.T. Hsieh, *Down-regulation of human DAB2IP gene expression mediated by polycomb Ezh2 complex and histone deacetylase in prostate cancer.* J Biol Chem, 2005. **280**(23): p. 22437-44.
183. Qi, W., et al., *An allosteric PRC2 inhibitor targeting the H3K27me3 binding pocket of EED.* Nat Chem Biol, 2017. **13**(4): p. 381-388.
184. Taplin, M.-E., et al., *ProSTAR: A phase Ib/II study of CPI-1205, a small molecule inhibitor of EZH2, combined with enzalutamide (E) or abiraterone/prednisone (A/P) in*

patients with metastatic castration-resistant prostate cancer (mCRPC). Journal of Clinical Oncology, 2019. **37**(7_suppl): p. TPS335-TPS335.
185. Duan, R., W. Du, and W. Guo, *EZH2: a novel target for cancer treatment.* Journal of Hematology & Oncology, 2020. **13**(1): p. 104.
186. Kung, P.P., et al., *Optimization of Orally Bioavailable Enhancer of Zeste Homolog 2 (EZH2) Inhibitors Using Ligand and Property-Based Design Strategies: Identification of Development Candidate (R)-5,8-Dichloro-7-(methoxy(oxetan-3-yl)methyl)-2-((4-methoxy-6-methyl-2-oxo-1,2-dihydropyridin-3-yl)methyl)-3,4-dihydroisoquinolin-1(2H)-one (PF-06821497).* J Med Chem, 2018. **61**(3): p. 650-665.
187. Mertz, J.A., et al., *Targeting MYC dependence in cancer by inhibiting BET bromodomains.* Proc Natl Acad Sci U S A, 2011. **108**(40): p. 16669-74.
188. Stathis, A. and F. Bertoni, *BET Proteins as Targets for Anticancer Treatment.* Cancer Discovery, 2018. **8**(1): p. 24-36.
189. Urbanucci, A., et al., *Androgen Receptor Deregulation Drives Bromodomain-Mediated Chromatin Alterations in Prostate Cancer.* Cell Reports, 2017. **19**(10): p. 2045-2059.
190. Welti, J., et al., *Targeting Bromodomain and Extra-Terminal (BET) Family Proteins in Castration-Resistant Prostate Cancer (CRPC).* Clinical Cancer Research, 2018. **24**(13): p. 3149-3162.
191. Asangani, I.A., et al., *Therapeutic targeting of BET bromodomain proteins in castration-resistant prostate cancer.* Nature, 2014. **510**(7504): p. 278-282.
192. Raina, K., et al., *PROTAC-induced BET protein degradation as a therapy for castration-resistant prostate cancer.* Proceedings of the National Academy of Sciences, 2016. **113**(26): p. 7124-7129.
193. Faivre, E.J., et al., *Selective inhibition of the BD2 bromodomain of BET proteins in prostate cancer.* Nature, 2020. **578**(7794): p. 306-310.
194. Coleman, D.J., et al., *BET bromodomain inhibition blocks the function of a critical AR-independent master regulator network in lethal prostate cancer.* Oncogene, 2019. **38**(28): p. 5658-5669.
195. Kumaraswamy, A., et al., *Recent Advances in Epigenetic Biomarkers and Epigenetic Targeting in Prostate Cancer.* European Urology, 2021. **80**(1): p. 71-81.
196. Lasko, L.M., et al., *Discovery of a selective catalytic p300/CBP inhibitor that targets lineage-specific tumours.* Nature, 2017. **550**(7674): p. 128-132.
197. Liu, J., et al., *p300/CBP inhibition enhances the efficacy of programmed death-ligand 1 blockade treatment in prostate cancer.* Oncogene, 2020. **39**(19): p. 3939-3951.
198. Ishino, Y., et al., *Nucleotide sequence of the iap gene, responsible for alkaline phosphatase isozyme conversion in Escherichia coli, and identification of the gene product.* J Bacteriol, 1987. **169**(12): p. 5429-33.
199. Bolotin, A., et al., *Clustered regularly interspaced short palindrome repeats (CRISPRs) have spacers of extrachromosomal origin.* Microbiology (Reading), 2005. **151**(Pt 8): p. 2551-2561.
200. Mojica, F.J., et al., *Intervening sequences of regularly spaced prokaryotic repeats derive from foreign genetic elements.* J Mol Evol, 2005. **60**(2): p. 174-82.
201. Pourcel, C., G. Salvignol, and G. Vergnaud, *CRISPR elements in Yersinia pestis acquire new repeats by preferential uptake of bacteriophage DNA, and provide additional tools for evolutionary studies.* Microbiology (Reading), 2005. **151**(Pt 3): p. 653-663.

202. Jansen, R., et al., *Identification of genes that are associated with DNA repeats in prokaryotes.* Mol Microbiol, 2002. **43**(6): p. 1565-75.
203. Brouns, S.J., et al., *Small CRISPR RNAs guide antiviral defense in prokaryotes.* Science, 2008. **321**(5891): p. 960-4.
204. Barrangou, R., et al., *CRISPR provides acquired resistance against viruses in prokaryotes.* Science, 2007. **315**(5819): p. 1709-12.
205. Jiang, F. and J.A. Doudna, *CRISPR–Cas9 Structures and Mechanisms.* Annual Review of Biophysics, 2017. **46**(1): p. 505-529.
206. Unniyampurath, U., R. Pilankatta, and M.N. Krishnan, *RNA Interference in the Age of CRISPR: Will CRISPR Interfere with RNAi?* Int J Mol Sci, 2016. **17**(3): p. 291.
207. Makarova, K.S., et al., *Evolutionary classification of CRISPR–Cas systems: a burst of class 2 and derived variants.* Nature Reviews Microbiology, 2020. **18**(2): p. 67-83.
208. Makarova, K.S., et al., *An updated evolutionary classification of CRISPR-Cas systems.* Nat Rev Microbiol, 2015. **13**(11): p. 722-36.
209. Faure, G., et al., *Comparative genomics and evolution of trans-activating RNAs in Class 2 CRISPR-Cas systems.* RNA Biol, 2019. **16**(4): p. 435-448.
210. Liu, L., et al., *Two Distant Catalytic Sites Are Responsible for C2c2 RNase Activities.* Cell, 2017. **168**(1-2): p. 121-134.e12.
211. Jinek, M., et al., *A programmable dual-RNA-guided DNA endonuclease in adaptive bacterial immunity.* Science, 2012. **337**(6096): p. 816-21.
212. Cong, L., et al., *Multiplex genome engineering using CRISPR/Cas systems.* Science, 2013. **339**(6121): p. 819-23.
213. Jinek, M., et al., *RNA-programmed genome editing in human cells.* Elife, 2013. **2**: p. e00471.
214. Mali, P., et al., *RNA-guided human genome engineering via Cas9.* Science, 2013. **339**(6121): p. 823-6.
215. Wang, K. and M. Nicholaou, *Suppression of Antimicrobial Resistance in MRSA Using CRISPR-dCas9.* American Society for Clinical Laboratory Science, 2017. **30**(4): p. 207-213.
216. Zhen, S., et al., *Harnessing the clustered regularly interspaced short palindromic repeat (CRISPR)/CRISPR-associated Cas9 system to disrupt the hepatitis B virus.* Gene Therapy, 2015. **22**(5): p. 404-412.
217. Sinha, R., et al., *Duchenne muscular dystrophy: Case report and review.* Journal of Family Medicine and Primary Care, 2017. **6**(3): p. 654-656.
218. Wu, K. and S.N. Malek, *CRISPR/Cas9-Based Gene Dropout Screens*, in *Chronic Lymphocytic Leukemia: Methods and Protocols*, S.N. Malek, Editor. 2019, Springer New York: New York, NY. p. 185-200.
219. Dufva, O., et al., *Integrated drug profiling and CRISPR screening identify essential pathways for CAR T-cell cytotoxicity.* Blood, 2020. **135**(9): p. 597-609.
220. Martinez-Lage, M., et al., *CRISPR/Cas9 for Cancer Therapy: Hopes and Challenges.* Biomedicines, 2018. **6**(4): p. 105.
221. Frangoul, H., et al., *CRISPR-Cas9 Gene Editing for Sickle Cell Disease and β-Thalassemia.* N Engl J Med, 2021. **384**(3): p. 252-260.
222. Khalaf, K., et al., *CRISPR/Cas9 in Cancer Immunotherapy: Animal Models and Human Clinical Trials.* Genes (Basel), 2020. **11**(8).

223. Moffat, J., et al., *A Lentiviral RNAi Library for Human and Mouse Genes Applied to an Arrayed Viral High-Content Screen.* Cell, 2006. **124**(6): p. 1283-1298.
224. Chen, S., et al., *Genome-wide CRISPR Screen in a Mouse Model of Tumor Growth and Metastasis.* Cell, 2015. **160**(6): p. 1246-1260.
225. Xue, H.Y., et al., *CRISPR-Cas9 for medical genetic screens: applications and future perspectives.* J Med Genet, 2016. **53**(2): p. 91-7.
226. Dhanjal, J.K., N. Radhakrishnan, and D. Sundar, *Identifying synthetic lethal targets using CRISPR/Cas9 system.* Methods, 2017. **131**: p. 66-73.
227. *Strategies for Enhancing the Homology-Directed Repair Efficiency of CRISPR-Cas Systems.* The CRISPR Journal, 2022. **5**(1): p. 7-18.
228. Yao, J. and H.L. Dai, *Is Pooled CRISPR-Screening the Dawn of a New Era for Functional Genomics.* Adv Exp Med Biol, 2018. **1068**: p. 171-176.
229. Bodapati, S., et al., *A benchmark of algorithms for the analysis of pooled CRISPR screens.* Genome Biology, 2020. **21**(1): p. 62.
230. Kampmann, M., *CRISPRi and CRISPRa Screens in Mammalian Cells for Precision Biology and Medicine.* ACS Chem Biol, 2018. **13**(2): p. 406-416.
231. Lei, H., et al., *CRISPR screening identifies CDK12 as a conservative vulnerability of prostate cancer.* Cell Death Dis, 2021. **12**(8): p. 740.
232. Palit, S.A., et al., *TLE3 loss confers AR inhibitor resistance by facilitating GR-mediated human prostate cancer cell growth.* Elife, 2019. **8**.
233. Das, R., et al., *An integrated functional and clinical genomics approach reveals genes driving aggressive metastatic prostate cancer.* Nat Commun, 2021. **12**(1): p. 4601.
234. Chen, J., et al., *Genome-Scale CRISPR-Cas9 Transcriptional Activation Screening in Metformin Resistance Related Gene of Prostate Cancer.* Front Cell Dev Biol, 2020. **8**: p. 616332.
235. Ye, R., et al., *CRISPR/Cas9 targeting of GPRC6A suppresses prostate cancer tumorigenesis in a human xenograft model.* Journal of Experimental & Clinical Cancer Research, 2017. **36**(1): p. 90.
236. Riedel, M., et al., *In vivo CRISPR inactivation of Fos promotes prostate cancer progression by altering the associated AP-1 subunit Jun.* Oncogene, 2021. **40**(13): p. 2437-2447.
237. Fu, Y., et al., *Improving CRISPR-Cas nuclease specificity using truncated guide RNAs.* Nat Biotechnol, 2014. **32**(3): p. 279-284.
238. Cho, S.W., et al., *Analysis of off-target effects of CRISPR/Cas-derived RNA-guided endonucleases and nickases.* Genome Res, 2014. **24**(1): p. 132-41.
239. Kim, S., et al., *Highly efficient RNA-guided genome editing in human cells via delivery of purified Cas9 ribonucleoproteins.* Genome Res, 2014. **24**(6): p. 1012-9.
240. Hsu, P.D., et al., *DNA targeting specificity of RNA-guided Cas9 nucleases.* Nature Biotechnology, 2013. **31**(9): p. 827-832.
241. Tang, X., et al., *Single transcript unit CRISPR 2.0 systems for robust Cas9 and Cas12a mediated plant genome editing.* Plant Biotechnol J, 2019. **17**(7): p. 1431-1445.
242. Gaudelli, N.M., et al., *Programmable base editing of A•T to G•C in genomic DNA without DNA cleavage.* Nature, 2017. **551**(7681): p. 464-471.
243. Yen, S.T., et al., *Somatic mosaicism and allele complexity induced by CRISPR/Cas9 RNA injections in mouse zygotes.* Dev Biol, 2014. **393**(1): p. 3-9.

244. Janik, E., et al., *Various Aspects of a Gene Editing System—CRISPR–Cas9.* International Journal of Molecular Sciences, 2020. **21**(24): p. 9604.
245. Gaj, T., C.A. Gersbach, and C.F. Barbas, 3rd, *ZFN, TALEN, and CRISPR/Cas-based methods for genome engineering.* Trends Biotechnol, 2013. **31**(7): p. 397-405.
246. Evers, B., et al., *CRISPR knockout screening outperforms shRNA and CRISPRi in identifying essential genes.* Nat Biotechnol, 2016. **34**(6): p. 631-3.
247. Dang, C.V., *MYC, metabolism, cell growth, and tumorigenesis.* Cold Spring Harb Perspect Med, 2013. **3**(8).
248. Hsieh, A.L., et al., *MYC and metabolism on the path to cancer.* Semin Cell Dev Biol, 2015. **43**: p. 11-21.
249. Poole, C.J. and J. van Riggelen, *MYC-Master Regulator of the Cancer Epigenome and Transcriptome.* Genes (Basel), 2017. **8**(5).
250. Wang, T., et al., *Genetic screens in human cells using the CRISPR-Cas9 system.* Science, 2014. **343**(6166): p. 80-4.
251. Hundley, F.V. and D.P. Toczyski, *Chemical-genetic CRISPR-Cas9 screens in human cells using a pathway-specific library.* STAR Protocols, 2021. **2**(3): p. 100685.
252. Joung, J., et al., *Protocol: Genome-scale CRISPR-Cas9 Knockout and Transcriptional Activation Screening.* bioRxiv, 2016: p. 059626.
253. Watson, P.A., et al., *Context-dependent hormone-refractory progression revealed through characterization of a novel murine prostate cancer cell line.* Cancer Res, 2005. **65**(24): p. 11565-71.
254. Tzelepis, K., et al., *A CRISPR Dropout Screen Identifies Genetic Vulnerabilities and Therapeutic Targets in Acute Myeloid Leukemia.* Cell Reports, 2016. **17**(4): p. 1193-1205.
255. Fujita, K. and N. Nonomura, *Role of Androgen Receptor in Prostate Cancer: A Review.* World J Mens Health, 2019. **37**(3): p. 288-295.
256. Zhang, G., et al., *FOXA1 defines cancer cell specificity.* Sci Adv, 2016. **2**(3): p. e1501473.
257. Lupien, M., et al., *FoxA1 translates epigenetic signatures into enhancer-driven lineage-specific transcription.* Cell, 2008. **132**(6): p. 958-70.
258. Nguyen, A.H., et al., *Gata3 antagonizes cancer progression in Pten-deficient prostates.* Hum Mol Genet, 2013. **22**(12): p. 2400-10.
259. Luo, Y.Z., P. He, and M.X. Qiu, *FOSL1 enhances growth and metastasis of human prostate cancer cells through epithelial mesenchymal transition pathway.* Eur Rev Med Pharmacol Sci, 2018. **22**(24): p. 8609-8615.
260. Zhang, K., et al., *Oncogenic K-Ras upregulates ITGA6 expression via FOSL1 to induce anoikis resistance and synergizes with αV-Class integrins to promote EMT.* Oncogene, 2017. **36**(41): p. 5681-5694.
261. Tang, F., et al., *Chromatin profiles classify castration-resistant prostate cancers suggesting therapeutic targets.* Science, 2022. **376**(6596): p. eabe1505.
262. Orellana, E.A., et al., *METTL1-mediated m7G modification of Arg-TCT tRNA drives oncogenic transformation.* Molecular Cell, 2021. **81**(16): p. 3323-3338.e14.
263. Beck, D.B., et al., *PR-Set7 and H4K20me1: at the crossroads of genome integrity, cell cycle, chromosome condensation, and transcription.* Genes Dev, 2012. **26**(4): p. 325-37.

264. Dave, N., et al., *Identification of retinoblastoma binding protein 7 (Rbbp7) as a mediator against tau acetylation and subsequent neuronal loss in Alzheimer's disease and related tauopathies.* Acta Neuropathologica, 2021. **142**(2): p. 279-294.
265. Ding, Y., et al., *Chromatin remodeling ATPase BRG1 and PTEN are synthetic lethal in prostate cancer.* J Clin Invest, 2019. **129**(2): p. 759-773.
266. Han, W., et al., *RB1 loss in castration-resistant prostate cancer confers vulnerability to LSD1 inhibition.* Oncogene, 2022. **41**(6): p. 852-864.
267. Ricketts, M.D. and R. Marmorstein, *A Molecular Prospective for HIRA Complex Assembly and H3.3-Specific Histone Chaperone Function.* Journal of Molecular Biology, 2017. **429**(13): p. 1924-1933.
268. Kim, J.Y., et al., *KDM3B is the H3K9 demethylase involved in transcriptional activation of lmo2 in leukemia.* Mol Cell Biol, 2012. **32**(14): p. 2917-33.
269. Kim, K.-Y., et al., *Uhrf1 regulates active transcriptional marks at bivalent domains in pluripotent stem cells through Setd1a.* Nature Communications, 2018. **9**(1): p. 2583.
270. Mohamed, W.I., et al., *The CRL4DCAF1 cullin-RING ubiquitin ligase is activated following a switch in oligomerization state.* The EMBO Journal, 2021. **40**(22): p. e108008.
271. Qiu, X., et al., *MYC drives aggressive prostate cancer by disrupting transcriptional pause release at androgen receptor targets.* Nature Communications, 2022. **13**(1): p. 2559.
272. Cancer Genome Atlas Research, N., *The Molecular Taxonomy of Primary Prostate Cancer.* Cell, 2015. **163**(4): p. 1011-1025.
273. Pomerantz, M.M., et al., *The androgen receptor cistrome is extensively reprogrammed in human prostate tumorigenesis.* Nat Genet, 2015. **47**(11): p. 1346-51.
274. Grasso, C.S., et al., *The mutational landscape of lethal castration-resistant prostate cancer.* Nature, 2012. **487**(7406): p. 239-243.
275. Wu, M., G. Chen, and Y.P. Li, *TGF-β and BMP signaling in osteoblast, skeletal development, and bone formation, homeostasis and disease.* Bone Res, 2016. **4**: p. 16009.
276. Mohammadnia, A., et al., *Signaling and Gene Regulatory Networks Governing Definitive Endoderm Derivation From Pluripotent Stem Cells.* J Cell Physiol, 2016. **231**(9): p. 1994-2006.
277. Tian, Q.H., et al., *METTL1 overexpression is correlated with poor prognosis and promotes hepatocellular carcinoma via PTEN.* J Mol Med (Berl), 2019. **97**(11): p. 1535-1545.
278. Xu, L., et al., *Roles for the methyltransferase SETD8 in DNA damage repair.* Clinical Epigenetics, 2022. **14**(1): p. 34.
279. Herviou, L., et al., *Targeting the methyltransferase SETD8 impairs tumor cell survival and overcomes drug resistance independently of p53 status in multiple myeloma.* Clinical Epigenetics, 2021. **13**(1): p. 174.
280. Veo, B., et al., *Combined functional genomic and chemical screens identify SETD8 as a therapeutic target in MYC-driven medulloblastoma.* JCI Insight, 2019. **4**(1).
281. Yu, N., et al., *RBBP7 is a prognostic biomarker in patients with esophageal squamous cell carcinoma.* Oncol Lett, 2018. **16**(6): p. 7204-7211.
282. Veland, N. and T. Chen, *Chapter 2 - Mechanisms of DNA Methylation and Demethylation During Mammalian Development*, in *Handbook of Epigenetics (Second Edition)*, T.O. Tollefsbol, Editor. 2017, Academic Press. p. 11-24.

283. Babbio, F., et al., *The SRA protein UHRF1 promotes epigenetic crosstalks and is involved in prostate cancer progression.* Oncogene, 2012. **31**(46): p. 4878-4887.
284. Schabla, N.M., K. Mondal, and P.C. Swanson, *DCAF1 (VprBP): emerging physiological roles for a unique dual-service E3 ubiquitin ligase substrate receptor.* Journal of Molecular Cell Biology, 2018. **11**(9): p. 725-735.
285. Kim, K., et al., *VprBP has intrinsic kinase activity targeting histone H2A and represses gene transcription.* Mol Cell, 2013. **52**(3): p. 459-67.
286. Kim, K., et al., *Vpr-binding protein antagonizes p53-mediated transcription via direct interaction with H3 tail.* Mol Cell Biol, 2012. **32**(4): p. 783-96.
287. Wen, T. and Q.Y. Chen, *Dynamic Activity of Histone H3-Specific Chaperone Complexes in Oncogenesis.* Frontiers in Oncology, 2022. **11**.
288. Saraç, H., et al., *Systematic characterization of chromatin modifying enzymes identifies KDM3B as a critical regulator in castration resistant prostate cancer.* Oncogene, 2020. **39**(10): p. 2187-2201.
289. Ying, X., et al., *METTL1-m7G-EGFR/EFEMP1 axis promotes the bladder cancer development.* Clinical and Translational Medicine, 2021. **11**(12): p. e675.
290. Poulose, N., et al., *VPRBP functions downstream of the androgen receptor and OGT to restrict p53 activation in prostate cancer.* bioRxiv, 2021: p. 2021.02.28.433236.

APPENDIX

Supplementary figures for chapter 3

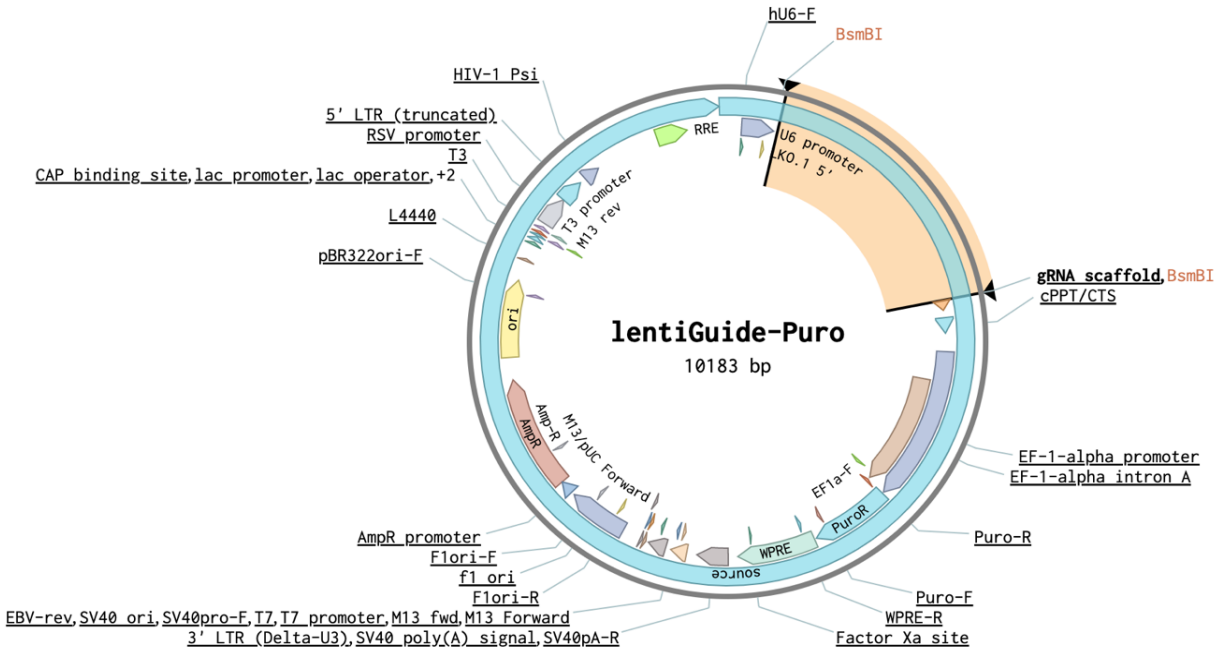

Figure 4-1. Map of LentiGuide-Puro.

BSMB1 cutting sites are depicted by the two black arrows. Plasmid designed using Benchling.

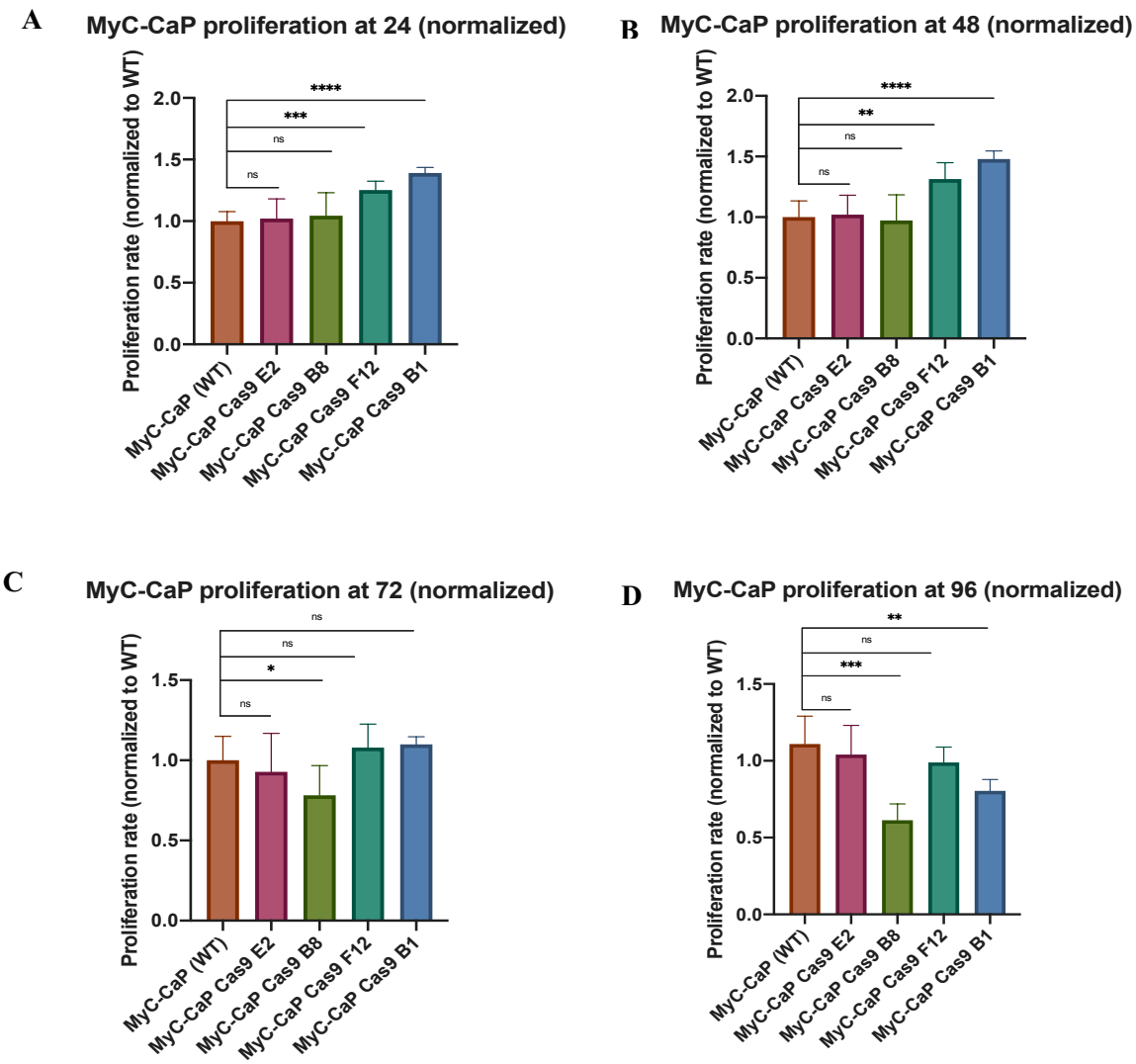

Figure 4-2. Proliferation rate of MyC-CaP Cas9 clones and MyC-CaP WT.

Proliferation rates of MyC-CaP Cas9 clones and MyC-CaP WT at 24h (**A**), 48h (**B**), 72h (**C**) and 96h (**D**). Mean ± SEM. Unpaired t-test. ns ≤ 0.05.

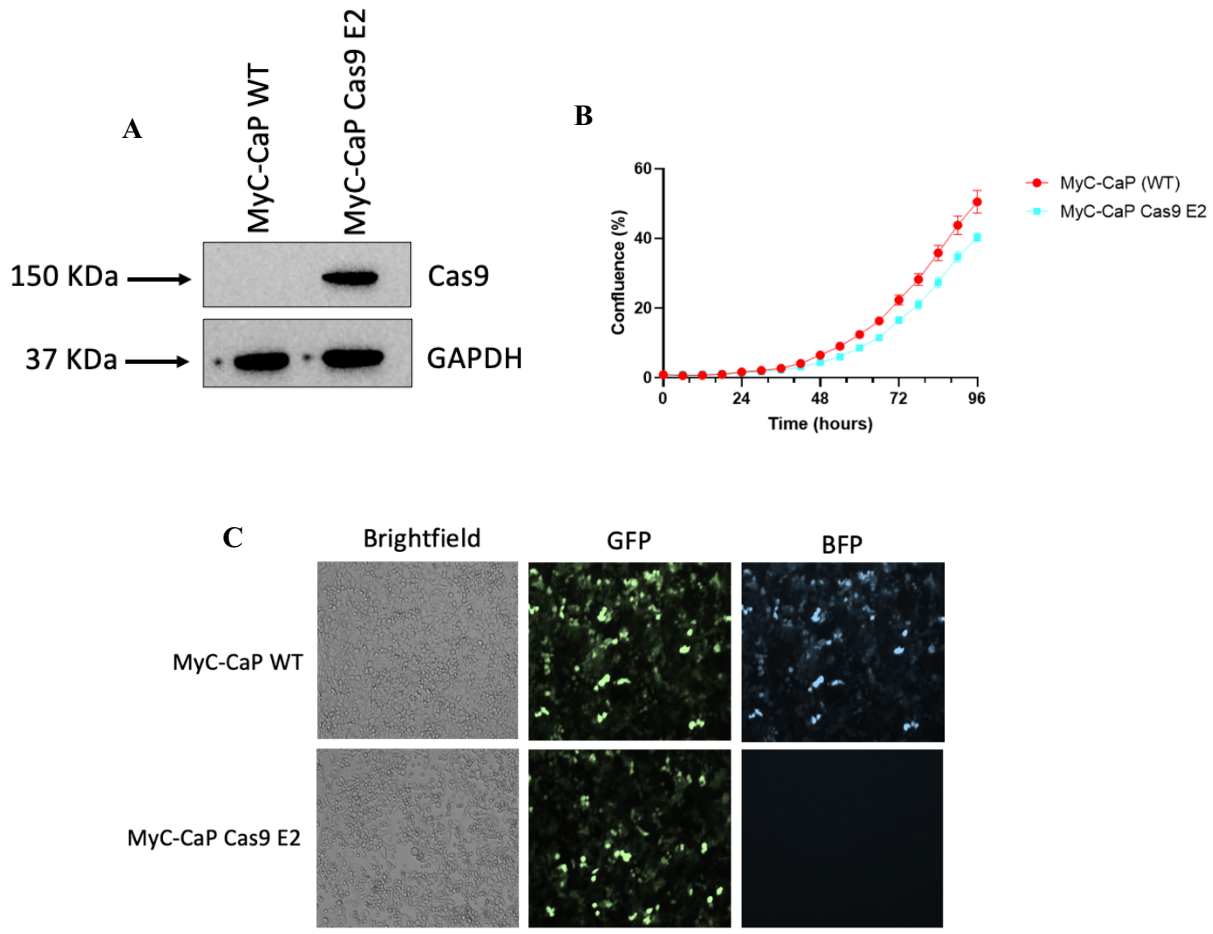

Figure 4-3. MyC-CaP Cas9 E2 clone re-characterization.

Re-characterization of MyC-CaP Cas9 E2 clone using Western Blot (**A**), proliferation assay (**B**), and Cas9 activity Assay (**C**).

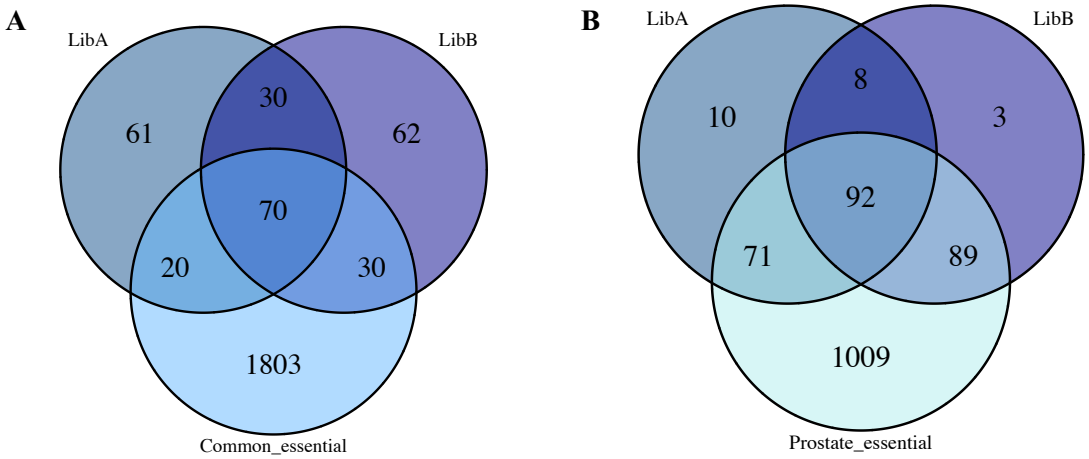

Figure 4-4. Overlap of *in vitro* MyC-CaP CRISPR/Cas9 KO screen hits and common essential genes in cancer cell lines.

Venn diagrams showing the overlap of significantly depleted genes in our screen with essential genes identified in other human cancer cell lines (**A**) and other human prostate cancer cell lines (22Rv1, LNCaP, DU-145, VCaP, BPH1, P4E6) (**B**).